MESTRADO
MEDICINA E ONCOLOGIA MOLECULAR

The role of glycans in modulating innate immunity towards cancer prevention

Pedro Filipe Neves de Almeida

M

2022/2023

FACULDADE DE **MEDICINA**

Pedro Filipe Neves de Almeida

The role of glycans in modulating innate immunity towards cancer prevention

Dissertação de Candidatura ao grau de Mestre em Medicina e Oncologia Molecular, submetida à Faculdade de Medicina da Universidade do Porto.

Orientadora: Prof. Doutora Salomé S. Pinho, PhD.

Coorientadoras: Doutora Ângela Fernandes, PhD; Doutora Inês Alves, PhD.

Agradecimentos

Em primeiro lugar, gostaria de agradecer à Professora Doutora Salomé Pinho, que me proporcionou a oportunidade de realizar a minha tese de mestrado no seu grupo. Obrigado por todo o apoio e motivação que me deu e por partilhar comigo a sua paixão pela ciência. Este ano foi um passo essencial na minha carreira científica e o seu auxílio foi uma constante que me permitiu evoluir consideravelmente.

Um obrigado muito especial à Ângela e à Inês. A vossa supervisão foi crucial para todos os sucessos deste projeto e o vosso apoio indispensável. Obrigado por todas as discussões científicas e todos os momentos de amizade que partilhamos, que foram igualmente importantes para ter conseguido chegar a este momento.

Aos restantes membros do ICG, dos mais novos que experienciaram muitos dos mesmos desafios pelos quais passei aos mais experientes que muitos conselhos deram, obrigado por todos os momentos de discussão que partilhamos e todos os momentos mais relaxados que disfrutamos. Desde o primeiro momento que me receberam de braços abertos e foram um pilar onde me pude suportar durante todo o mestrado.

Ao Professor Doutor Henrique Almeida, agradeço todo o apoio que nos deu enquanto diretor do Mestrado em Medicina e Oncologia Molecular e pela excelência do programa que nos proporciona.

A todos os meus amigos, desde as amizades que mantenho desde os 3 anos até àqueles que só conheci no início do mestrado, um enorme obrigado por todos os momentos de diversão e descontração que vivemos, vocês foram essenciais em manter-me na motivado para enfrentar os desafios que enfrentei ao longo de todo o meu percurso académico.

À minha família, em particular aos meus pais, avós e, claro, ao Bolt, obrigado por sempre acreditarem em mim e me motivarem para nunca desistir. Vocês foram as pessoas que mais portas me abriram, quer no meu percurso académico, quer na vida pessoal, e espero que vos tenha deixado orgulhosos com tudo o que consegui atingir até agora. Ao avô Ernesto, quem me dera que pudesses estar aqui, eu sei o quão feliz ficavas quando me vias a cruzar metas importantes, e esta foi mais uma que dedico a ti.

Abstract

In 2020, over 500 000 cases of Bladder Cancer (BC) were diagnosed, which resulted in around 200 000 deaths directly related to this malignancy, which highlights the urgent need to better comprehend the molecular mechanisms behind it.

The majority of cases (around 80%) are diagnosed in the non-muscle invasive (NMIBC) stage. Bacillus Calmette-Guérin (BCG) is often used as an adjuvant immunotherapy in early high risk NMIBC together with the resection of the tumour and has been shown to significantly improve recurrence-free survival. It is described that this bug induces an epigenetic reprogramming of innate immune cells, such as monocytes, triggering a memory-like enhanced immune phenotype named "Trained Immunity" (TI). This process translates into a higher pro-inflammatory cytokine production, an improved anti-tumoral response and T-cell independent protection against other infections. However, the mechanism that promotes this immune response in BC is not fully understood, and not all patients have a positive response.

Glycans are macromolecular sugar structures added by enzymes to lipids or proteins, and they cover the cell membrane of all cells, forming the glycocalyx. This carbohydrate shield plays a major role in several cellular processes in homeostasis, and in pathological settings, being involved in tumour immunoediting and progression. Previous work from our group demonstrated that aberrant expression of complex branched *N*-glycans is linked to tumour evasion in colorectal cancer, and the removal of these structures lead to a reinvigorated immune response. In another setting, we also demonstrated that the surface expression of mannose glycans can be recognised by immune cells triggering inflammatory/autoreactive responses. Notably, BCG has relevant glycan structures on its surface, namely lipomannans, which can be sensed by innate cells carrying Pattern-Recognizing Receptors (PRRs).

With all of this in mind, the main goal of this thesis is to understand the role of pathogen-derived glycans as relevant triggers of a more pro-inflammatory "trained" phenotype on monocytes, and whether this glycan-mediated training increased the capacity of these cells to sense and kill tumour cells. *In silico* analysis showed that monocytes previously exposed to certain stimuli with pro-inflammatory priming/training capabilities presented an increased expression of glycan binding

receptors, such as DC-SIGN and Dectin-1. Furthermore, we demonstrated that monocytes isolated from healthy donors and exposed to different glycan structures revealed an increased expression of certain PRRs, namely DC-SIGN and Dectin-1. Additionally, pro-inflammatory cytokine production, specifically TNF-α and IL-6, was also increased. Interestingly, co-cultures with glycan trained monocytes (isolated from healthy donors) and BC cell lines showed that glycan-treated immune cells exhibited elevated anti-tumoral activity. Lastly, we complemented our analysis by studying monocytes from one NMIBC patient blood sample in the maintenance stage of BCG therapy and evaluating the receptors that these cells were expressing.

Taken together, our results suggest that certain pathogen-derived glycan structures have the ability to prime and improve innate immune responses through the induction of TI. Moreover, this enhanced immune phenotype could be used to induce tumour cell death *in vitro*, making it a possible relevant avenue to explore as a potential treatment for bladder malignancies.

Resumo

Em 2020, foram diagnosticados mais de 500 mil casos de Cancro da Bexiga (CB), o que resultou em cerca de 200 mil mortes causadas diretamente pela doença, destacando a necessidade urgente de desvendar os mecanismos moleculares empregues pela mesma.

A maioria dos casos (cerca de 80%) foi diagnosticado em estadios Não-Músculo Invasivos (CBNMI). Injeções intravesicais de Bacillus Calmette-Guérin (BCG) são frequentemente administradas em estadios inicias de CBNMI de alto risco em conjunto com remoção do tumor, sendo que esta imunoterapia adjuvante já mostrou ser eficaz a aumentar a sobrevivência livre de recorrência. Este patogénio tem a capacidade de induzir a reprogramação epigenética de células imunes inatas, nomeadamente de monócitos, levando ao desenvolvimento de um fenótipo de "memória imune inata", denominado de "Imunidade Treinada" (IT). Este processo leva a uma maior produção de citocinas pró-inflamatórias, uma resposta anti-tumoral mais eficaz e proteção contra infeções secundárias independente de células T. Todavia, o mecanismo que leva a esta resposta imune aprimorada não é completamente compreendido no contexto do CB, e nem todos os pacientes respondem positivamente.

Os glicanos são estruturas macromoleculares constituídas por açúcares enzimaticamente ligadas a proteínas ou lípidos que cobrem a membrana de todas as células, formando o glicocálice. Este revestimento de carbo-hidratos tem um papel importante em vários processos celulares em homeostasia e em contexto patológico, estando envolvido na evasão imune e progressão dos tumores. Trabalhos prévios do nosso grupo demonstraram que a expressão aberrante de *N*-glicanos está ligada a maior evasão tumoral em cancro colorretal e a remoção destas estruturas levou a uma resposta imune revigorada. Noutro contexto, demonstramos que a expressão de glicanos ricos em manose pode ser reconhecida por células imunes, desencadeando respostas inflamatórias/auto-reativas. Notavelmente, o patogénio BCG apresenta diversas e relevantes estruturas de glicanos na sua superfície, tais como os lipomananos, que podem ser reconhecidos por *Pattern Recognizing Receptors* (PRRs).

Com tudo isto em mente, o objetivo principal desta tese consiste em explorar o papel dos glicanos derivados de patogénios como desencadeadores de um fenótipo pró-

inflamatório "treinado", e se o treino mediado por glicanos se traduz num aumento da capacidade destas células de detetar e eliminar células tumorais. A análise de dados *in silico* de monócitos previamente expostos a estímulos pró-inflamatórios com capacidade de treino revelou um aumento da expressão de recetores específicos para glicanos, tais como DC-SIGN e Dectin-1. Além disso, demonstramos que monócitos isolados de dadores saudáveis posteriormente colocados em contacto com diferentes glicanos apresentavam um aumento da expressão de certos PRRs, nomeadamente DC-SIGN e Dectin-1 . Ainda mais, examinamos a expressão de citocinas pró-inflamatórias, em particular TNF-α e IL-6, que se encontrava aumentada. Co-culturas de monócitos treinados com glicanos (isolados de dadores saudáveis) e linhas celulares de CB demonstraram que células imunes tratadas com glicanos apresentavam maior atividade anti-tumoral. Por fim, complementamos a nossa análise estudando monócitos extraídos de uma amostra de sangue de um paciente de CBNMI na fase de manutenção do tratamento com BCG e estudamos a expressão de recetores destas células.

Em suma, os nossos resultados sugerem que o uso de certas estruturas de glicanos derivados de patogénios tem a capacidade de melhorar a resposta imune inata através da indução da IT. Além disso, este fenótipo conduziu a maior morte tumoral *in vitro*, realçando que este mecanismo pode ser um potencial caminho a explorar para o desenvolvimento de terapias contra o CB.

Index

Agradecimentos.....II

Abstract.....III

Resumo.....V

Figure Index.....IX

Table Index.....XIII

Abbreviation List.....XIV

INTRODUCTION.....1

1. Cancer.....2
    1.1. Global Overview.....2
    1.2. Bladder Cancer.....4
2. Glycosylation.....8
    2.1. Protein Glycosylation.....8
    2.2. *N*-glycosylation.....10
    2.3. Glycan alterations as a key feature of malignant transformation.....12
3. The immune system.....14
    3.1. The principles of immunity.....14
    3.2. Immune evasion in cancer and the role of glycans.....18
4. Trained Immunity.....22
    4.1. Standing up to the dogma: innate cell "memory".....22
    4.2. BCG mediated trained immunity in the context of Bladder Cancer.....24

AIMS.....28

MATERIALS AND METHODS.....30

1. *In silico* analysis.....31
2. Human samples.....32
3. Isolation of monocytes.....32
4. Glycan priming of monocytes.....33
5. Restimulation of patient-derived monocytes.....34
6. Bladder cancer cell lines culture.....35
7. Co-culture assays.....36
8. Western Blot (Lectin Blot).....36
9. Flow cytometry staining.....37
    9.1. Monocyte glycan-binding protein staining.....37

9.2. Bladder cancer cell line lectin staining……40
9.3. Annexin-PI assay……42
10. Enzyme-Linked ImmunoSorbent Assays (ELISAs)……46
11. Real Time quantitative Polymerase Chain Reaction (RT-qPCR)……46
12. Statistical Analysis……48

RESULTS……49
1. Trained immunity alters glycan-binding protein expression pattern - an *in silico* analysis……50
2. Monocytes supplemented with α-mannan evidenced a primed phenotype……54
3. Bladder cancer cell lines and glycan-primed monocyte co-cultures……60
3.1. Bladder cancer cell line glycoprofile characterization……60
3.2. α-mannan primed monocytes displayed higher tumoricidal activity……62
4. Characterization of surface receptor expression in monocytes derived from non-muscle invasive bladder cancer patients treated with BCG instillations……65

DISCUSSION……67
CONCLUSION AND FUTURE PERSPECTIVES……78
REFERENCES……81
Appendix 1……90
Appendix 2……93

Figure Index

Figure 1. Forecast of total number of newly diagnosed cancer cases in 2040, stratified in accordance with the 4-tier Human Development Index. Sourced from (1)……2

Figure 2. The hallmarks of cancer. Sourced from (6)……4

Figure 3. Pie-charts illustrating cancer incidence rates in 2020 for both sexes (A), for males (B) and mortality rates in males (C). Bladder cancer is represented in dark green. Adapted from https://gco.iarc.fr/today/home……5

Figure 4. Worldwide incidence (A) and mortality (B) rates for bladder cancer normalized per 100 000 inhabitants, for both sexes and all ages in 2020. Adapted from https://gco.iarc.fr/today/home……5

Figure 5. Different stages and histological classifications of bladder cancer. Sourced from (7)……7

Figure 6. Main classes of glycoconjugates found in mammals. Glycans can be linked to lipids, originating glycosphingolipids. Glycoproteins can be connected to a glycosylphosphatidylinositol (GPI) anchor on the plasma membrane, to the nitrogen atom of an Asn residue (*N*-glycans) or to the oxygen atom of a Ser or Thr (*O*-glycans). Glycosaminoglycans are linear polymers frequently found associated with proteoglycans or, in the case of hyaluronic acid, freely roaming in the extracellular matrix. Sourced from (24)……9

Figure 7. *N*-glycan biosynthesis schematic. This process starts in the ER, where dolichol-phosphate acts as a carrier for the assembly of the lipid-linked oligosaccharide (LLO). The LLO is transferred to an asparagine residue of a nascent protein and is further processed in the ER. Then, it is transported to the Golgi apparatus, where an assortment of mannosidases, glycotransferases and other enzymes further process and mature the glycan, leading to the diverse cellular glycome. Adapted from (35)……11

Figure 8. Relevant glycans found in the context of cancer. Sialylation is one of the most prevalent alterations identified in tumours, being associated with both *N*- and *O*-linked branched glycans, truncated *O*-glycans and other structures, namely Lewis (Le) antigens. Other non-protein elements, such as glycosphingolipids, can also be sialylated. Other noteworthy events are an increase in core fucosylation and increase in β-1,6-GlcNAc branching mediated by GnT-V. Sourced from (24)……14

Figure 9. The three E's of cancer immunoediting. (a) Elimination is the process where the immune system identifies the tumour cells and effectively destroys them. (b) However, this allows for the selection of the fittest clones that are able to survive the attacks by the immune cells, establishing an equilibrium. (c) Eventually, these selected variants become very competent at escaping the immune surveillance, culminating in their uncontrolled replication. Sourced from (84)……18

Figure 10. The opposite responses induced by innate immune memory. After an initial stimulus, innate cells can follow a program of tolerance, where the pro-inflammatory response gives way to a suppressive one, often with the intent to protect the host and culminating in a lower baseline strength for the immune response. In dissonance, these cells can adopt a primed phenotype, where a second stimulus induces a much greater response. This reaction is dependent on several mechanisms, namely: (A) epigenetic reprogramming, allowing more access to crucial genes for the immune response; (B) metabolic adjustments, intimately connected to the chromatin alterations; (C) higher responsiveness and pro-inflammatory activity and (D) long-term bone marrow progenitor reprogramming, essential for a longer lasting effect. Adapted from (117)……24

Figure 11. Proposed mechanism for monocyte/macrophage-mediated trained immunity in bladder cancer treated with BCG instillations. (1) Naïve monocytes enter the bladder and are met with the pathogen, recognizing it through several PRRs, namely NOD-2. (2) There is an initial immune response, with cytokine production. (3) These cells differentiate into macrophages and acquire typical TI markers, such as increased metabolic activity and gather chromatin alterations that allow for a stronger immune response. (4 and 5) Successive BCG exposures and DAMP release from dead cancer cells restimulates the primed

macrophages that head the anti-tumoral response, displaying increased cytokine expression. Sourced from (145)……27

Figure 12. Example of the gating strategy employed in the flow cytometry analysis of the glycan binding protein analysis of monocytes. (A) Initially, cells were gated based size (FSC) versus complexity (SSC). (B) This was followed by single cell selection using a plot of event area (FCS-A) by event height (FSC-H). (C) Then, live cells were selected based on the non-incorporation of the viability dye (FVD), as cells that have a compromised membrane integrate it, becoming stained. (D) To guarantee the purity of the extraction process, CD14 was used to assure we had a pure monocyte population. The expression levels of the antibodies enumerated in Table 1 were then assessed utilising the Mean Fluorescence Intensity (MFI) values, as is exemplified in graphs (E) for CD86 and (F) for DC-SIGN……39

Figure 13. Example of the gating strategy employed in the flow cytometry analysis of the surface glycan expression. (A) Initially, cells were gated based size (FSC) versus complexity (SSC). (B) This was followed by single cell selection using a plot of event area (FCS-A) by event height (FSC-H). (C) Then, live cells were selected based on the non-incorporation of the viability dye (FVD). The expression levels of the lectins enumerated in Table 1 were then assessed utilising the Mean Fluorescence Intensity (MFI) values, as is exemplified in graphs (D) for DC-SIGN BM and (E) for L-PHA……41

Figure 14. Example of the gating strategy employed in the flow cytometry analysis of tumour cell death in the co-culture experiment. (A) Initially, cells were gated based size (FSC) versus complexity (SSC). (B) This was followed by single cell selection using a plot of event area (FCS-A) by event height (FSC-H). (C) Then, tumour cells were selected based on the absence of CD45 expression, a marker of immune populations. (D) Finally, cells were subdivided into four subsets based on the staining with Annexin V and PI. As is explained previously, double negative cells are live cells. Annexin V single positives are early apoptotic cells, whilst PI single positives are considered necrotic cells. Double stained cells are late apoptotic. The antibodies used in this section are indicated in Table 1 and the data was represented in relative percentages of the different subsets……43

Figure 15. Normalised gene counts comparing glycan-binding protein (GBP) levels in uninfected controls (white bar, n = 4) and HIV infected (blue bar, n = 7-8) individuals. Several pattern recognizing receptors (PRRs) display a significant increase in their expression in the HIV-positive group, except for MICL, that still exhibits a similar trend. Outlier tests were followed by Mann-Whitney U tests. Data is represented as Mean $\pm$ Standard Deviation (SD). * $p < 0.05$, ** $p < 0.01$……51

Figure 16. Normalised gene counts comparing glycan-binding protein (GBP) levels in uninfected controls (white bar, n = 4) and Sars-CoV-2 infected (blue bar, n = 3-4) individuals. Two different stimuli were used to rechallenge the monocytes: LPS and recombinant spike protein (SP). DC-SIGN and MICL were the only receptors that presented a significant increase in their levels after Sars-CoV-2 exposure, but trends are discernible for MR and MGL as well. The remaining PRRs did not present significant alterations. Outlier tests were followed by Mann-Whitney U tests. Data is represented as Mean $\pm$ SD. * $p < 0.05$……52

Figure 17. Normalised gene counts comparing glycan-binding protein (GBP) levels in non-primed (white bar, n = 4-5) and BCG-primed (blue bar, n = 4-5) monocytes extracted from 5 different individuals. Two different BCG strains were used to train the monocytes: BCG Bulgaria and BCG Denmark. This priming translated into higher DC-SIGN and Dectin-2 levels, whereas Dectin-1 and MICL did not display clear tendencies. MGL and MR were not detected in this dataset. Outlier tests were followed by Mann-Whitney U tests. Data is represented as Mean $\pm$ SD. * $p < 0.05$……53

Figure 18. (A) Diagram representation of the experimental procedure employed for the glycan priming of monocytes. After the isolation of the cells, they were exposed to carbohydrate stimuli for 24 hours. This was followed by a 5 day resting period and a 6 hour restimulation period with LPS. (B) Schematic illustration of the structure of the glycan stimuli utilised in the training of the monocytes. α-mannan is built from mannose residues, with an α-1,6 linked backbone connected to several branches. diGlcNAc exposes several GlcNAc adorned domains. β-glucan is constituted by a β-1,3-linked glucose backbone with

occasional β-1,6 branches that possess smaller β-1,3 linked chains. Images were created with BioRender……55

Figure 19. Glycan supplementation of monocytes induced higher levels of CD86 and reprogrammed the expression levels of several pattern recognizing receptors (PRRs). Cultured cells were isolated from two healthy donors and three technical replicates were established from each one (n = 4-9). Monocytes were stained for (A) CD86, (B) DC-SIGN, (C) Dectin-1, (D) Dectin-2 and (E) MR. Results are presented as the fold change of the Median Fluorescence Intensity values normalised to "Basal + LPS" conditions. Outlier tests were followed by Ordinary One-Way ANOVA or Kruskal-Wallis non-parametric ANOVA (depending on normality) and Dunnett's multiple comparison test. Data is represented as Mean ± SD. * $p < 0.05$, ** $p < 0.01$……57

Figure 20. β-glucan and α-mannan primed monocytes to secrete higher levels of pro-inflammatory cytokines. Cultured cells were isolated from two healthy donors and three technical replicates were established from each one (n = 2-6). ELISA assays were performed for IL-6 and TNF-α. Outlier tests were followed by Ordinary One-Way ANOVA and Dunnett's multiple comparison test. Data is represented as Mean ± SD. ** $p < 0.01$, *** $p < 0.001$, **** $p < 0.0001$……58

Figure 21. Glycan supplementation of monocytes produced inconsistent RT-qPCR results for (A) *TNF-α* and (B) *DC-SIGN*. For this experiment, only one donor was selected and three technical replicates were established (n = 3). *GAPDH* was used as the housekeeping gene. Outlier tests were followed by Ordinary One-Way ANOVA or Kruskal-Wallis non-parametric ANOVA (depending on normality) and Dunnett's multiple comparison test. Data is represented as Mean ± SD. * $p < 0.05$, ** $p < 0.01$, **** $p < 0.0001$……..59

Figure 22. Bladder cancer cell line surface glycan expression profile. Results shown in graphs A to E are the outcome of three different experiments, each one with three technical replicates (n = 9). GNA to L-PHA ratios (graph F) were calculated for each individual experiment for both cell lines, yielding an n = 3. Outlier tests were followed by Mann-Whitney U tests. Data is represented as Mean ± SD. ** $p < 0.01$, **** $p < 0.0001$……61

Figure 23. Lectin blot of the total protein lysate for the RT112 and T24 bladder cancer cell lines. Vinculin was used as the housekeeping gene. (A) Scans of the obtained gels. (B) Ratio between the measured Optical Density (OD) of the detected bands using the different lectins and their respective vinculin control……62

Figure 24. Schematic representation of the co-culture experimental procedure. Initially, monocytes underwent training *in vitro*. Afterwards, the immune cells were restimulated with LPS for 6 hours and cultured with RT112 or T24 bladder cancer cell lines in a 1:10 target:effector ratio. Two different timepoints were used to better evaluate the tumoricidal ability of monocytes: 24 and 48 hours……63

Figure 25. T24 cell line viability after 48 hours of co-culture with trained monocytes. The immune cells were supplemented with either β-glucan or α-mannan at 2,5 ug/ml and 200 ug/mL, respectively, and restimulated for 6 hours with LPS before co-culture with tumour cells. Non-trained monocytes were used as control for the priming of these cells. A further control with only tumour cells was added in this experiment. Monocytes were isolated from one donor and three technical replicates were established (n = 2-3). Cells were stained with CD45, allowing the distinction of tumoral and immune fractions. Furthermore, Annexin V and PI facilitated the evaluation of cell viability, with the percentage (%) of live, early apoptotic, late apoptotic and necrotic cells being displayed for each condition. Outlier tests were followed by a Two-way ANOVA and Dunnett's multiple comparison test. Data is represented as Mean ± SD……64

Figure 26. Schematic representation of the experimental procedure employed for the analysis of patient-derived monocytes. Patients underwent a BCG instillation regime that trained the circulating monocytes. We then isolated these cells and rechallenged them with LPS for 6 hours……66

Figure 27. GBP landscape in a BCG treated NMBIC patient. Cultured cells were isolated from one donor and three technical replicates were established (n = 3). Monocytes were stained for (A) CD86, (B) DC-SIGN, (C) Dectin-1, (D) Dectin-2 and (E) MR. Outlier tests were followed by Mann-Whitney U tests. Data is represented as Mean ± SD……66

Table Index

Table 1. List of glycan-binding protein genes tested in the gene expression analysis. The glycan affinity might not represent the only type of glycan residue these receptors bind, but the ones that are most strongly bound by them……31

Table 2. List of monoclonal antibodies and lectins utilised in flow cytometry and western blot experiments. *The concentration of these lectins used in the western blot experiments is indicated in the correspondent section of the Materials and Methods……44

Table 3. List of used lectins in flow cytometry and western blot experiments. L-PHA recognizes complex β-1,6-branched *N*-glycans. GNA recognizes terminal α-1,3 bound mannose residues, whilst SNA targets terminal α-2,6-linked sialic acid. ConA and DC-SIGN BM share the affinity to highly mannosylated *N*-glycans, but the latter also binds fucose residues (not only α-1,4-linked fucose residues, but also α-1,2 and α-1,3)……45

Table 4. List of probes utilised in RT-qPCR experiments……48

Abbreviations List

ACK	Ammonium Chloride Potassium lysing buffer
APC	Allophycocyanin
APCs	Antigen-Presenting Cells
Asn	Asparagine
BC	Bladder Cancer
BCG	Bacillus Calmette-Guérin
BCR	B-Cell Receptor
βG	Beta-glucan
BSA	Bovine Serum Albumin
CAFs	Cancer Associated Fibroblasts
CD	Cluster of Differentiation
cDNA	Complementary DNA
CHIP	Chromatin Immunoprecipitation
CHIP-seq	CHIP sequencing
ConA	Concanavalin-A
COVID-19	Coronavirus Disease 2019
CRD	Carbohydrate-Recognizing Domain
CTLs	C-Type Lectins
CTLA-4	Cytotoxic T Lymphocyte Associated protein 4
Cy5.5/7	Cyanine 5.5/7
DAMPs	Danger Associated Molecular Patterns
DC	Dendritic Cell
DC-SIGN	Dendritic Cell-Specific Intercellular adhesion molecule-3-Grabbing Non-integrin
DC-SIGN BM	DC-SIGN binding motifs
dGN	diGlcNAc
DMSO	Dimethyl Sulfoxide
DNGR-1	Dendritic cell Natural killer lectin Group receptor 1
dNTPs	Deoxynucleotide Triphosphates
DolP	Dolichol-Phosphate
DTT	Dithiothreitol
ECM	Extracellular Matrix
ELISA	Enzyme-Linked ImmunoSorbent Assay

ER	Endoplasmic Reticulum
FBS	Fetal Bovine Serum
FITC	Fluorescein
FSC-A	Forward Scatter Area
FSC-H	Forward Scatter Height
Fuc	Fucose
FUT3/4/6/7/8	Fucosyltransferase 3/4/6/7/8
FVD	Fixable Viability Dye
Gal	Galactose
GalNAc	*N*-acetylgalactoseamine
GBPs	Glycan-Binding Proteins
GlcNAc	*N*-acetylglucosamine
Glu	Glucose
GluA	Glucuronic Acid
GM-CSF	Granulocyte-Macrophage Colony Stimulating Factor
GNA	*Galanthus Nivalis* Agglutinin
GnT-I to V	*N*-acetylglucosaminyltransferase I to V
GTP	Guanosine Triphosphate
HIF-1α	Hypoxia-Inducible Factor 1 alfa
HIV	Human Immunodeficiency Virus
HPV	Human Papillomavirus
IdoA	Iduronic Acid
IFN	Interferon
Igs	Immunoglobulins
IL	Interleukin
ILCs	Innate Lymphoid Cells
IPO-Porto	*Instituto Português de Oncologia do Porto*
LBB	Lectin Binding Buffer
Le	Lewis antigens
lncRNA	Long Non-Coding RNA
L-PHA	*Phaseolus Vulgaris* leukoagglutinin
LPS	Lipopolysaccharide
Man	Mannose
MAN1A1/1A2/1C1/2A1/2A2	Mannosyl Mannosidase IA/IB/IC/IIA/IIB

Man-LAMs	Mannose-capped Lipoarabinomannans
MBL2	Mannose Binding Lectin 2
MDP	Muramyl Dipeptide
MDSCs	Myeloid-Derived Suppressor Cells
MFI	Median Fluorescence Intensity
MGAT1 to 5	Mannosyl *N*-Acetylglucosaminyltransferase 1 to 5
MGL	Macrophage Galactose-type Lectin
MHC-I/II	Major Histocompatibility Complex Class I or II
MIBC	Muscle Invasive Bladder Cancer
MICL	Myeloid Inhibitory C-type Lectin
Mincle	Macrophage inducible Ca^{2+}- dependent lectin receptor
miRNA	Micro RNA
MPI	Mannosyl-Phosphatidyl-myo-Inositol
MR	Macrophage Mannose Receptor
mTOR	Mammalian Target of Rapamycin
Na_3VO_4	Sodium Orthovanadate
NK	Natural-Killer cells
NMIBC	Non-muscle Invasive Bladder Cancer
NOD-2	Nucleotide-binding Oligomerization Domain containing 2
OSG	Oligosaccharyltransferase
PAMPs	Pathogen-Associated Molecular Patterns
PBS	Phosphate-Buffered Saline
PBST	PBS Tween 0,05%
PBMCs	Peripheral Blood Mononuclear Cells
PD-1	Programmed cell Death 1 receptor
PD-L1/2	Programmed cell Death Ligand 1/2
PE	Phycoerythrin
PenStrep	Penicillin-Streptomycin
PercP	Peridinin-Chlorophyll-protein
PI	Propidium Iodate
PI3K	Phosphoinositide 3-Kinase
PMSF	Phenylmethylsulphonyl Fluoride
PUNLMP	Papillary Urothelial Malignancy of Low Malignant Potential
PRR	Pattern Recognizing Receptor

RPMI 1640	Roswell Park Memorial Institute 1640
RQ	Relative Quantification values
RSV	Respiratory Syncytial Virus
RT-qPCR	Real Time quantitative Polymerase Chain Reaction
SA	Sialic Acid
SD	Standard Deviation
Ser	Serine
Siglecs	Sialic Acid-Binding Immunoglobulin-like Lectins
SNA	*Sambucus Nigra* Agglutinin
SSC-A	Side Scatter Area
ST6GAL1	Sialyltransferase 1
TAGs	Tumour-Associated Glycans
TAMs	Tumour Associated Macrophages
TBST	Tris Buffered Saline with 0,05% Tween
TCR	T-Cell Receptor
TGF-β	Tumour Growth Factor beta
Th	T helper $CD4^+$ cells
Thr	Threonine
TI	Trained Immunity
TIM-3	Mucin-domain containing-3
TLRs	Toll-Like Receptors
TMB	Trimethylbenzene
TME	Tumour Microenvironment
TNF-α	Tumour Necrosis Factor alpha
Tregs	T Regulatory cells
TURBT	Transurethral Resection of the Bladder Tumour
VEGF	Vascular Endothelial Growth Factor
WHO	World Health Organization
Xyl	Xylose

INTRODUCTION

1. Cancer

1.1 Global Overview

Cancer is a pathology best characterized by an unbalance between cell proliferation and cell death mechanisms, culminating in uncontrolled cell growth. The prevalence of this pathology has been consistently rising in the entire world due to generalized socioeconomic development, which is reflected in the rise of the average life expectancy and better treatment for other types of ailments, such as cardiovascular disease[1]. In fact, in 2040, estimates point towards an increase of 47% in the number of diagnosed cancer cases in comparison with 2020 (from 19,3 million to 28,4 million diagnosed cases – **Figure 1**). The burden of cancer is also going to be negatively impacted in the near future by the Coronavirus Disease 2019 (COVID-19) health crisis, as the lockdown imposed by multiple governments at the start of the pandemic combined with the general reluctance of people to go to hospitals due to fear of getting infected severely hampered cancer screening programs, particularly in early-mid 2020[2,3]. Considering this, it is clear that research into more advanced diagnostic methods and therapies is profoundly relevant.

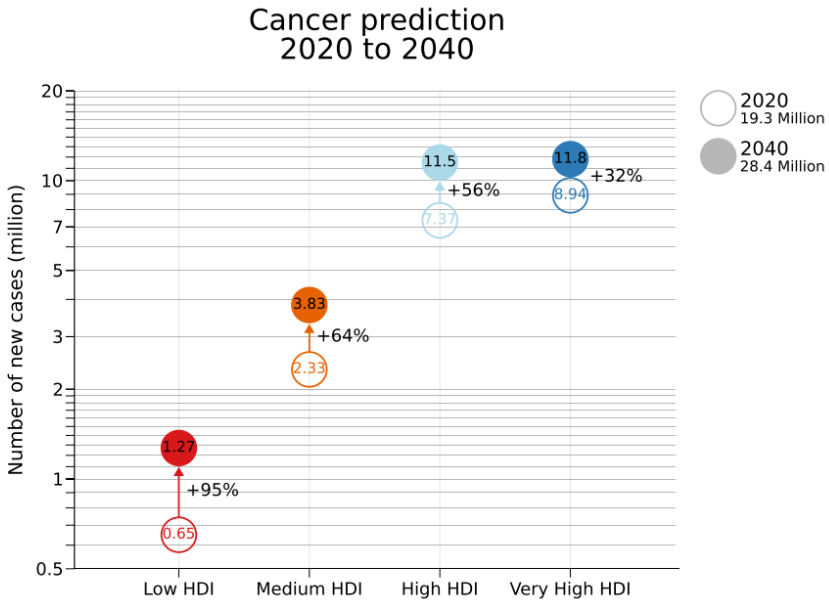

Figure 1. Forecast of total number of newly diagnosed cancer cases in 2040, stratified in accordance with the 4-tier Human Development Index. Sourced from (1).

For cancer to develop, cells need to undergo some considerable functional and genetic alterations, conferring certain traits that allow them to proliferate freely. In

2000, Hanahan and Weinberg[4] described six essential hallmarks that were present in the numerous neoplastic diseases: (i) self-sufficiency in growth signals, (ii) insensitivity to anti-growth signals, (iii) tissue invasion and metastasis, (iv) limitless replicative potential, (v) sustained angiogenesis and (vi) evading apoptosis. Furthermore, the authors also emphasize the importance of viewing tumours as complex tissues, where not only the cancer cells, but all the cell types play a role for in the progression of the disease.

As this realization gained more traction, about a decade later, the hallmarks of cancer were revised in order to cement the perspective that tumours were a lot more than clusters of neoplastic cells. This led to the addition of new emerging hallmarks that accentuated the importance of the "Tumour Microenvironment" (TME): (vii) deregulation of cellular energetics and (viii) avoidance of immune destruction[5]. Moreover, Hanahan and Weinberg described two enabling characteristics that make the acquisition of the various hallmarks possible: (a) genome instability and mutation and (b) tumour-promoting inflammation.

In 2022, another update was published on this matter where, even though the previously described hallmarks were validated, it was clear new ones needed to be proposed to better explain the complexity of the biology of cancer[6]. With that in mind, two more traits were added to the list: (ix) unlocking phenotypic plasticity and (x) senescent cells. Furthermore, another two enabling characteristics were also included: (c) polymorphic microbiomes and (d) non-mutational epigenetic reprogramming. All of the established and newly proposed hallmarks of cancer (**Figure 2**) highlight the intricacy of the biology behind neoplastic transformation and are a great resource for discussion around this topic in the scientific community.

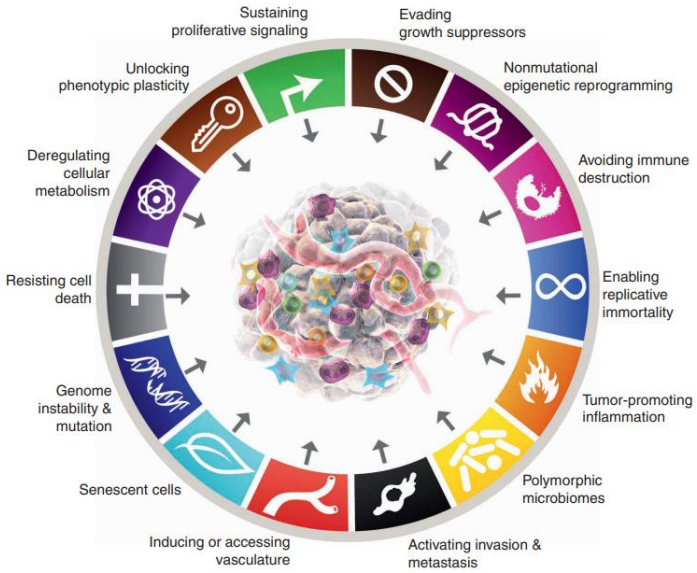

Figure 2. The hallmarks of cancer. Sourced from (6).

1.2 Bladder Cancer

Bladder cancer (BC) is the most common cancer of the urinary track, being the 10th most diagnosed cancer and 13th deadliest worldwide for both sexes (**Figure 3-A**)[1]. However, men are around 3 to 4 times more likely than women to develop this disease, which translates into bladder cancer being the 6th most common and 9th deadliest cancer among men (**Figure 3-B and C**) [1,7]. BC is a disease associated with developed countries, with North America and Europe being the regions where it is the most prevalent (**Figure 4-A**). Some parts of Northern Africa (mainly Egypt) and Western Asia also present high incidence[7]. In addition, BC mainly affects populations over the age of 55 years-old (about 90% of cases) and is more prevalent in Caucasians, even though Black patients tend to be diagnosed in later stages of the disease[8]. Mortality is highest in Eastern and Southern Europe, Northern Africa and certain regions of the Middle East (**Figure 4-B**).

The biggest risk factor for BC is unquestionably cigarette smoking, with some reports estimating it might be responsible for half of the diagnosed cases[7,9]. This could partially explain the higher prevalence of the disease in developed countries and in males, as it is a habit more commonly undertaken by these populations. Other risk factors consist of a poor/westernized diet (low in fruits and vegetables, frequent consumption of processed and red meats), sedentary lifestyle, occupational hazards leading to exposure to carcinogenic molecules, namely aromatic amines, among

others[7,9–11]. Of note, certain pathogens have also been linked with a higher predisposition to BC, such as *Schistosoma haematobium*, which is endemic to Northern Africa and accounts for a large percentage of the diagnosed cases in countries like Egypt[9,11].

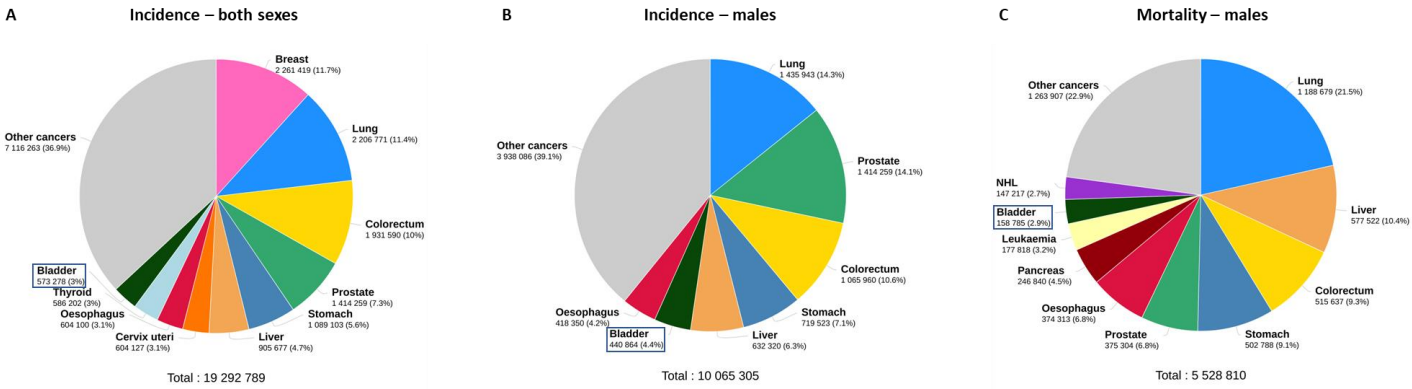

Figure 3. Pie-charts illustrating cancer incidence rates in 2020 for both sexes (A), for males (B) and mortality rates in males (C). Bladder cancer is represented in dark green. Adapted from https://gco.iarc.fr/today/home.

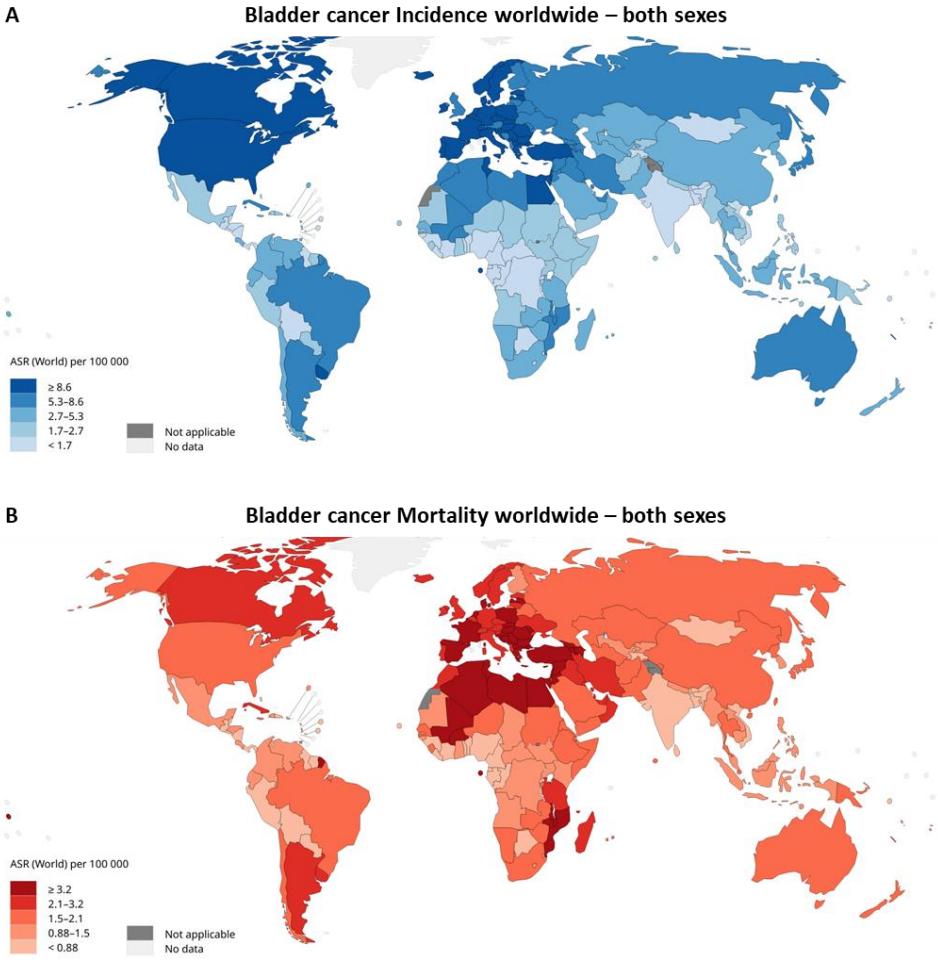

Figure 4. Worldwide incidence (A) and mortality (B) rates for bladder cancer normalized per 100 000 inhabitants, for both sexes and all ages in 2020. Adapted from https://gco.iarc.fr/today/home.

The vast majority of the diagnosed BC cases are transitional cell carcinomas (around 90%), but in regions endemic to Schistosomiasis there is a relevant number of squamous cell carcinomas[7,8,12]. There are two main types of BC: non-muscle invasive BC (NMIBC), that represent around 70-80%[7,10] of cases, and muscle invasive BC (MIBC). NMIBC comprises stages pTis to pT1 in the cascade (**Figure 5**) and is characterized by localized disease, usually limited to hyperplastic lesions in the urothelial layer (pTa) or the lamina propria (pT1). Of note, *carcinoma in situ*, particularly when associated with other stages of BC, has been shown to indicate a worse prognosis[7,13]. Many molecular alterations have been described for NMIBC, with the most common being a mutation in the *FGFR3* gene, leading to the activation of the RAS-MAPK pathway[7,14]. When the muscle layer (MIBC) of the bladder is invaded, the tumour is classified as pT2a or pT2b, depending on the depth achieved. The pT3 stage is defined as the invasion of the perivesical fat layer, whereas pT4 describes the spread of the tumour to other organs in the abdominal cavity[7,13]. Some of the key genes mutated in the context of the more aggressive and invasive BCs are *TP53* and *Rb1*[7,14]. For histological grading, the World Health Organization (WHO) published the original three-tier system of grade 1, 2 and 3 in 1973, where the higher grade represented more invasive phenotypes (**Figure 5**). In 2004, this was updated to only feature low-tier or high-tier tumours, where the latter group encompasses grade 2 and 3 neoplasms (**Figure 5**). WHO also added the notion of papillary urothelial malignancy of low malignant potential (PUNLMP) that describes a non-cancerous lesion that consists of the thickening of the urothelial layer with very low risk of progression[7,15].

The most common symptom for BC is either macroscopic or microscopic haematuria, commonly known as blood in the urine. Other frequent complaints are increased urination frequency, dysuria (burning or pain sensation during urination), nocturia (urge to urinate during the night) and, in rarer cases, difficulty micturating due to partial obstruction of the urethra by the tumour[8,16].

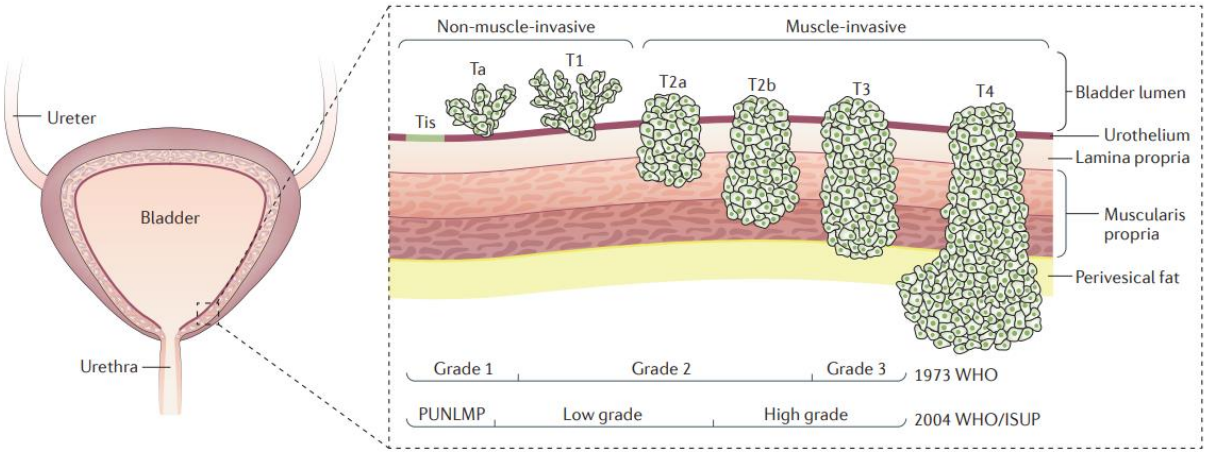

Figure 5. Different stages and histological classifications of bladder cancer. Sourced from (7).

After haematuria and other initial symptoms, patients need to perform more tests before a BC diagnosis is given, including cystoscopy, urine cytology, renal function assessment and, when necessary, upper urinary tract imaging (computerized tomography is preferred)[8,17].

When abnormal findings are reported, the first step is usually transurethral resection of the bladder tumour (TURBT), that will provide further pathological information. If the patients present non-muscle invasive disease, the procedure is followed by a chemotherapy instillation in suspected low-grade tumours or BCG instillation in intermediate or high-risk scenarios[8,10,18]. For the latter population, the risk of recurrence is quite high, and BCG immunotherapy has been shown to be an important tool in improving recurrence free-survival[19], and instillations regimes (1 or 3 years for BCG responders, depending on the risk assessment of the tumour) with this pathogen have proven to be efficient tools in the arsenal of clinicians. Unfortunately, as with any gold-standard treatment, some side effects are to be expected. Locally, up to 75% of patients treated with BCG experience local adverse reactions, such as cystitis, haematuria and increased urination frequency. Systemic side effects can be seen in over a quarter of patients, and include fever, tiredness and flu-like symptoms. In rare occasions, BCG can induce a disseminated infection, which requires a long antibiotic treatment regimen. These adverse manifestations are a serious barrier to this therapy, as studies report up to 16% of patients need to temporarily or permanently halt treatment due to such reactions[20–22]. In the case of BCG failure, for high-risk NMIBC patients, repeat resection might be recommended

and, in more extreme scenarios, partial or total cystectomy can be required. Other alternative treatments, like immune-checkpoint inhibitor therapy (for example, pembrolizumab, an antibody that targets the receptor Programmed cell Death 1 - PD-1) are also options[8,10,18]. With all of this in mind, further investigations are required to improve the quality of life and treatment options for high-risk NMIBC patients that are unresponsive to BCG instillations or that develop adverse effects.

As for MIBC disease, briefly, more severe intervention is required. When diagnosed in a non-metastatic stage, cisplatin chemotherapy followed by radical cystectomy is the first line treatment. If the tumour already presents metastasis, the prognosis becomes much more reserved (5% and 36% 5-year survival rate for distant and regional metastasis respectively), with a regimen of combined chemotherapy agents being the standard of care. In case of failure or if the tumour presents PD-L1 expression, immune checkpoint inhibitors are recommended[8,10,23].

2. Glycosylation

2.1 Protein glycosylation

Glycosylation is a modification that consists of the enzymatic addition of carbohydrates (or glycans) to other macromolecular structures, namely lipids, proteins or even other saccharides[24,25]. There is a huge variety of possible glycan conjugates that form the glycome and these structures are frequently exposed at the cell surface, forming a layer known as the glycocalyx. This sugar coat is crucial to many cellular processes[26], including molecular trafficking, cell-to-cell adhesion, self and non-self-self-recognition, receptor activation, among others, which elucidates the prevalent role that glycosylation can have in the balance between homeostasis and disease.

Setting our sights on protein glycosylation in mammals, there are ten monosaccharide building blocks from which the estimated over 7000 glycan structures are assembled from: Fucose (Fuc), Galactose (Gal), Glucose (Glu), Mannose (Man), Syalic Acid (SA), Xylose (Xyl), *N*-acetylgalactoseamine (GalNAc), *N*-acetylglucoseamine (GlcNAc), Glucuronic Acid (GlcA) and Iduronic Acid (IdoA)[27]. The main substrates are glucose and fructose, from which the various other sugars can be formed. Before they can be used in glycan synthesis, the monosaccharides need to be

phosphorylated and paired with a nucleoside triphosphate, such as Guanosine Triphosphate (GTP)[28]. The addition of these post-translational modifications requires the action of two different main enzyme groups: glycosyltransferases, which are responsible for creating the glycan chains, and glycosidases, that facilitate the catalysation of glycan linkages[26,29]. This process takes place in two particular organelles where the various enzymes are housed: the Endoplasmic Reticulum (ER) and the Golgi apparatus[30]. Their activity is highly regulated by substrate availability, gene transcription levels and enzyme localization inside the organelles that harbour them[29].

Glycoconjugates are mainly classified according to their non-glycan component, leading to the formation of glycosphingolipids if the carbohydrates are added to a lipid backbone or glycoproteins and proteoglycans when covalently attached to a polypeptide structure[24,27] (**Figure 6**). Narrowing the scope to protein glycosylation, the most frequent types are *N*-glycosylation, in which the glycans are attached via the nitrogen atom of asparagine (Asn) residues, and *O*-glycosylation, where the connection occurs through the oxygen atom of serine (Ser) or threonine (Thr) residues (**Figure 6**)[24,26,31].

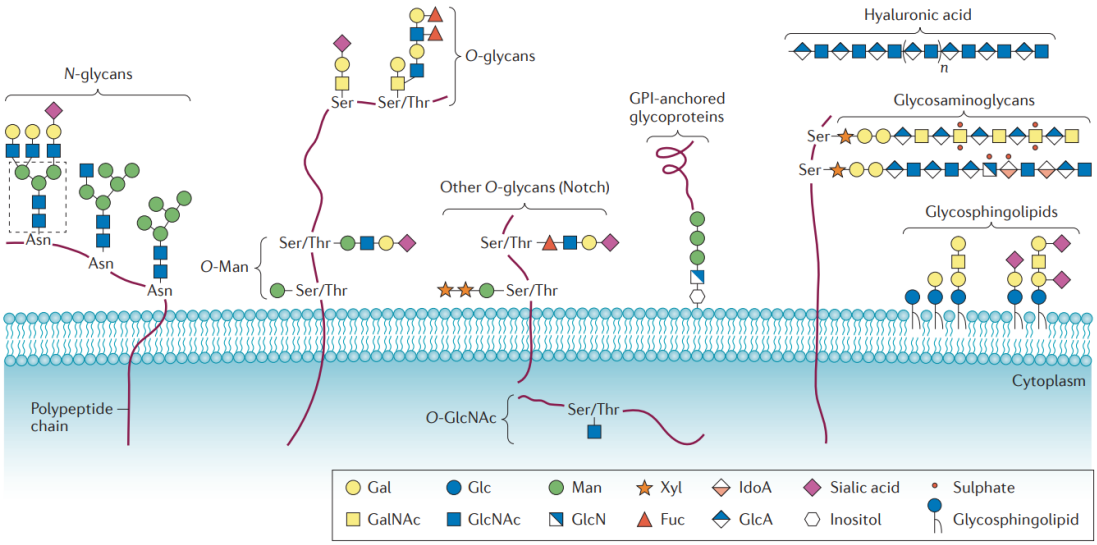

Figure 6. Main classes of glycoconjugates found in mammals. Glycans can be linked to lipids, originating glycosphingolipids. Glycoproteins can be connected to a glycosylphosphatidylinositol (GPI) anchor on the plasma membrane, to the nitrogen atom of an Asn residue (*N*-glycans) or to the oxygen atom of a Ser or Thr (*O*-glycans). Glycosaminoglycans are linear polymers frequently found associated with proteoglycans or, in the case of hyaluronic acid, freely roaming in the extracellular matrix. Sourced from (24).

2.2 *N*-glycosylation

N-glycosylation will be the main focus of this thesis, which prompts an in depth look at the biosynthesis of these glycans, that can be divided in three different classes: high-mannose, hybrid and complex glycans[24,29,32]. The pathway (**Figure 7**) starts in the ER, where a lipid carrier named dolichol-phosphate (DolP) is used as an anchor. Initially, a hepta-saccharide is built on the cytoplasmatic side of the ER through the glycosyltransferase mediated addition of two GlcNAc and 5 Man residues to DolP. This structure is then flipped to the lumen side of the organelle, where DolP-Man and DolP-Glc are used as substrate donors to form a $Glc_3Man_9GlcNAc_2$ lipid-linked oligosaccharide[32–34].

This structure then is transferred *en bloc* with the help of the oligosaccharyltransferase (OST) to the Asn-X-Ser/Thr region of a nascent protein[32]. Further processing steps occur in the ER, leading to the trimming of three Glc and one Man residue, yielding a $Man_8GlcNAc_2$ saccharide that is transported to the Golgi apparatus. In the cis region of this organelle, α-1,2 mannosidases IA, IB and IC (encoded by the genes *MAN1A1*, *MAN1A2* and *MAN1C1*), which are enzymes that remove mannose residues, further refine this structure, originating the important intermediary $Man_5GlcNAc_2$, crucial for the synthesis of hybrid and complex glycans (high-mannose saccharides can also be incorporated into proteins without further processing)[32,35].

In the medial-Golgi, the *N*-acetylglucosaminyltransferase I (GnT-I, encoded by the *MGAT1* gene) initiates the biosynthesis of hybrid glycans, catalysing the addition of a GlcNAc residue to the available α-1,3 core mannan in the $Man_5GlcNAc_2$ saccharide. Two further mannose residues can be trimmed by α-mannosidase IIA or IIB (encoded by the genes *MAN2A1* and *MAN2A2*), which is followed by the addition of a second GlcNAc by GnT-II (encoded by the *MGAT2* gene) to the α-1,6 arm, paving the path for the formation of complex glycans. Additionally, the $GlcNAcMan_3GlcNAc_2$ glycan can be processed by other glycosyltransferases, such as GnT-IV and GnT-V (encoded by the *MGAT4* and *MGAT5* genes, respectively), incorporating more branching and yielding tri and tetra-antennary glycans. Furthermore, GnT-III (encoded

by the *MGAT3* gene) can add a bisecting GlcNAc residue to the mannan core, but it is usually not extended[32,35].

Hybrid and complex glycans can be decorated with a variety of structures to further mature them. The most important alteration to the core of glycans is the addition of a fucose residue catalysed by α-1,6 fucosyltransferase (encoded by *FUT8*), and it requires previous GnT-I activity. The various branches presented by these glycans can be extended, usually through the addition of galactose residues to the available GlcNAc building blocks, forming a sequence known as LacNAc. This disaccharide can be repeated, forming poly-LacNAc tandem repeats. In some cases, instead of Gal, GalNAc can be added to GlcNAc, producing LacdiNAc. Lastly, hybrid and complex glycans can be capped with various sugars, including SA, Fuc, Gal and GlcNAc. These terminations tend to protrude away from the rest of the glycan structure, facilitating their recognition[32,35].

Wrapping up this section, a large variety of structures can be found in the cellular glycome, with this diversity resulting from the competition between the various enzymes present in the described pathway[27].

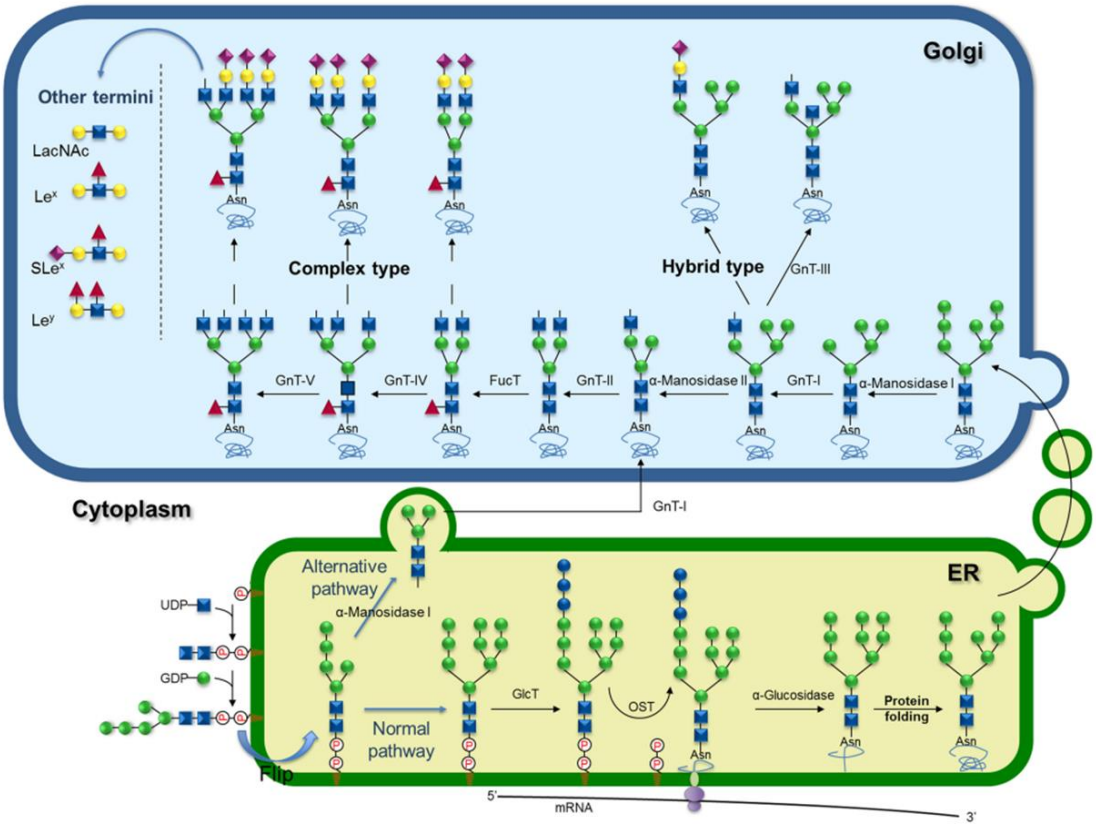

Figure 7. *N*-glycan biosynthesis schematic. This process starts in the ER, where dolichol-phosphate acts as a carrier for the assembly of the lipid-linked oligosaccharide (LLO). The LLO is transferred to an

asparagine residue of a nascent protein and is further processed in the ER. Then, it is transported to the Golgi apparatus, where an assortment of mannosidases, glycotransferases and other enzymes further process and mature the glycan, leading to the diverse cellular glycome. Adapted from (35).

2.3 Glycan alterations as a key feature of malignant transformation

Given the crucial function of glycans in several cellular processes, their impact in the transition from healthy to a malignant cancerous phenotype isn't unforeseen. In fact, in an effort to highlight the importance of aberrant glycan expression in malignant transformation, Munkley and Elliot[36] established an association between the previously mentioned cancer hallmarks and carbohydrate alterations in the context of cancer.

Tumour-associated glycans (TAGs) derive either from an incomplete or *de novo* synthesis process[24,37]. The first is a consequence of the disruption of the normal complex glycan production pathways, originating truncated structures and being more prevalent in earlier stages of cancer. Neo-synthesis is commonly associated with further advanced stages of this disease and derives from an increased expression of certain glycogenes. Of note, these alterations aren't random events, but rather another mechanism that allows tumour cells to select the fittest clones for survival in the environment they are in[38].

Typical modifications found in TAGs (**Figure 8**) are *O*-glycan truncation, *N*-linked branching, sialylation and fucosylation[24,38–42]. These confer several advantages to cancer cells. For example, increased sialyation is present in many malignancies and has been associated to a poor prognosis in colon cancer[24], facilitates immune evasion and reduces cell to extracellular matrix (ECM) adhesion[40]. Furthermore, upregulation of certain sialyltransferases, such as α-2,6-sialyltransferase 1 (encoded by the *ST6GAL1* gene), has been linked to a higher metastatic potential in various cancer models[43].

Different types of fucosylation are associated with contrasting outcomes in relation to the pathological effect of cancer. Higher α-1,2-fucosylation is linked to a tumour suppressive effect in melanoma and gastric cancers but has a harmful effect in bladder and prostate malignancies[41]. Other types of fucosylation, such as α-1,3 or α-1,4-fucosylation, appear to have a more consistent role in cancer and are mainly

mediated by fucosyltransferases 3, 4, 6 and 7 (encoded by *FUT3/4/6/7* genes). For instance, fucosyltransferase 4 inhibition has been shown to restrict tumour invasiveness in breast and colorectal cancer models[44,45].

O-glycan truncation is also commonly found in TAGs. This type of glycans consist of the monosaccharide GalNAc (known as Tn antigen) or GalNAc connected to a galactose residue (known as "core 1" or T antigen) and their sialylated forms (ST and STn)[24]. Their expression has been linked to a more proliferative and invasive phenotype in various malignancies, including pancreatic cancer[46] and gastric cancer[47].

Furthermore, branched glycans are a key alteration found in tumour glycosylation and it is mainly mediated by the GnT-V enzyme. Increased branching has been correlated with loss of contact inhibition, higher cell motility and increased invasion and metastasis[24]. Previous work from our group has demonstrated that *MGAT5* gene is overexpressed patient's samples from colon adenocarcinoma and branched *N*-glycans are increased when compared to healthy tissue[48]. Additionally, using an *MGAT5* knock-out mouse model, it was shown that the ablation of branched *N*-glycans supressed tumoral growth. Additionally, N-glycans can be further modified by the GnT-III enzyme, originating bisecting glycans. Unlike GnT-V, this enzyme has been associated to a potential tumour suppressive role, for example, through the mitigation of metastasis by increasing the stability of E-cadherin at the cell surface in gastric cancer[49]. However, this effect might be tissue specific, as overexpression of GnT-III in ovarian cancer was linked to a considerable decrease in patient survival[50].

Carbohydrate alterations can vary between different models. Centering the spotlight on bladder cancer, the most relevant glycan modifications consist of an increase in GnT-III levels (and, consequently, in bisecting *N*-glycans), diminished GnT-V activity and higher short *O*-glycan expression (STn, T and ST antigens), with all correlating with a worse prognosis, higher disease stage and grade and shorter disease-free survival[51,52]. Moreover, late-stage bladder malignancies display a loss of ABO(H) blood group expression[51–53], a phenomenon accompanied by an increase in structurally similar Lewis antigens[51,52]. High-mannose *N*-glycans have also been described as upregulated in bladder cancer cell lines and patient samples[54].

Overall, it is clear that glycans have a clear role in the development of several cancer types. Therefore, there is growing attention being placed in carbohydrates, which will hopefully lead to their potential as therapeutic targets to be fully explored.

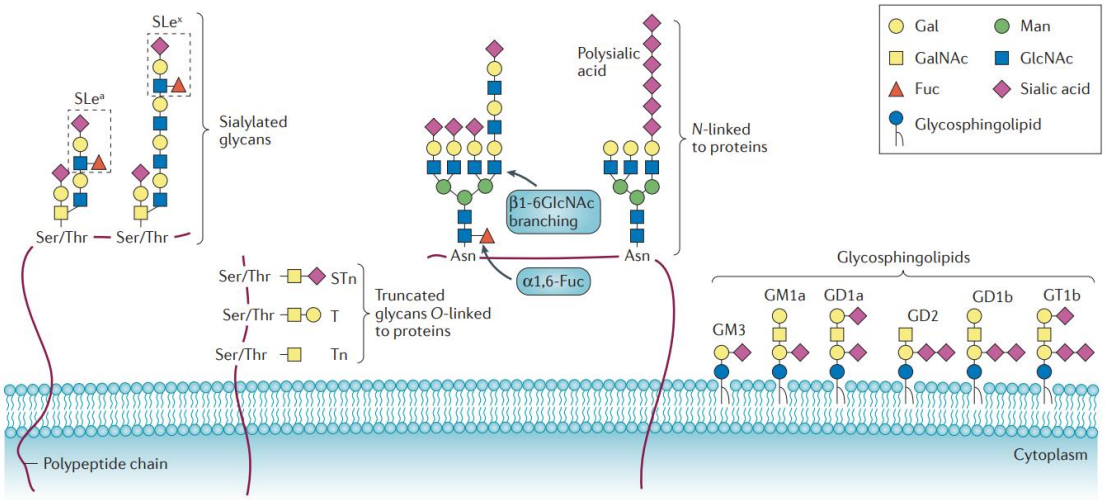

Figure 8. Relevant glycans found in the context of cancer. Sialylation is one of the most prevalent alterations identified in tumours, being associated with both *N*- and *O*-linked branched glycans, truncated *O*-glycans and other structures, namely Lewis (Le) antigens. Other non-protein elements, such as glycosphingolipids, can also be sialylated. Other noteworthy events are an increase in core fucosylation and increase in β-1,6-GlcNAc branching mediated by GnT-V. Sourced from (24).

3. The immune system

3.1 The principles of immunity

The immune system consists of an extensive family of cells and molecules that defend our organism against a plethora of challenges, from infectious pathogens to rogue cells from the host that could originate cancers. Furthermore, an essential feature of this system is the ability to distinguish between "self" and "non-self", as the disruption of this discrimination leads to autoimmune disorders.

Diving deeper, the immune system has two main branches: innate and adaptive immunity. Innate immunity consists of the first line of defences against immune challenge and the response is quickly mounted and not target-specific. On a more primary level, innate host defence begins with the physical and chemical barriers, exemplified by tight junctions in the skin, mucus excretion in certain membranes, certain molecules/enzymes with protective capacities present in secretions, among others[55–58].

When these blockades are not sufficient, the innate immune system is armed with a vast array of cells. A major group of these are the myeloid cells, with the main constituents being neutrophils, monocytes, macrophages and dendritic cells (DCs)[59].

Neutrophils are polymorphonuclear granulocytic cells that are produced in abundant fashion in steady-state and inflammatory settings. They are very short-lived and can exert their function either via phagocytosis or through the production of several molecules with immune-regulating properties[59,60]. In cancer, neutrophils have a somewhat controversial role, as their reduced life span raises some doubts about these cell's ability to influence tumour biology. However, more recently, this view has started to shift and neutrophils have been linked to both pro and anti-tumoral effects, being susceptible to polarization depending on the factors present in the TME[60,61].

Monocytes are mononuclear phagocytic cells that represent around 10% of the leukocytes in circulation[62]. These cells possess the ability to differentiate into macrophages and dendritic cells and are highly heterogeneous[62–64]. The large majority of monocytes presents high Cluster of Differentiation (CD) 14 expression, being labelled "Classical" or "Inflammatory" monocytes ($CD14^{++}$, $CD16^{-}$)[62–64]. Other subsets express CD16, with "Intermediate" monocytes maintaining relatively high CD14 levels ($CD14^{+}$, $CD16^{+}$) and "Resident" or "Non-classical" monocytes considerably restricting CD14 expression ($CD14^{low}$, $CD16^{++}$)[62–64]. All monocytes share functional similarities, but the "Classical" subset is typically recruited in reaction to injury or inflammatory signals, contributing to the immune response through threat recognition and elimination, resorting to cytokine secretion and phagocytosis[64]. The "Intermediate" cells also participate in the pro-inflammatory response, using similar defence mechanisms[64]. However, these monocytes also participate in wound healing. Finally, "Resident" monocytes patrol the endothelium as innate surveyors[64].

As mentioned before, **macrophages** originate from circulating blood monocytes (or from embryonic progenitors[65]) and, similarly to their parent cells, have crucial roles in inflammatory responses and in the maintenance of tissues homeostasis[66,67]. In fact, these cells display an immense phenotypical diversity. Once again, phagocytosis is an essential part of their effector functions, but macrophages are potent immunomodulators that can secrete a large array of cytokines, including Interleukin (IL)-1β, IL-6, Tumour Necrosis Factor alpha (TNF-α), Interferon (IFN)-α and

β, IL-10, IL-12, among others[67]. As previously described for neutrophils, macrophages are also susceptible to polarization depending on the factors present in the environment, forming a spectrum where the two extremes are represented by the M1 or "classically activated" phenotype and the M2 or "alternatively activated" phenotype[68,69]. M1 cells are pro-inflammatory and mediate pathogen resistant/microbiocidal responses that can lead to tissue destruction. They secrete several cytokines, such as IL-1β and TNF-α and present high levels of major histocompatibility complex class II (MHC-II) and costimulatory molecules (CD80 and 86) on their surface[68,69]. M2 macrophages are typically associated to a more anti-inflammatory phenotype, displaying high IL-10 excretion. They play a pivotal role in allergic and parasite responses, tissue remodelling and angiogenesis. Conventional markers are CD163, CD206 (also known as the Macrophage Mannose Receptor or MR) and Arginase-1[68,69]. Another relevant subset of macrophages is the Tumour Associated Macrophages (TAMs). These cells represent a major population in the TME (up to 50% of cells) and secrete high levels of IL-10 and Tumour Growth Factor beta (TGF-β), inhibiting other immune populations and further contributing to tumour growth[68,70]. Furthermore, TAMs can promote metastatic disease[71,72].

Dendritic cells are essential for an adequate immune response as they are the mediators between innate and adaptative immunity. This stems from their function as professional antigen-presenting cells (APCs): when DCs sense danger, they ingest and process antigens, making them readily available through MHC molecules on the cell surface. Then, they migrate to nearby lymphatic organs, where T cells get exposed to the antigen, triggering their differentiation and a powerful immune response[59,73].

The other major group of innate immune cells has a lymphoid origin. However, these lack the expression of the antigen receptors generated by the combination of several genetic elements typical of their adaptative lymphoid counterparts. The major cells of this group are the **Innate Lymphoid Cells (ILCs) 1, 2 and 3** and the **Natural Killer (NK) cells**[74].

NK cells are a heavily cytotoxic subset that express high levels of perforin and circulate in the blood stream, playing a key role in anti-viral and tumoral immunity. They eliminate cells that demonstrate signs of stress or that display no MHC class I expression on their surface[74,75].

Different ILC subsets present distinct transcription factor requirements for their development and favour the expression of different cytokines. ILC1s have some common traits with NKs, producing high levels of IFN-γ and require T-bet to exert their function. However, they are weakly cytotoxic and are tissue-resident cells. ILC2s are important for the anti-parasite response and typically produce type 2 cytokines, namely IL-4, IL-5 and IL-13. They play a significant role in tissue repair and their development is GATA3 dependant. Finally, ILC3s are a heterogeneous population that is relevant to extracellular bacteria immunity and intestinal commensal regulation. RORγt is the central transcription factor and they secrete high amounts of IL-17, IL-22 and Granulocyte-Macrophage Colony Stimulating Factor (GM-CSF). Interestingly, the various subsets demonstrate an interesting parallel to their T helper (Th) counterparts[74,76].

The immune system has another arm: adaptive immunity. The response triggered by this branch is very specific and takes a longer time to mount, relying primarily on the antigen-receptors expressed by **T and B lymphocytes**. These receptors are assembled after the recombination of several genes, which allows these cells to target a vast repertoire of threats. Importantly, the adaptive response has the pivotal capacity to create immune memory[77].

Focusing T cell subsets, the vast majority express the αβ T-cell receptor (TCR) and can be further stratified in to CD4 or CD8 positive. The first group is often labelled as "helper", being crucial for the mounting and suppression of the immune response[77]. $CD4^+$ T cells can present distinct phenotypes, which allows them to be further stratified into Th1, Th2 and Th17 subsets, carrying out diverse functions and producing distinct soluble factors[78]. Another relevant group of CD4+ T cells are the T regulatory (Tregs), potent immunosuppressors that are crucial for homeostasis, but also play a major role in cancer[78,79]. $CD8^+$ T cells are the intrinsically cytotoxic elements, being important in antimicrobial and tumour immunity[77,80]. They exert their activity through the release of granules containing granzymes, perforin and other molecules (for example, cytokines, such as INF-γ) or via certain receptors that induce the death of the target cell[80]. Some T cells commit to a different lineage, expressing the γδ TCR. However, γδ T cells can recognize targets in an MHC independent way and

respond quicker than their αβ analogues, as certain subsets do not require clonal expansion[81].

Finally, B cells are responsible for humoral immunity, that is, when the B-cell receptor (BCR) binds its ligand, these cells begin a differentiation program that culminates in the production of antibodies or immunoglobulins (Igs). B cells also possess the ability to modulate the immune environment through cytokine secretion[82].

3.2. Immune evasion in cancer and the role of glycans

For tumours to successfully grow, they must develop strategies that allow them to dodge the hosts' immune system. Indeed, the concept of cancer immunosurveillance was proposed as early as 1909 and it states that the various immune cells contribute to the elimination and control of cancer[83]. Later, this idea was perfected, with the suggestion that tumour cells expressed neo-antigens that have the ability to instigate an immune reaction. Nonetheless, this is a one-dimensional view of the widely accepted cancer immunoediting hypothesis. This notion states that the development of neoplastic disease has three stages (3 E's of cancer immunoediting – **Figure 9**)[83–85]. Initially, the elimination phase of tumour cells is achieved via immunosurveillance. However, this eradication generates a selective pressure, culminating in the survival of the more genetically unstable fittest clones that bear the capability of co-existing with the hosts' immune system, creating an equilibrium stage. The sculpting of the tumour eventually climaxes in the last stage of cancer development, the escape phase, where there is uncontrolled division of the more apt variants, as the immune system is unable to detect and control their spread[83–85].

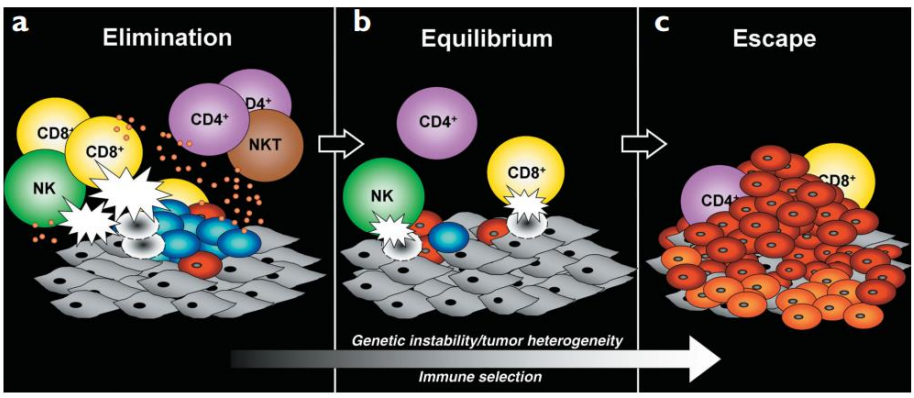

Figure 9. The three E's of cancer immunoediting. (a) Elimination is the process where the immune system identifies the tumour cells and effectively destroys them. (b) However, this allows for the

selection of the fittest clones that are able to survive the attacks by the immune cells, establishing an equilibrium. (c) Eventually, these selected variants become very competent at escaping the immune surveillance, culminating in their uncontrolled replication. Sourced from (84).

The neoplastic cells have a deep roster of mechanisms that allow them to achieve immune evasion. T lymphocytes, particularly $CD8^+$ cells, are elemental players in the immune response that seeks to limit cancer growth. However, tumour cells can supress the machinery responsible for antigen presentation, effectively corrupting the MHC class I pathway and impeding $CD8^+$ mediated cytotoxicity[86]. Furthermore, certain immune populations express, among other similar receptors, PD-1 and Cytotoxic T Lymphocyte Associated protein 4 (CTLA-4) that, when bound to their ligands (PD 1 Ligand 1/2 – PD-L1/2 – and CD80/86, respectively), compromise their activity[86–88]. PD-1 activation translates into diminished activation, proliferation, cytokine secretion and T cell survival, whilst CTLA-4 is a homologue of CD28 (a key player in the APC mediated activation of T cells) that blocks the binding of CD80 and CD86 co-stimulatory molecules.

Another important tool in the arsenal of tumours is the creation of an immunosuppressive microenvironment. The release of pro-tumoral soluble factors by neoplastic cells facilitates this phenomenon, calling on other populations that amplify it, such as cancer associated fibroblasts (CAFs), Myeloid-Derived Suppressor Cells (MDSCs), Tregs[89] and TAMs[68–70,72]. Those factors can be cytokines, for example TGF-β and IL-10, that hinder the pro-inflammatory immune response or other growth promoting molecules, namely Vascular Endothelial Growth Factor (VEGF), a potent angiogenic factor[86,90].

Besides all of this, tumour cells also change their glycan expression considerably, as was explored in section 2.2, and these alterations impact more than the biological behaviour of tumour cells, as it also manipulates the interaction with various elements of the immune system, contributing to the shaping of the TME. Surface glycosylation can be recognized through Glycan-Binding Proteins (GBPs) or lectins, that have a high specificity for particular sugars dictated by the Carbohydrate-Recognizing Domain (CRD) they carry[91]. GBPs can be further subdivided based on the CRDs they express, with some of the most relevant families being Galectins, Sialic Acid-Binding Immunoglobulin-like Lectins (Siglecs) and C-type lectins (CTLs)[92–94].

Galectins are soluble proteins with immunomodulatory properties that recognize galactose-containing motifs, such as N-acetyllactosamine (Galβ-1,3-GlcNAc or Galβ-1,4-GlcNAc), and can exert their activity either intra or extracellularly. They can display one or two CRDs, being categorized as proto-type or tandem repeat galectins, respectively[92]. Galectin-3 is considered a chimera-type, as it exhibits a single CRD and a terminal polypeptide tail that can oligomerise[95]. These GBPs have important roles in several biological processes, intervening in signalling pathways, cell-to-ECM binding, mRNA splicing, apoptosis and tissue regeneration to name a few[95,96]. In addition, galectins have garnered some attention regarding a potential role in cancer development. Indeed, the majority of studies state that galectins are overexpressed in neoplastic samples when compared to healthy tissue[96]. Galectin-1 has been linked to an immunosuppressive role, as it is capable of inducing T-cell apoptosis[97] and favouring the proliferation of T regulatory cells and tolerogenic DCs[98]. This immunosuppressive demeanour is shared by other members of this lectin family, for example, Galectin-9 interacts with T cell immunoglobulin and mucin-domain containing-3 (TIM-3), with similar consequences for anti-tumoral T cell activity to the previously enumerated for Galectin-1[99].

Siglecs are also relevant players in the establishment of tumoral tolerance. As the name implies, they mainly recognize sialic acid residues and they have at least one immunoglobulin-like fold in their structure. The majority of these receptors contain motifs that allow them to directly intervene in cellular signalling[94,100]. Siglecs are expressed by most immune populations and the abundance of sialylation found in many tumours directly affects the immune response. In fact, Siglec-7 and 9 present a relevant immunosuppressive role in cancer, as they contribute to the inhibition of NK cell activity and can polarize macrophage populations towards a tumour-benefiting phenotype[101,102].

Lastly, **C-type lectins** are a large family of mostly calcium-dependant GBPs that includes, among others, collectins, selectins, endocytic receptors and proteoglycans. They often form oligomers and play an important role in innate immunity, with many of them being Pattern Recognizing Receptors (PRRs)[93,102]. These receptors display a large array of binding motifs and, therefore, can recognize a panoply of carbohydrates, namely mannose, GlcNAc, Fuc and glucose through the EPN (Glutamic acid – Proline

– Asparagine) domain and galactose and GalNAc using the QPD motif (Glutamine – Proline – Aspartic acid)[103]. Some examples of CTLs containing the EPN sequence are the Dendritic Cell-Specific Intercellular adhesion molecule-3-Grabbing Non-integrin (DC-SIGN/CD209) and the Mannose Receptor (MR/CD206)[104]. DC-SIGN has been linked to an immunosuppressive role in cancer, as its binding to fucose-rich Lewis antigens in a colorectal cancer model supressed DC response[105]. However, previous work from our group has demonstrated that DC-SIGN and MR were able to improve DC function through the recognition of high-mannose epitopes[48], which suggests that this receptor can have polarizing roles depending on the carbohydrate domains it binds. Dectin-2 is another CTL that harbours the EPN domain and has also been associated with a role in cancer suppression. Indeed, Kupffer cells (liver resident macrophages) expression Dectin-2 have been connected to a metastasis supressing role in mouse models of several cancers[106]. Shifting the focus to CTLs that favour galactose recognition, Macrophage Galactose-type Lectin (MGL/CD301) is one of the most well-known receptors and it has also been linked to a potential dual role in neoplastic disease. On the one hand, the co-expression of this lectin and Tn antigens correlated with more aggressive tumoral phenotypes and recruitment of immunosuppressive macrophages[107,108]. Looking at the flipside, MGL can uptake antigens and present them via MHC, priming a strong adaptative immune response, which highlights the potential of targeting this CTL using specific antigens that mimic tumour associated glycans[109,110]. Another important C-type lectin is Dectin-1, that will be further explored in the next chapter, and it plays an important role in fungal immunity by recognizing fungal β-glucans[103]. However, this receptor has been shown to also bind endogenous molecules in different scenarios, including neoplastic disease, where it can trigger a pro-tumoral response after binding galectin-9[111] or pilot a DC + macrophage/NK axis to eliminate cancer cells[112].

4. Trained Immunity

4.1 Standing up to the dogma: innate cell "memory"

As was described in the preceding sections, the immune system has been traditionally subdivided into two groups, the innate response, labelled as quick and unspecific, and the adaptative arm, delayed, but powerful and targeted. However, evidence has been mounting throughout the years that points to this view being too simplistic. Indeed, several PRRs modulate their response depending on the Pathogen-Associated Molecular Pattern (PAMP) that is recognized, which is a demonstration that the innate immune system can have a more specific response that also has the capacity to modulate adaptative immunity[113,114]. Furthermore, early studies in mice showed that certain immune challenges, including BCG and *Candida albicans*, could lead to unspecific protection against other pathogens[115], even in athymic animals (that, therefore, lacked a T-cell response)[116].

In 2011, Mihai Netea *et al.* compiled a large body of articles in this research field, coining the term "Trained Immunity" (TI) to refer to this phenomenon[117]. More specifically, TI is compared to an innate immune memory, confronting the previous notion that only the adaptative faction of the immune system was capable of such achievements. Unlike traditional memory, trained immunity relies on epigenetic reprogramming mechanisms upon the clash with a given stimuli[118]. Indeed, "trained" cells display the removal of typically repressing chromatin markers and the addition of promoting ones in several immune genes, modulating their activity[118,119]. After the return to a steady-state, a secondary encounter with the same or even a different challenge allows the primed innate cells to better respond, commanding a more powerful secondary reaction. This phenotypical switch can also induce a more tolerant state, where the reprogrammed response leads to the suppression of immune activity[118]. A prominent example of this is Lipopolysaccharide (LPS) induced tolerance in cells like macrophages, a phenomenon that has been correlated with chromatin alterations[118,120].

Other than epigenetic alterations, "trained" innate cells undergo several other modifications. For starters, chromatin changes are intimately connected with a shake-up in metabolic pathways[118]. When PRRs are triggered during the primary challenge,

it acts as a prompt for the upregulation of glycolysis and tricarboxylic acid cycle, among others. This will in turn translate into the formation of a series of intermediate metabolites, including fumarate and acetyl coenzyme A[121,122], that have the ability to either promote or inhibit the activity of an array of enzymes responsible for the handling of histone modifications. Additionally, the training process also imposes adjustments in DNA methylation and modulates microRNA (miRNA) and long-noncoding RNA (lncRNA) expression, further tweaking the transcriptomic landscape[123].

Another relevant aspect of trained immunity is the reprogramming of bone marrow progenitors[118]. Peripheral TI, that is, the priming of innate cells such as circulating monocytes and tissue macrophages, was the originally described effector pathway for this enhanced immune phenotype. However, a relevant question arises from this: the majority mature myeloid cells have relatively short life spans[124–126] (from a day to 7 days), therefore, how does training persist over longer periods of time? Indeed, the answer lies in the ability of bone marrow progenitors to respond to different immune stimuli, namely β-glucan and BCG, two classical inducers of TI[127,128]. These immune challenges shape haematopoiesis, favouring myelopoiesis and imprinting long-standing central trained immunity.

β-glucan (βG) is one of the most studied stimuli in the context of training. This polysaccharide is one of the main components of the cell wall of many fungi, including *Candida albicans* and *Saccharomyces Cerevisiae*[129]. In 2012, Netea *et al.* published an article where they explored *C. albicans* mediated protection against secondary challenges in mice and the role βG could play[130]. Indeed, the authors demonstrated that this polysaccharide could prime monocytes *in vitro*, increasing their pro-inflammatory cytokine secretion (TNF-α and IL-6, for instance) upon a secondary restimulation. Moreover, a shift in the epigenetic landscape was detected, with many marks compatible with higher chromatin availability recorded both in *in vitro* and *in vivo* experiments. This phenomenon was mediated by the recognition of β-glucan through Dectin-1, a PRR belonging to the C-type lectin family expressed on the surface on various myeloid populations. The crucial pathway triggered is the non-canonical serine threonine kinase Raf-1 and, in fact, knockout mice were not able to reap the benefits of the priming effect that *C. albicans* demonstrated in the wild type

counterparts. Raf-1 then recruits phosphoinositide 3-kinase (PI3K), followed by mammalian target of rapamycin (mTOR) and culminating in Hypoxia-Inducible Factor 1α (HIF-1α), all crucial steps for TI instigation[131].

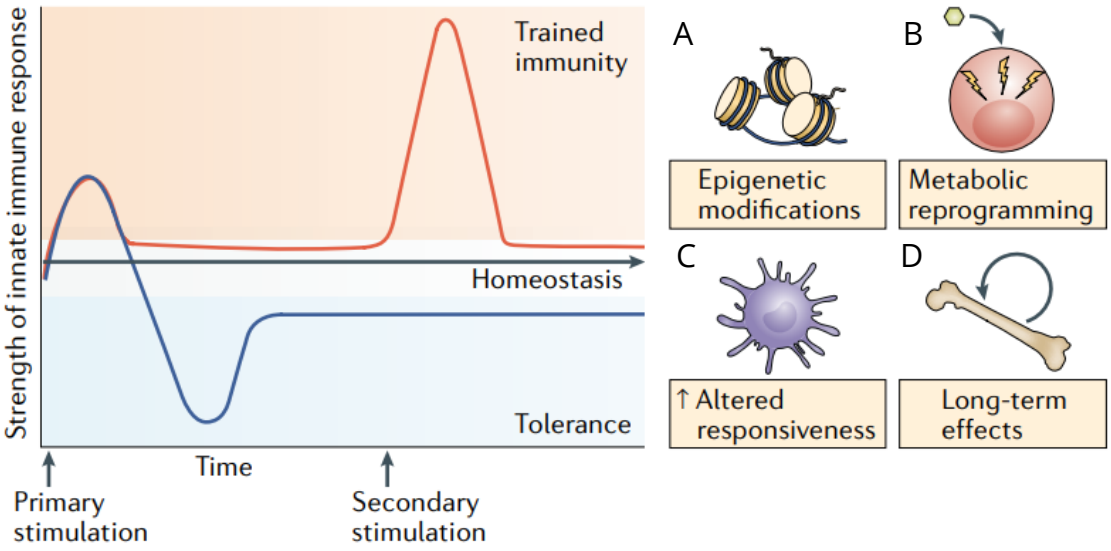

Figure 10. The opposite responses induced by innate immune memory. After an initial stimulus, innate cells can follow a program of tolerance, where the pro-inflammatory response gives way to a suppressive one, often with the intent to protect the host and culminating in a lower baseline strength for the immune response. In dissonance, these cells can adopt a primed phenotype, where a second stimulus induces a much greater response. This reaction is dependent on several mechanisms, namely: (A) epigenetic reprogramming, allowing more access to crucial genes for the immune response; (B) metabolic adjustments, intimately connected to the chromatin alterations; (C) higher responsiveness and pro-inflammatory activity and (D) long-term bone marrow progenitor reprogramming, essential for a longer lasting effect. Adapted from (117).

4.2 BCG mediated trained immunity in the context of Bladder Cancer

As was iterated in the previous section, BCG is a classical inducer of trained immunity. This pathogen has been administered as a vaccine for tuberculosis for a century now and has proven to be effective at mitigating its devastating consequences, demonstrating considerable clinical impact in children against pulmonary, miliary and meningeal tuberculosis[132]. However, the degree of protection varied considerably with distance to the equator (the higher the latitude, the better the protection) and seemed to be less powerful in adults and in previously infected individuals (independently of age). Furthermore, BCG vaccination has been linked with cross protection against other viral and lower respiratory tract infections, including

Respiratory Syncytial Virus (RSV), Influenza A, Human Papillomavirus (HPV) and Yellow Fever[133–135].

BCG displays several PAMPs that can be recognized by receptors in immune cells that are deeply involved in the following response. For starters, at the cell surface, certain Mycobacteria species, including BCG and *M. tuberculosis*, abundantly express Mannose-capped Lipoarabinomannans (Man-LAMs)[136]. This lipoglycan has three main structural components: a mannosyl-phosphatidyl-myo-inositol (MPI) domain that acts as an anchor to the cell wall; a saccharide backbone rich in D-mannose and D-arabinose residues and several mannosylated caps. These terminations can be recognized by a variety of PRRs, namely the C-type lectins MR and DC-SIGN[136–140]. The first of these has been associated with an important role in the phagocytosis of the Man-LAM bearing pathogen, potentially being an important player in antigen presentation[140]. Contradictorily, MR was also linked to the suppression of the immune response and favouring of bacterial survival[137,139]. In unison, DC-SIGN mediated Man-LAM recognition is believed to trigger increased IL-10 production, contributing to the suppression of immune response[138,141]. More recently, Dectin-2, a CTL with affinity for fungal α-mannans, has been correlated with a Man-LAM driven pro-inflammatory response, increasing production of IL-6, TNF-α and IL-2, but it also led to higher IL-10 levels[142]. All in all, this points to a potential dual role of these saccharide structures in modulating immune response and, currently, it is unknown if triggering the mentioned receptors could induce TI.

Another widely studied PAMP displayed by BCG is muramyl dipeptide (MDP). This small molecule is recognized by the Nucleotide-binding Oligomerization Domain containing 2 (NOD-2) and Netea *et al.* have demonstrated it has an essential role in triggering BCG-mediated trained immunity[143]. Both BCG and MDP lead to increased TNF-α levels in primed monocytes and when these cells were extracted from recently vaccinated adult patients, increased levels of open chromatin markers (including trimethylation of lysine 4 of the third histone – H3K4me3) were detected in immune genes, such as IL-6.

As was alluded to previously, BCG is used in the treatment of NMIBC. Various mechanisms might be unfolding in this process[144,145]: some evidence suggests the pathogen can directly interact with the tumour cells, being internalized and

potentiating the release of pro-inflammatory cytokines; adaptive immune cells, like $CD4^+$ T cells, are often detectable in the urine of responding patients and animal models have pointed to a crucial role for both $CD4^+$ and $CD8^+$ T cells; innate cells, namely monocytes, display various PRRs that recognize BCG and trigger a pro-inflammatory response that could command a potent anti-tumoral reaction, especially when trained by exposure to this pathogen[146]. Focusing this last part, it is understood that after a BCG instillation, naïve monocytes recognize the mycobacteria and undergo a differentiation process where they concomitantly acquire epigenetic and metabolic characteristic related with trained immunity (**Figure 11**). This allows the primed macrophages to be better equipped to fight the neoplastic cells and posterior challenges with BCG can further stimulate these cells. Curiously, dying tumour cells release Danger Associated Molecular Patterns (DAMPs), which can themselves elicit an anti-tumoral response[146].

Taking all these facts into account and given the relevance of carbohydrates in both cancer immunity and modulation of the innate immune system, it is relevant to study the impact of glycans in reprogramming monocytes and instructing an anti-tumoral phenotype in these cells.

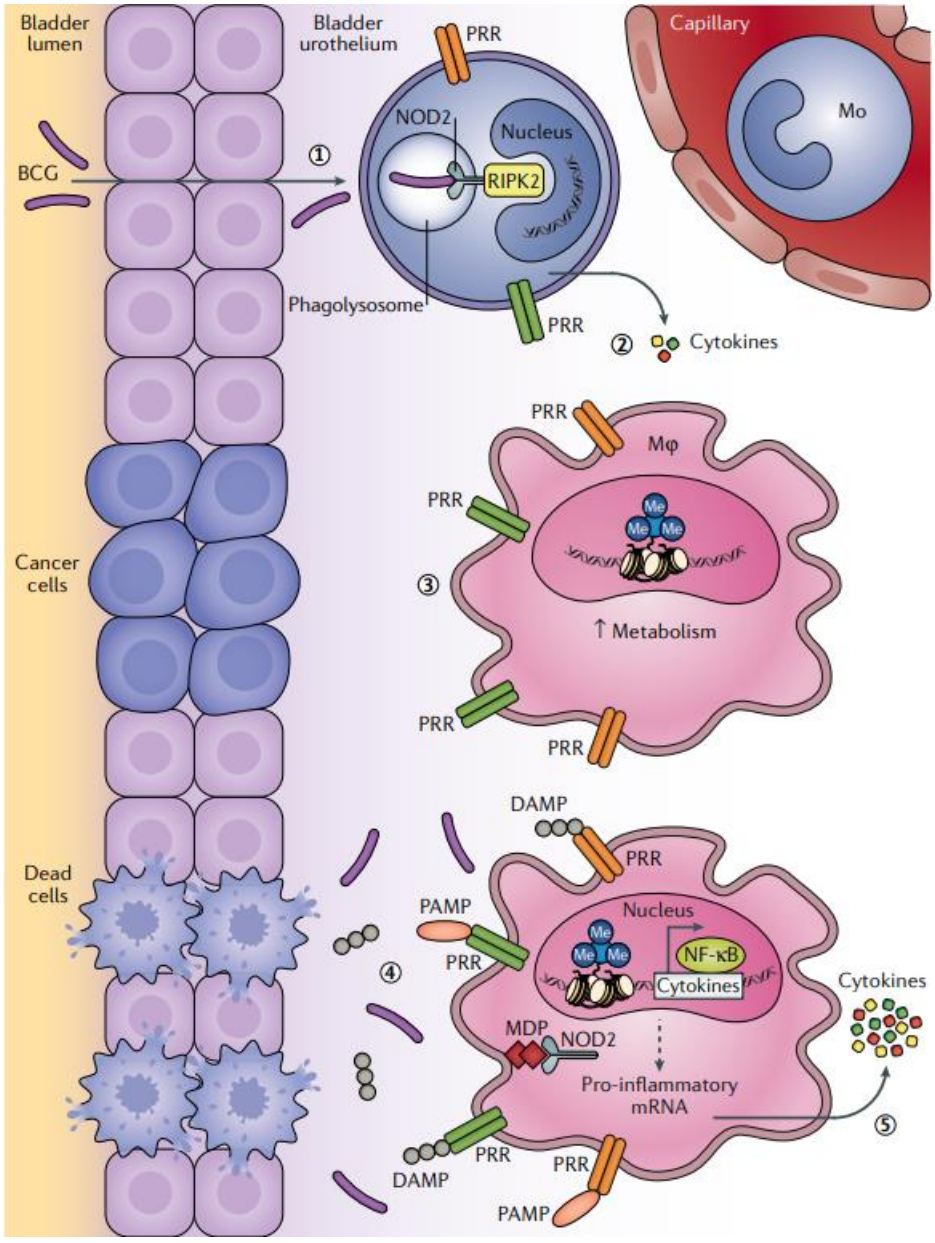

Figure 11. Proposed mechanism for monocyte/macrophage-mediated trained immunity in bladder cancer treated with BCG instillations. (1) Naïve monocytes enter the bladder and are met with the pathogen, recognizing it through several PRRs, namely NOD-2. (2) There is an initial immune response, with cytokine production. (3) These cells differentiate into macrophages and acquire typical TI markers, such as increased metabolic activity and gather chromatin alterations that allow for a stronger immune response. (4 and 5) Successive BCG exposures and DAMP release from dead cancer cells restimulates the primed macrophages that head the anti-tumoral response, displaying increased cytokine expression. Sourced from (145).

AIMS

The main goal of this thesis was to explore if pathogen-derived glycans that are rich in mannose structures, like fungal mannan, could have a role in inducing trained immunity in monocytes. Moreover, we aimed to understand if this enhanced phenotype could alter the pattern recognizing receptor (PRR) expression profile displayed by these cells upon a second stimulus and if their reprogramming could induce an effective anti-tumoral immune response that could limit tumour growth based on the recognition of high-mannose glycans. Therefore, three major aims were designed:

1. *In silico* and *ex vivo* characterization of the expression profile of glycan recognizing receptors in monocytes after exposure to a glycan stimulus.

2. Assessment of the glycan priming of monocytes as a mechanism to improve the anti-tumoral response exerted by these cells using an *in vitro* approach with two bladder cancer cell lines – T24 and RT112.

3. Evaluation of the glycan binding receptors expressed in monocytes isolated from a blood sample from a non-muscle invasive bladder cancer (NMIBC) patient treated with BCG instillations.

For the *ex vivo* characterization, monocytes ($CD14^+$ cells) were isolated from healthy donor buffy coats and cultured with different glycan stimuli. Afterwards, flow cytometry was used to evaluate the expression of PRRs of interest that were selected based on a bioinformatic preliminary analysis. Furthermore, ELISA was employed to study the impact of glycan supplementation in the secretion of pro-inflammatory cytokines. As a comparator, monocytes isolated from a blood sample from a NMIBC patient (currently in the maintenance stage of the BCG instillations therapy) were subjected to the same flow cytometry analysis. Glycan-primed monocytes were co-cultured with the RT112 and T24 bladder cancer cell lines and their tumoricidal activity was evaluated using an Annexin V/Propidium Iodate staining protocol (viability assessment).

MATERIALS AND METHODS

1. *In silico* analysis

RNA-sequencing data was obtained from different studies through the National Centre for Biotechnology Information's Gene Expression Omnibus (GSE). Three different datasets were utilised, GSE160184, GSE173488 and GSE168468. A small contextualisation of the experimental setting given for each one in section 1 of the Results. The first two mentioned datasets already provided processed data, in the form of normalised gene counts in Excel files. As for the third, the provided counts data was given in a raw format, that is, not normalised and with limited quality control applied. Therefore, to extract the normalised counts, we used part of the protocol provided by Sanchis *et al.*[147] as a basis. The R software was employed for this analysis. Briefly, we started by organising and compiling the provided files into a single data frame. Then, using the *DEseq2* package, the dataset was processed and a normalised count matrix was extracted. Genes that presented a low expression (under 100 reads across all the samples) were filtered out, yielding the final product of this analysis. We then searched for the glycan-binding proteins of interest (Table 1) in all the datasets, with the counts data for the available gene being then extracted into the GraphPad Prism 9 software (GraphPad Software®) for statistical analysis of gene expression.

Table 1. List of glycan-binding protein genes tested in the gene expression analysis. The glycan affinity might not represent the only type of glycan residue these receptors bind, but the ones that are most strongly bound by them.

Genes	Glycan affinity
CD209/DC-SIGN	Mannose
CLEC2A	Unknown
CLEC2B	Unknown
CLEC2D	Sulphated polysaccharides
CLEC2L	Unknown
CLEC4E/Mincle	Mannose
CLEC6A/Dectin-2	Mannose
CLEC7A/Dectin-1	β-glucan
CLEC9A/DNGR-1	Mannose
CLEC10A/MGL	Galactose
CLEC12A/MICL	Mannose
CD206/MRC1	Mannose
CD280/MRC2	Mannose
MBL2	Mannose

2. Human samples

Buffy coats from healthy donors were obtained from the blood bank of *Centro Hospital Universitário de São João* and were used for monocyte extraction and subsequent culture and experimentation (described below). The non-muscle invasive bladder cancer patient blood sample was acquired through a partnership with *Instituto Português de Oncologia do Porto* (IPO-Porto), with the kind collaboration of Professor Cármen Jerónimo. The patient was in the maintenance stage of the immunotherapy treatment with BCG instillations. Once again, the blood sample was utilized for monocyte isolation and further experimentation with those immune cells (described below).

3. Isolation of monocytes

Buffy coats from healthy donors were mixed with Phosphate-Buffered Saline (PBS) in a 1:3 ratio and carefully pipetted onto Lymphoprep™ (Stemcell Technologies®) solution at a 2:1 proportion. Lymphoprep™ is a density gradient medium designed to facilitate the separation of Peripheral Blood Mononuclear Cells (PBMCs). Following a centrifugation at 900g for 30 minutes at room temperature, different layers are formed, where a white ring, that corresponds to the interphase, harbours the PBMCs. Therefore, this layer was isolated and washed with PBS and centrifuged at 300g for 10 minutes at room temperature. Cell pellets were resuspended in Ammonium Chloride Potassium lysing buffer (ACK, Gibco™) for 3 mins to eliminate erythrocytes. Following this, cells were once again resuspended in PBS and centrifuged at 300g for 10 minutes at room temperature. PBMCs were then resuspended in MACS Buffer (PBS supplemented with 0,5% BSA and 2 mM EDTA) and a small volume of cell suspension (10 μL) was diluted in a Trypan Blue (Thermo Fischer Scientific®) solution for cell counting in a Neubauer chamber. The formula utilised for this was the following:

$$Live\ cells = \frac{Number\ of\ live\ cells\ counted}{Number\ of\ divisions} \times Dilution\ Factor \times 10^4$$

The volume of cell suspension that contained the necessary number of cells for further experimentation was calculated and transferred into a different falcon

tube. We then added the required volume of CD14 labelled positive selection magnetic beads (Miltenyi Biotec®, 20 μL for every 10^7 cells) and MACS buffer (80 μL for every 10^7 cells) and incubated the cell suspension for 30 minutes at 4º C. This step allows for the discrimination of the monocyte population from the remaining PBMCs when exposed to a magnetic field. The cells were then washed with MACS buffer (1-2 mL for every 10^7 cells) and centrifuged at 300g for 10 minutes at room temperature. The pellet was resuspended in the appropriate volume of MACS buffer (500 μL for every 10^8 cells) and the cellular suspension was then filtered through a column attached to a magnet (Miltenyi Biotec®), that facilitated the elution of non-CD14 positive cells. The column was then removed from the magnet and 5 mL of MACS buffer were quickly added and pushed through with the help of an embolus, allowing for the collection of the monocytes.

4. Glycan priming of monocytes

In the day before the glycan priming experiments, 96 well plates with a binding surface (Thermo Fischer Scientific®) were coated with α-mannan (Sigma-Aldrich®, final concentrations of 10, 100 and 200 μg/mL, also referred to as "Mannan" in this thesis) and diGlcNAc (kindly provided by Professor Javier Rojo, final concentrations of 10, 100 and 200 μg/mL), as these stimuli appeared to better stimulate the monocytes under these conditions. For this, these glycans were dissolved in Coating Buffer (Bicarbonate buffer, pH = 9,6) and placed in the wells overnight at 4º C. Then, before the monocytes were placed in the wells, the Coating Buffer was aspirated.

After the isolation process, monocytes derived from buffy coats from healthy donors were centrifuged at 300g for 10 minutes at room temperature and resuspended in 1 mL of culture medium that was constituted by Roswell Park Memorial Institute 1640 (RPMI 1640) + GlutaMAX™ (Gibco™), 20% Fetal Bovine Serum (FBS, Biowest®) and 1% Penicillin-Streptomycin (PenStrep, Gibco™). The cells were once again counted following the procedure detailed in section 3 and the volume containing the desired number of cells was separated into a different tube. Culture medium was added until the dilution corresponded to 1 million monocytes for each mL of medium. Cells were then placed in 96 well plates for 24 hours and each well

contained 200 μL of the cell suspension (200 000 monocytes per well). β-glucan (Sigma-Aldrich®) was only added to the culture media at this stage (2,5 μg/mL), whereas the other stimuli of interest followed the protocol provided at the beginning of this section. After this period, monocytes are adhered to the bottom of the wells. Nevertheless, the medium of each well was transferred to a new 96-well plate that underwent a centrifugation at 300g for 5 minutes at room temperature to rescue any floating cells. 25 μL of TrypLE™ Express (Gibco™) was then added to each of the empty well for 10 minutes at 37° C, which leads to the detachment of the cells from the bottom of the plate. Following this period, 125-150 μL of culture medium was added to each well to inactivate the TrypLE™ Express and the cells were resuspended and transferred to a new plate that was also centrifuged under the same conditions. In the end, the cells were all joined on the same plate with 200 μL of culture medium per well. A 5-day resting period followed, where the medium was exchanged at the third day mark. On the sixth day, LPS was added to the relevant conditions (10 ng/mL) for 6 hours to promote the activation of the monocytes. After this, the 96 well plate was centrifuged at 300g for 5 minutes at room temperature and the supernatants were stored for further analysis at -80° C. The monocytes were detached using TrypLE™ Express following the procedure detailed previously in this section, preparing them for further experimentation. **Figure 18** (in section 2 of the Results) provides a graphical overview of this experimental procedure.

5. Restimulation of patient-derived monocytes

Monocytes isolated from patient samples did not need to undergo a training protocol, as they had been exposed to BCG *in vivo*, which acted as the priming stimulus. Therefore, after extraction, 200 000 cells were cultured per well in a 96 well plate with 200 μL of the culture medium previously described. Moreover, the cells were exposed to LPS (10 ng/mL) for 6 hours, as previously described. Afterwards, the plate was centrifuged at 300g for 5 minutes and the supernatants were stored at -80° C for further analysis (namely, flow cytometry, as described in section 9). Following detachment using TrypLE™ Express in the same conditions as before, the monocytes

were ready for other evaluations. **Figure 26** (in section 4 of the Results) provides a graphical overview of this experimental procedure.

6. Bladder cancer cell lines culture

Two different cell lines – RT112 and T24 - were utilised in the experiments performed in this thesis and both were kindly provided by Professor Cármen Jerónimo, from IPO-Porto. RT112 was established from a transitional cell carcinoma of histological grade 2 (low grade according to the most recent classification guidelines) that was excised from a woman of unknown age[148]. The T24 cell line was isolated from an 82-year-old Swedish woman with a transitional cell carcinoma of histological grade 3 (high grade)[149].

Both cell lines were kept in the same conditions, having been cultured with RPMI 1640 + GlutaMAX medium supplemented with 10% FBS and 1% PenStrep. Cells were maintained in sterile culture flasks (T25 or T75) in a humidified incubator at 37º C and 5% CO_2, in order to promote exponential growth. When cells reached 80-90% confluence, they were transferred into a new flask. In order to achieve this, we started by removing the medium and washing the cells with sterile PBS. Trypsin was then added for 3 minutes at 37º C to detach the cells (Gibco™, 2 mL for T25 flasks and 4 mL for T75 flasks), being inactivated by double the volume of culture medium with FBS. Following this, cells were transferred into new tubes and centrifuged at 300g for 5 minutes at room temperature, with the pellet being resuspended in a small volume of culture medium. The cells were then placed into new flasks and maintained at 37º C 5% CO_2.

With the intention of preserving the cell lines, some vials were frozen. To achieve this, confluent cells were detached and centrifuged like previously described. The cells were then resuspended in freezing medium constituted by 90% FBS and 10% Dimethyl Sulfoxide (DMSO, ITW Reagents®) and stored in 1 mL vials at -80º C.

All the experiments that used these cell lines were performed at the exponential growing phase.

7. Co-culture assays

For the co-culture assays, the T24 and RT112 bladder cancer cell lines were cultured with trained monocytes in a 96 well U-bottom plate. The target to effector ratio was 1:10. For this, the tumour cell lines were detached from the flasks using the procedure described in the previous section and centrifuged at 300g for 5 minutes at room temperature. The cells were then resuspended in 1 mL of culture media (RPMI 1640 supplemented with 20% FBS and 1% PenStrep) and counted following the procedure described in Section 3. Then, for each well, 20 000 tumour cells were transferred into a plate where 200 000 monocytes had previously been seeded after the training protocol presented in section 4. After each timepoint (24 and 48 hours), the cells were detached using trypsin and stained with Annexin V and PI (as is presented in section 9.3), with the intent to evaluate tumour cell death. **Figure 24** (in section 3.2 of the Results) provides a graphical overview of this experimental procedure.

8. Western Blot (Lectin blot)

Western Blot was performed in order to evaluate the surface glycan expression of the bladder cancer cell lines RT112 and T24. Initially, cells were transformed into lysates with the help of a catenin lysis buffer (1% NP-40 (Sigma-Aldrich®), 1% Triton X100, cOmplete™ (Roche®), 100 mM Phenylmethylsulphonyl Fluoride (PMSF, Sigma-Aldrich®), Sodium Orthovanadate (Na_3VO_4, Sigma-Aldrich®) and PBS) that was incubated for 15 minutes on ice and resuspended every 5 minutes. The lysates were then centrifuged at 20800g for 10 minutes at 4º C and the supernatant was transferred into a new eppendorf tube. The lysates be stored at -80º C at this stage.

Total protein quantification was estimated using a Bradford Assay (Bio-Rad®) and duplicate Bovine Serum Albumin (BSA, Sigma-Aldrich®) standard curves. Absorbance was read at 750nm in a BioTek uQuant plate reader. This allowed us to standardize the mass of protein for all samples, that it, the same mass was used for every sample (30 μg). Initially, the cell lysates were resolved in a 10% SDS-PAGE gel at 125 volts, being then transferred to a nitrocellulose membrane using an adequate transfer system (Bio-Rad®) running at 90 volts for 90 minutes. Afterwards, unspecific

binding was blocked using a 4% BSA solution in PBS Tween 0,05% (PBST, Tween from Sigma®) incubated overnight at 4º C. This was followed by incubation with the lectins of interest (more complete information found in Tables 2 and 3), namely L-PHA (3,5 µg/mL), GNA (3,5 µg/mL) and DC-SIGN Binding Motifs (DC-SIGN BM, 17,5 µg/mL). These were diluted in a 1% BSA in PBST solution and incubated for 1 hour at room temperature. The membranes were then washed with PBST three times for 10 minutes and incubated for 1 hour with an Avidin - Biotinylated Horseradish Peroxidase conjugate from a commercial kit (Vector Laboratories). Protein levels were measured using ECL or ECL Prime Western Blotting Detection Reagents (GE Healthcare®) with signals being captured in Hyperfilm ECL (GE Healthcare®).

After the lectin analysis, we stripped the membranes using a commercial stripping solution (NZYtech®) for 3 minutes. This was followed by a 10-minute washing step with Tris Buffered Saline with 0,05% Tween (TBST, TBS from Fischer Bioreagents™) that was repeated twice. The membranes were incubated in 5% skim milk diluted in TBST for 1 hour to block unspecific interactions, followed by another 1-hour incubation with the anti-vinculin antibody (Sigma-Aldrich®, clone V284, 1:500 dilution in 1% skim milk in TBST). After two 5-minute washes with TBST, the membranes were incubated with the ECL™ anti-mouse IgG HRP conjugated secondary antibody (GE Healthcare®, 1:2000 in 1% skim milk in TBST) and washed again with TBST twice for 10 minutes. Protein levels were measured using ECL or ECL Prime Western Blotting Detection Reagents (GE Healthcare®) with signals being captured in Hyperfilm ECL (GE Healthcare®).

9. Flow cytometry staining

9.1 Monocyte glycan-binding protein staining

After the protocol described in section 4, monocytes were ready to undergo flow cytometry staining. Following detachment, the cells were washed with 100 µL of FACS buffer (2% FBS in PBS) and centrifuged at 300g for 5 minutes at room temperature. Cells were then stained with Fixable Viability Dye (FVD, Labclinics®) diluted at 1:2000 ratio in PBS and were kept protected from light for 30 minutes on ice. This dye infiltrates cells that have had their membrane integrity compromised and

binds to certain cellular proteins (amines), allowing the distinction between dead and live cells. After another washing step (with PBS), monocytes were centrifuged as previously described and stained with the fluorophore-labelled antibodies for 30 minutes, on ice and protected from light. The utilised antibodies and respective dilutions are denoted in Table 2 and were diluted in FACS buffer. Following this period, cells were once again washed with FACS buffer and centrifuged in the same conditions as stated above. Cells were then stained with a FITC-labelled secondary antibody (Table 2) that bound the anti-DC-SIGN primary unconjugated antibody for 30 minutes on ice and in the dark. The monocytes were washed and centrifuged one final time and were then kept in 100-150 μL of FACS buffer at 4º C protected from light until they were acquired in a BD Bioscience® FACS Canto II cytometer. The gating strategy we utilised for this analysis is depicted in **Figure 12**. Single stains for each antibody were done with beads, whilst FVD single stains were performed using cells. Furthermore, an unstained control was used. Data was analysed using FlowJo Version 10 (Tree Star®).

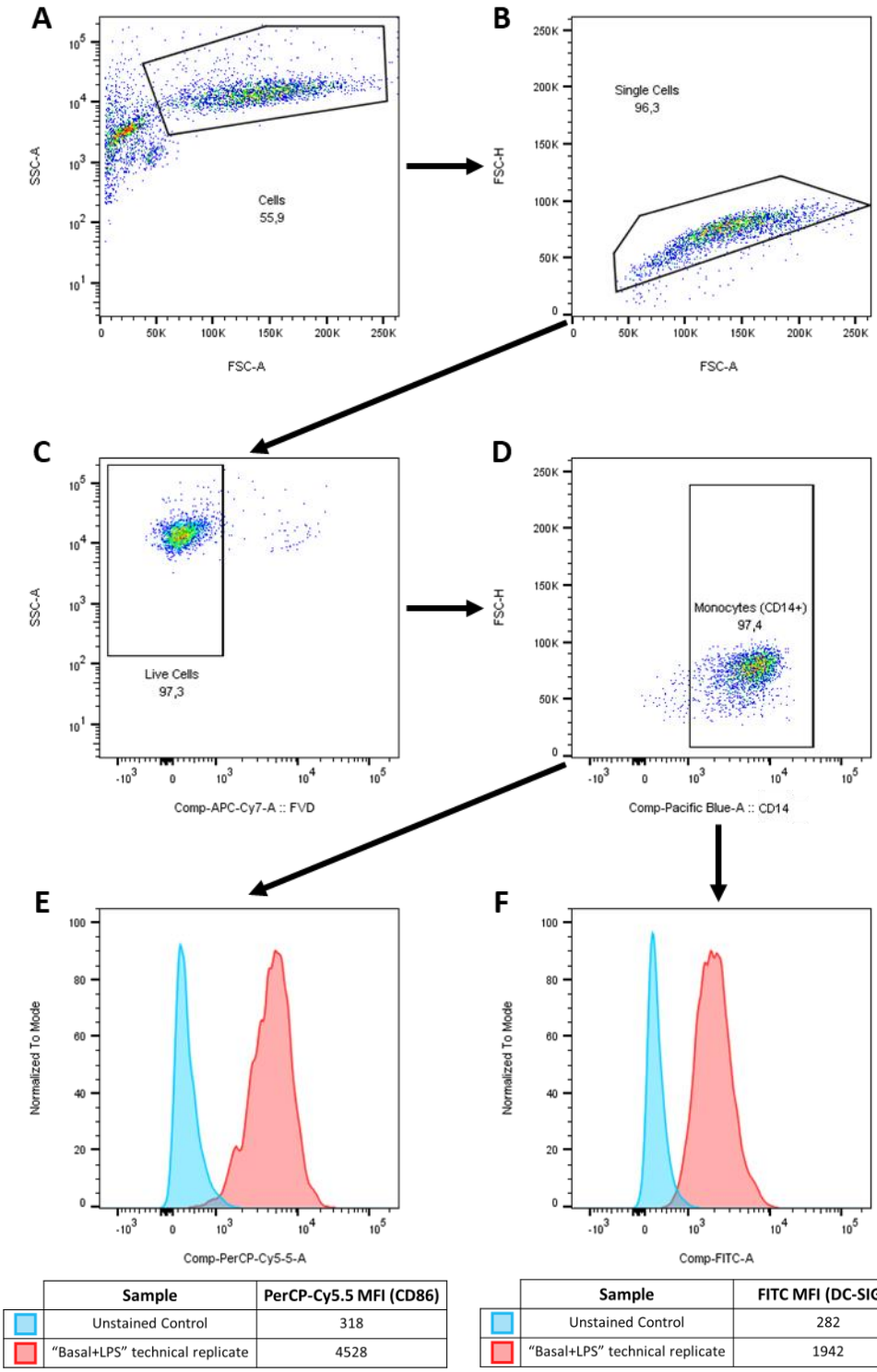

	Sample	PerCP-Cy5.5 MFI (CD86)
	Unstained Control	318
	"Basal+LPS" technical replicate	4528

	Sample	FITC MFI (DC-SIGN)
	Unstained Control	282
	"Basal+LPS" technical replicate	1942

Figure 12. Example of the gating strategy employed in the flow cytometry analysis of the glycan binding protein analysis of monocytes. (A) Initially, cells were gated based size (FSC) versus complexity (SSC). (B) This was followed by single cell selection using a plot of event area (FCS-A) by event height (FSC-H). (C) Then, live cells were selected based on the non-incorporation of the viability dye (FVD), as cells that have a compromised membrane integrate it, becoming stained. (D) To guarantee the purity of the extraction process, CD14 was used to assure we had a pure monocyte population. The expression levels of the antibodies enumerated in Table 1 were then assessed utilising the Mean Fluorescence Intensity (MFI) values, as is exemplified in graphs (E) for CD86 and (F) for DC-SIGN.

9.2 Bladder cancer cell line lectin staining

To evaluate the surface glycan expression of both bladder cancer cell lines, cells were detached with trypsin. Following washing with culture medium and centrifugation at 300g for 5 minutes at room temperature, the cells were pelleted in three technical replicates per cell line in 96 well U-bottom plates. The first step in the staining process was once again the resuspension of the cells in FVD (1:2000 dilution in PBS) for 30 minutes on ice and protected from light. The cells were then washed with PBS and centrifuged at 300g for 1 minute, which was followed by the staining with various lectins for 15 minutes on ice and in the dark. The utilised lectins, dilutions and their affinities are displayed in Table 2 and Table 3 and were diluted in FACS Buffer, unless DC-SIGN BM was present in the mix, in which case Lectin Binding Buffer (LBB, 50 mM HEPES (Sigma-Aldrich®), 5mM $MgCl_2$ and 5mM $CaCl_2$ diluted in distilled water) was used in place of FACS Buffer. Following this, cells were washed with FACS Buffer and centrifuged at 300g for 1 minute and stained with a PeCy7 conjugated secondary antibody (allowed for the detection of the unconjugated lectins ConA and DC-SIGN BM) for 30 minutes in ice and protected from light. After, cells were washed with FACS Buffer and centrifuged in the previously stated conditions, being then resuspended in 100-150 μL of FACS Buffer and stored at 4º C protected from light until acquirement in a BD Bioscience® FACS Canto II cytometer. The gating strategy we utilised for this analysis is depicted in **Figure 13**. Single stains for each lectin and FVD were performed using cells. Furthermore, an unstained control was used. Data was analysed using FlowJo Version 10 (Tree Star®).

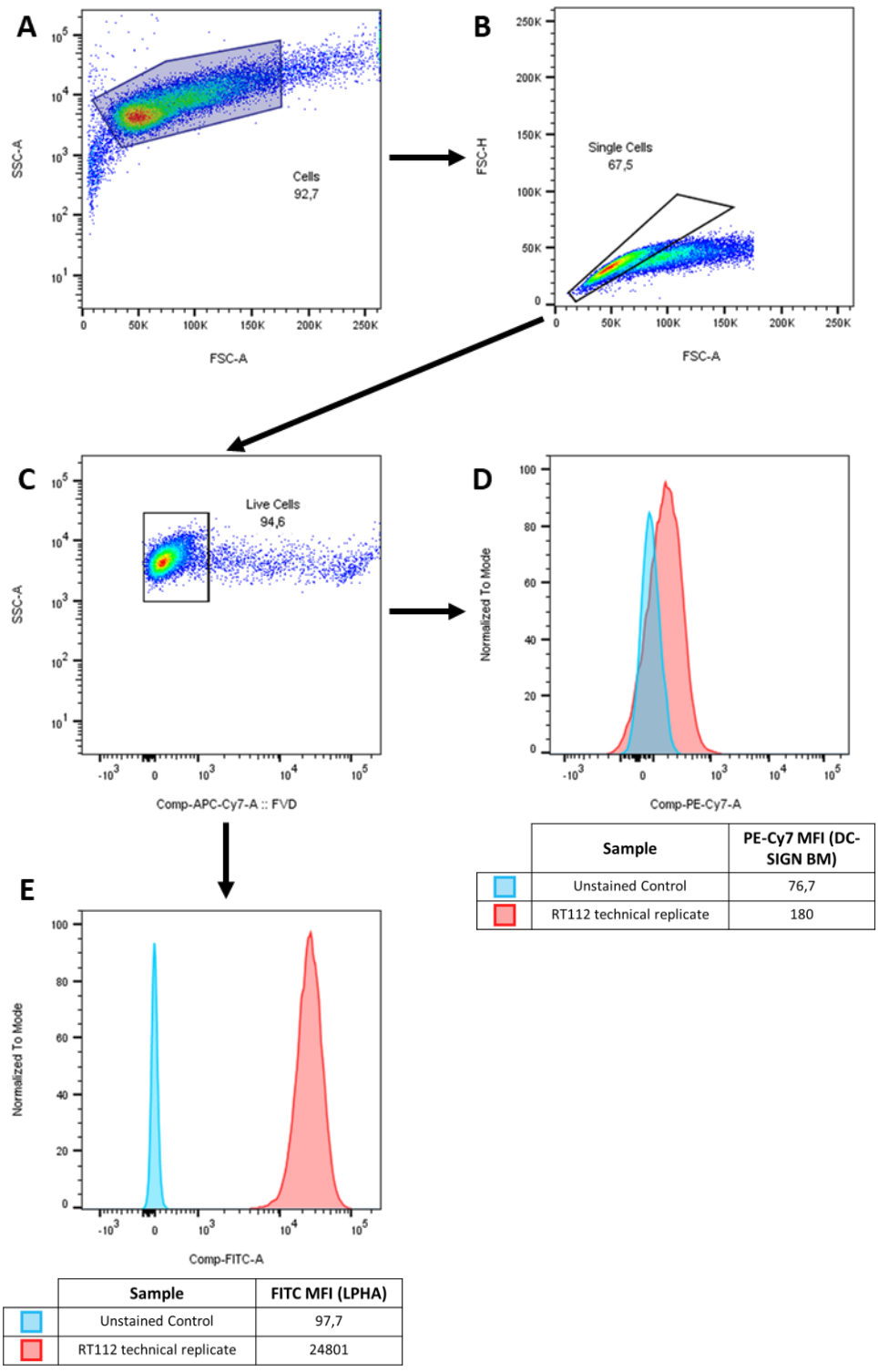

	Sample	PE-Cy7 MFI (DC-SIGN BM)
	Unstained Control	76,7
	RT112 technical replicate	180

	Sample	FITC MFI (LPHA)
	Unstained Control	97,7
	RT112 technical replicate	24801

Figure 13. Example of the gating strategy employed in the flow cytometry analysis of the surface glycan expression. (A) Initially, cells were gated based size (FSC) versus complexity (SSC). (B) This was followed by single cell selection using a plot of event area (FCS-A) by event height (FSC-H). (C) Then, live cells were selected based on the non-incorporation of the viability dye (FVD). The expression levels of the lectins enumerated in Table 1 were then assessed utilising the Mean Fluorescence Intensity (MFI) values, as is exemplified in graphs (D) for DC-SIGN BM and (E) for L-PHA.

9.3 Annexin-PI assay

To characterise the ability of trained monocytes to induce tumour cell death in the co-culture assays, we stained the cells with Annexin V – Propidium Iodate (PI). Detailed information about all the antibodies utilised in this protocol is indicated in Table 2. Firstly, cells were detached using trypsin (25 µL in each well for 3 minutes), which was followed by a washing step with FACS buffer and a centrifugation at 300g for 1 minute. Then, cells were stained with an anti-CD45 antibody for 20 minutes protected from light and on ice, allowing the distinction between the immune ($CD45^+$) and tumoral ($CD45^-$) counterparts. Once more, cells were washed with FACS buffer and centrifuged at 300g for 1 minutes. Another washing step was performed, this time with Annexin Binding Buffer (ABB, HEPES buffer at 100mM, NaCl at 140mM and $CaCl_2 \cdot 2H_2O$ at 2,5 mM), followed by centrifugation in the same conditions. Cells were then stained with Annexin V diluted in ABB for 15 minutes protected from light at room temperature. This antibody binds phosphatidylserine, a component of the cell membrane that becomes exposed once they enter an apoptotic state. After another washing and centrifugation step, cells were resuspended in 100 µL of ABB. Before acquisition on the flow cytometer, PI was added, staining only the cells that had their membrane integrity compromised – necrose detection. Importantly, the acquisition needs to be performed no more than 15 minutes after this step. This staining procedure allows the differentiation between live cells (Annexin V^-, PI^-), early apoptotic cells (Annexin V^+, PI^-), late apoptotic cells (Annexin V^+, PI^+) and necrotic cells (Annexin V^-, PI^+). Data was acquired in a BD Bioscience® FACS Canto II cytometer. The gating strategy we utilised for this analysis is depicted in **Figure 14**. Single stains for CD45, Annexin V and PI were performed using cells. Furthermore, an unstained control was used. Data was analysed using FlowJo Version 10 (Tree Star®).

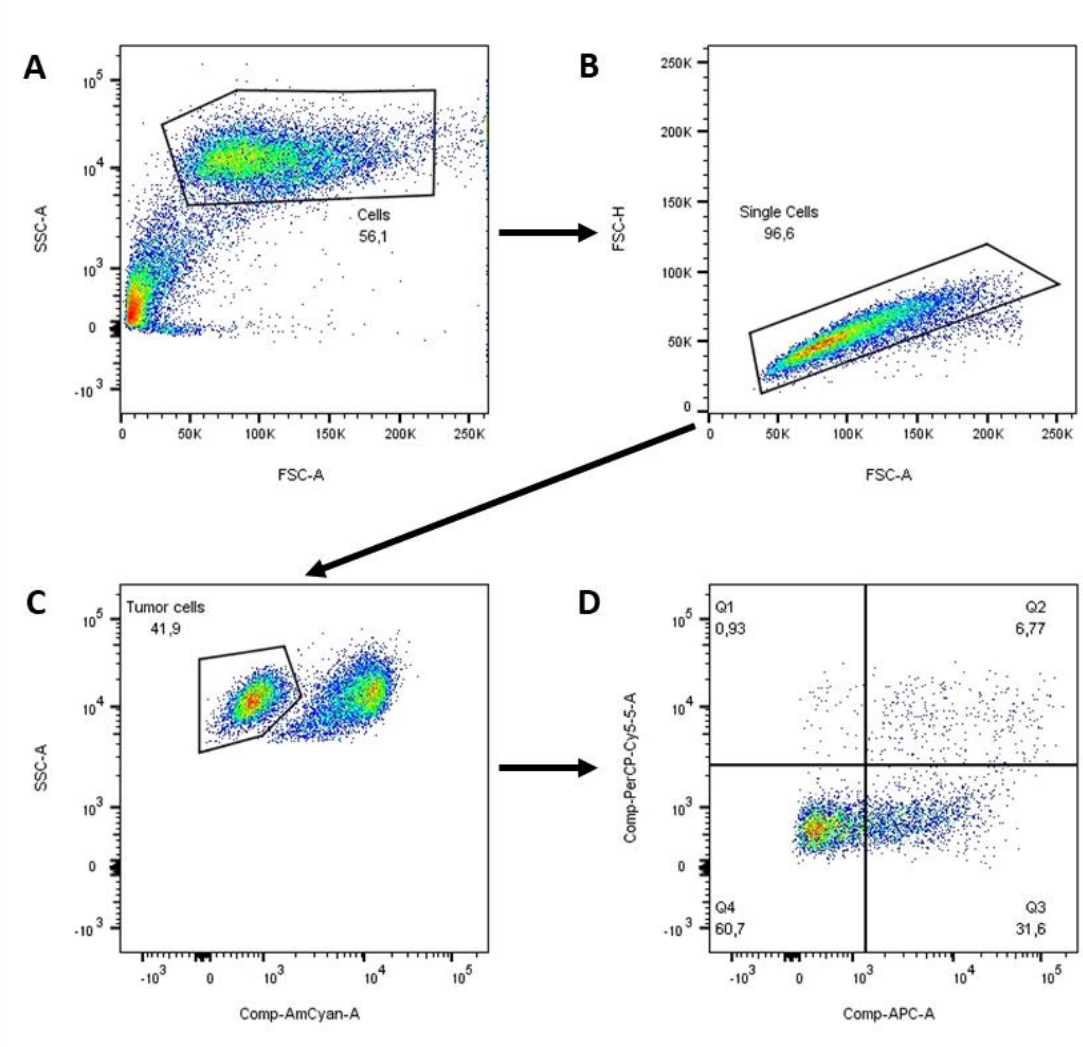

Quartil	Cell status
Q1 (Annexin V-, PI+)	Necrotic cells
Q2 (Annexin V+, PI+)	Late Apoptotic cells
Q3 (Annexin V+, PI-)	Early Apoptotic cells
Q4 (Annexin V-, PI-)	Live cells

Figure 14. Example of the gating strategy employed in the flow cytometry analysis of tumour cell death in the co-culture experiment. (A) Initially, cells were gated based size (FSC) versus complexity (SSC). (B) This was followed by single cell selection using a plot of event area (FCS-A) by event height (FSC-H). (C) Then, tumour cells were selected based on the absence of CD45 expression, a marker of immune populations. (D) Finally, cells were subdivided into four subsets based on the staining with Annexin V and PI. As is explained previously, double negative cells are live cells. Annexin V single positives are early apoptotic cells, whilst PI single positives are considered necrotic cells. Double stained cells are late apoptotic. The antibodies used in this section are indicated in Table 1 and the data was represented in relative percentages of the different subsets.

Table 2. List of monoclonal antibodies and lectins utilised in flow cytometry and western blot experiments. *The concentration of these lectins used in the western blot experiments is indicated in the correspondent section of the Materials and Methods.

	Antibody/Lectin	Fluorophore/Conjugate	Dilution Factor	Clone	Supplier
Antibody (Human)	Fixable Viability Dye	eFluor 780	1:2000	-	eBioscience™
	CD14	Brilliant Violet 421	1:100	63D3	Biolegend®
	Dectin-1	PE	1:100	15E2	Biolegend®
	Dectin-2	Alexa Fluor 488	1:100	545925	R&D Systems™
	DC-SIGN	Unconjugated	1:100	AHP627	BioRad®
	Mannose Receptor	PE-Cy7	1:100	15-2	Biolegend®
	CD86	PerCP-Cy5.5	1:100	IT2.2	Invitrogen™
	Annexin V	APC	1:20	-	Biolegend®
	Propidium Iodate	PE	1:200	-	eBioscience™
	CD45	Brilliant Violet 510	1:200	HI30	BioLegend®
Lectin	L-PHA	FITC	1:1000*	-	Vector Laboratories
	GNA	FITC	1:1000*	-	Vector Laboratories
	SNA	APC	1:1000	-	Vector Laboratories
	DC-SIGN Binding Motifs	Unconjugated	1:1000*	-	Vector Laboratories
	ConA	Unconjugated	1:1000	-	Vector Laboratories
Secondary antibody	Anti-rabbit secondary antibody	FITC	1:20	-	Dako
	Streptavidin	PE-Cy7	1:200	-	Invitrogen™

Table 3. List of used lectins in flow cytometry and western blot experiments. L-PHA recognizes complex β-1,6-branched *N*-glycans. GNA recognizes terminal α-1,3 bound mannose residues, whilst SNA targets terminal α-2,6-linked sialic acid. ConA and DC-SIGN BM share the affinity to highly mannosylated *N*-glycans, but the latter also binds fucose residues (not only α-1,4-linked fucose residues, but also α-1,2 and α-1,3).

Lectin	Structural affinity	Glycan illustration
***Phaseolus Vulgaris* leukoagglutinin (L-PHA)**	2,6-branchd tri and tetra antenary complex *N*-glycans	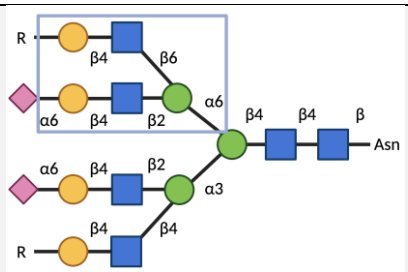
***Galanthus Nivalis* Agglutinin (GNA)**	Terminal α-1,3 mannose-linked residues	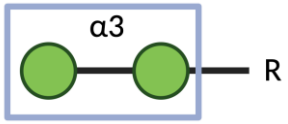
***Sambucus Nigra* Agglutinin (SNA)**	α-2,6-linked sialic aid residues	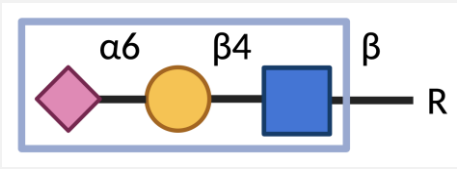
Concavalin-A (ConA)	Oligomannose-type *N*-glycans	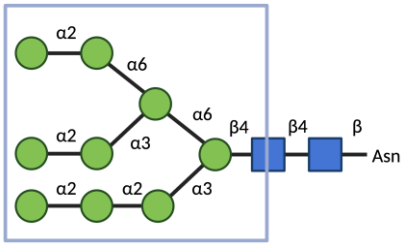
DC-SIGN Binding Motifs (DC-SIGN BM)	*N*-linked high mannose glycans and fucose residues	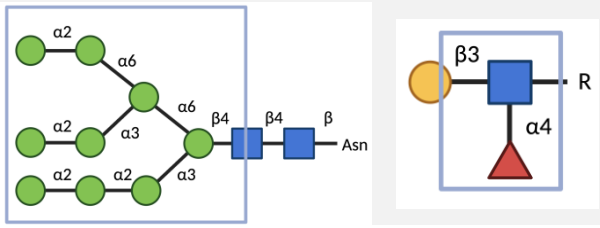

10. Enzyme-Linked ImmunoSorbent Assays (ELISAs)

To analyse the levels of cytokine secreted by monocytes in the various conditions tested in the *ex vivo* cell culture procedures, we used ELISA kits that target TNF-α and IL-6 (Invitrogen™) present in the stored supernatants. The assays were performed according to manufacturers' recommendations. Briefly, 96 well plates were coated overnight at 4º C with capture antibody diluted 250 times in PBS 1x. The next day, each well was washed using PBST with this process being repeated 2 times per washing step. This was followed by a blocking step with diluted ELISPOT (1:4 ratio in PBS) provided in the kits for 1 hour at room temperature. After a washing step, standards and samples were added to the wells and incubated for 2 hours at room temperature. Once again, the plates were washed and the detection antibody (diluted 250 times in PBS) was added for 1 hour at room temperature. Following another washing step, streptavidin-conjugated horseradish peroxidase diluted 100 times in PBS was added to the plates for 30 minutes at room temperature. Lastly, trimethylbenzene (TMB, eBioscience®) was added for a maximum period of 15 minutes, allowing for the discrimination of the intensity of binding. The reaction was stopped with a 1 M / 2 N sulfuric acid solution, which was followed by the reading of absorbance at 450 nm and 570 nm in a BioTek uQuant plate reader.

11. Real Time quantitative Polymerase Chain Reaction (RT-qPCR)

After the monocyte *ex vivo* cultures were finished as depicted in section 4, cells were ready for further analysis. For the RT-qPCR analysis, we started by isolating the RNA. TRIzol (Sigma-Aldrich®) was added to the wells for 15 minutes at room temperature and the cells were resuspended vigorously. At this stage, the lysate could be stored at -80º C. After this, glycogen was added to each sample to allow for the RNA to have a visible colour, which was followed by the addition of chloroform (40% of the volume of TRIzol initially used, Sigma-Aldrich®) for 5 minutes at room temperature. The samples were then centrifuged at 18000g for 10 minutes at 4º C, which lead to the formation of multiple layers. RNA is found on the top transparent

layer, with this part being carefully separated into a new tube. After this, isopropanol was added (50% of the volume of TRIzol initially used, Sigma-Aldrich®) and incubated at room temperature for 15 minutes. Samples were then centrifuged at 18000g for 30 minutes at 4º C. Following this step, the supernatant was removed, and the pellet was immersed in cold 70% ethanol. To detach the pellets, a vortex was set to maximum speed and the tubes were very briefly put in contact with the vortex, which allowed for the pellet to be visibly floating. The samples were then centrifuged for 8 minutes at 7500g at 4º C. Afterwards, the maximum volume of ethanol supernatant was removed and the pellets were left to dry. The RNA was then dissolved in ultrapure water (Invitrogen™) and quantified in a Nanodrop 1000 UV-Vis Spectrophotometer system (ThermoFisher Scientific®).

At this stage, the RNA could be stored at -20º C. Next it line from RNA isolation is complementary DNA (cDNA) synthesis. It is mandatory that the same mass of RNA is used for every sample in these steps (in this case, approximately 230 ng), which requires prior calculations based on the RNA concentration readings obtained in the nanodrop. With this in mind, samples were diluted in ultrapure water and incubated with random primers (Invitrogen™) and deoxynucleotide triphosphates (dNTPs, Thermo Fischer Scientific®). Samples were then placed in a T100TM thermocycler (Bio-Rad®), where a cycle of 5 minutes at 65º C was ran followed by an infinite hold at 4º C. Afterwards, samples were incubated with a reaction mix constituted by 5x SSIV buffer solution (Invitrogen™), dithiothreitol (DTT, New England BioLabs®), RNase Out enzyme (Invitrogen™) and SuperScript™ IV reverse transcriptase enzyme (Invitrogen™) and, once again, placed in the thermocycler, where a cycle of 10 minutes at 23º C, 10 minutes at 50º C, 10 minutes at 80º C and an infinite hold at 4º C was ran. Samples were frozen at -20º C until further use.

Lastly, the expression levels of the genes of interest were measured using RT-qPCR. The utilised probes are identified in Table 4. For starters, the samples were added to a 96 well plate, which was then complemented with a reaction mix constituted by ultrapure water, TaqMan™ Universal PCR Master Mix (Thermo Fischer Scientific®) and the respective probe. All the samples were ran as three technical replicates in a 7500 real-time PCR system (Applied Biosystems®) and subjected to the

following cycle: holding stage for 20 seconds at 50º C; denaturation for 10 minutes at 95º C and 45 amplification cycles consisting of 15 seconds at 95º C (annealing) and 1 minute at 60º C (extension). Relative quantification values (RQ) were calculated with the formula $2^{-(\Delta Ct)}$, where ΔCt is the difference between the CT of the housekeeping gene (GAPDH) and the CT of the gene of interest.

Table 4. List of probes utilised in RT-qPCR experiments.

GENE	PROBE	CONJUGATE	SUPPLIER
GAPDH	Hs02786624_g1	FAM	Thermo Fishcer Scientific®
DC-SIGN	Hs01588349_m1	FAM	Thermo Fishcer Scientific®
TNF	Hs00174128_m1	FAM	Thermo Fishcer Scientific®

12. Statistical analysis

Statistical analysis was done with the GraphPad Prism 9 software (GraphPad Software®). When the sample number (n) was greater than 3, the ROUT method was employed to check for outliers with a False Discovery Rate of 1% and any hits were removed from further analysis. All the data was tested for normality. When this was verified, Student's T-tests or One-Way ANOVA followed by Dunnett's multiple comparisons test were performed, depending on if there we were comparing 2 or more conditions, respectively. When normality was not present, Mann-Whitney U-Tests or Kruskal-Wallis tests followed by Dunn's multiple comparison tests were performed, once again considering 2 or more conditions, respectively. For the co-culture assays, Two-Way ANOVA tests were used followed by Dunnett's multiple comparison tests. Statistical significance was defined as a p value equal or inferior to 0,05 (* $p < 0.05$, ** $p < 0.01$, *** $p < 0.001$, **** $p < 0.0001$.).

RESULTS

1. Trained immunity alters glycan-binding protein expression pattern - an *in silico* analysis

As was explained in previous sections, the literature has demonstrated that innate immune cells, when exposed to infectious stimuli or carbohydrates displayed by these pathogens, such as *Candida albicans* and β-glucan respectively, can trigger a primed pro-inflammatory state that, upon a secondary challenge, can lead to a heightened response. This response is mediated via certain pattern recognizing receptors (PRRs) with glycan-binding capabilities, namely Dectin-1, a receptor capable of piloting a complex metabolic and epigenetic rewiring of monocytes when activated by β-glucan. Therefore, we hypothesized that these and other infectious stimuli presented different glycan structures, including ones rich in mannose residues, that could trigger similar programs. Furthermore, we speculated that the reprogramming of monocytes would reshape the glycan-binding protein (GBP) expression landscape, potentially increasing the levels of certain receptors with affinity for important pathogen-associated glycan structures.

With this in mind, we initially set our sights on an *in silico* approach. Publicly available RNA sequencing databases from studies with various infectious stimuli were selected and analysed, allowing us to better understand the expression pattern of different glycan receptors. The first dataset pertains to a study where the authors linked the persistent inflammation observed in Human Immunodeficiency Virus (HIV) patients with a strengthened pro-inflammatory trained state in monocytes[150]. This virus displays glycoproteins at its surface that are crucial for its pathological activity inside the human body, with most well-known example being gp120[151,152]. Normalised gene counts were displayed for 8 patients and 4 age and sex-matched uninfected controls (GSE160184). The quality control procedure applied to the data is detailed in the material and methods section of the related paper.

First, we looked for a wide variety of GBPs, including several C-type lectins and other receptors with a panoply of glycan affinities (**Table 1**). Normalised counts were extracted for the available genes of interest. Interestingly, our results show that monocytes from HIV patients presented significantly higher levels of some mannose-binding PRRs, including DC-SIGN and Mannose Receptor (**Figure 15**). As for Myeloid

Inhibitory C-type Lectin-like receptor (MICL), a non-significant tendency is found. Receptors with other glycan affinities, such as Dectin-1 and MGL, are also found to be upregulated in HIV patients (**Figure 15**). These results, combined with the findings from the cited paper, demonstrate that the virus responsible for the Acquired Immunodeficiency Syndrome can reconfigure the GBP landscape in monocytes in a trained immunity environment, supporting our hypothesis.

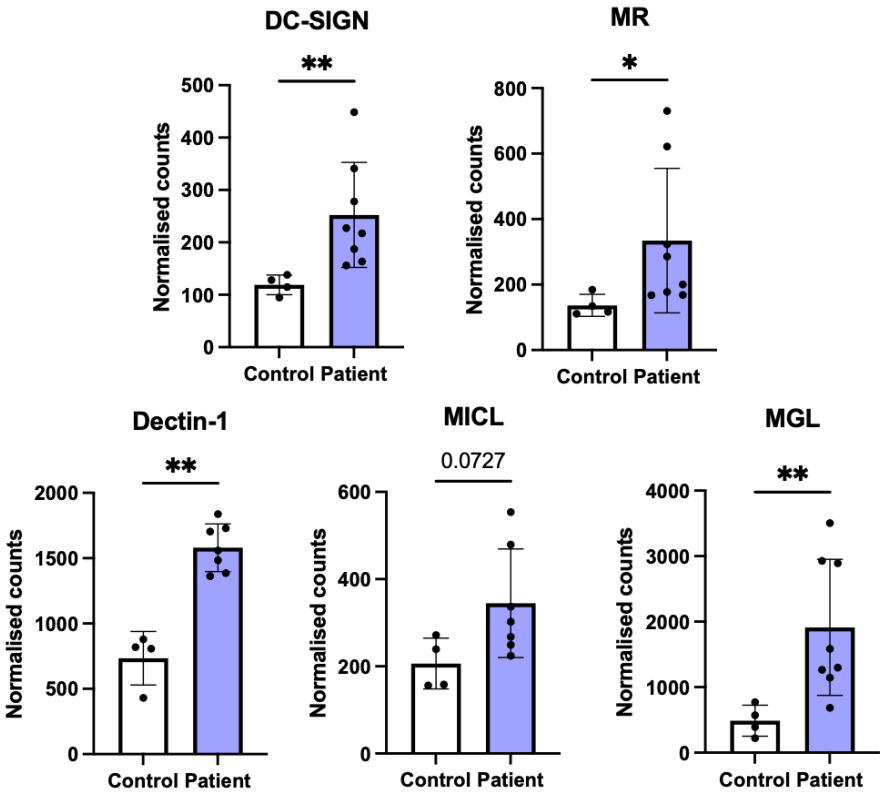

Figure 15. Normalised gene counts comparing glycan-binding protein (GBP) levels in uninfected controls (white bar, n = 4) and HIV infected (blue bar, n = 7-8) individuals. Several pattern recognizing receptors (PRRs) display a significant increase in their expression in the HIV-positive group, except for MICL, that still exhibits a similar trend. Outlier tests were followed by Mann-Whitney U tests. Data is represented as Mean ± Standard Deviation (SD). * $p < 0.05$, ** $p < 0.01$.

Another pathogen that exposes relevant glycans at their surface is Sars-CoV-2, the virus responsible for the Covid-19 pandemic[153,154]. Therefore, we selected a dataset (GSE173488) derived from an article where the authors once again linked the infection with this virus to a long-lasting reprogrammed myeloid phenotype[155]. The researchers extracted monocytes from 4 uninfected controls and 4 recovered (convalescent) Covid-19 patients, with the only important difference in experimental procedure being the restimulation of the immune cells with two stimuli: LPS and a

recombinant version of the Sars-CoV-2 spike protein. The provided data came in the form of normalised gene counts, and the same statistical analysis was applied.

In accordance with the data previously shown and in line with the hypothesis of this thesis, we observe that mannose-binding CTLs alter their expression after the exposure to Sars-CoV-2, with DC-SIGN and MR displaying an increasing trend for both stimuli, even though the latter is not statistically significant (**Figure 16**). MGL and MICL also present higher levels in the trained myeloid cells (**Figure 16**). Other GBPs, like Dectin-1 and Dectin-2 (another C-type lectin with high affinity for high-mannose ligands that did not figure in the first dataset) did not exhibit relevant changes.

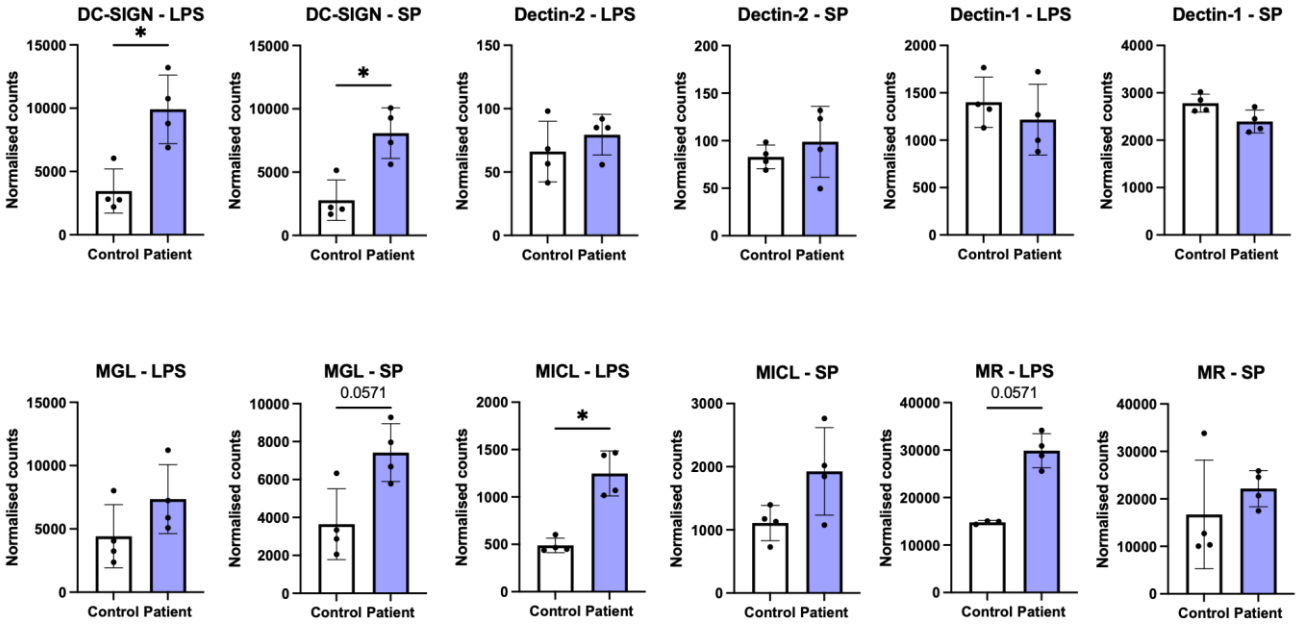

Figure 16. Normalised gene counts comparing glycan-binding protein (GBP) levels in uninfected controls (white bar, n = 4) and Sars-CoV-2 infected (blue bar, n = 3-4) individuals. Two different stimuli were used to rechallenge the monocytes: LPS and recombinant spike protein (SP). DC-SIGN and MICL were the only receptors that presented a significant increase in their levels after Sars-CoV-2 exposure, but trends are discernible for MR and MGL as well. The remaining PRRs did not present significant alterations. Outlier tests were followed by Mann-Whitney U tests. Data is represented as Mean ± SD. * $p < 0.05$.

Lastly, as one of the focal points of this study was BCG and its link to an anti-tumoral response, we selected a dataset (GSE168468) from an article where the authors explored the role of BCG vaccination in the priming of monocytes[156]. This pathogen also has relevant glycan moieties at its surface, including Man-LAMs, that have been linked to an important role in the pathogenic activity of the *Mycobacterium* family[136]. The transcriptomic data we analysed was derived from *ex vivo* experiments performed by extracting monocytes from 5 naïve donors and exposing the immune

cells to two different strains of BCG, namely Bulgaria and Denmark. However, the authors supplied raw data, which required an initial processing step detailed in section 1 of the Materials and Methods. After this, we produced a data matrix with the normalised gene counts.

Maintaining the trend previously observed, DC-SIGN increased its levels after exposure to both strains of BCG, with Dectin-2 also displaying a significant expression boost after monocyte priming (**Figure 17**). As for Dectin-1 and MICL, neither achieved statistical significance (**Figure 17**). Unfortunately, MR and MGL were not detected in this dataset.

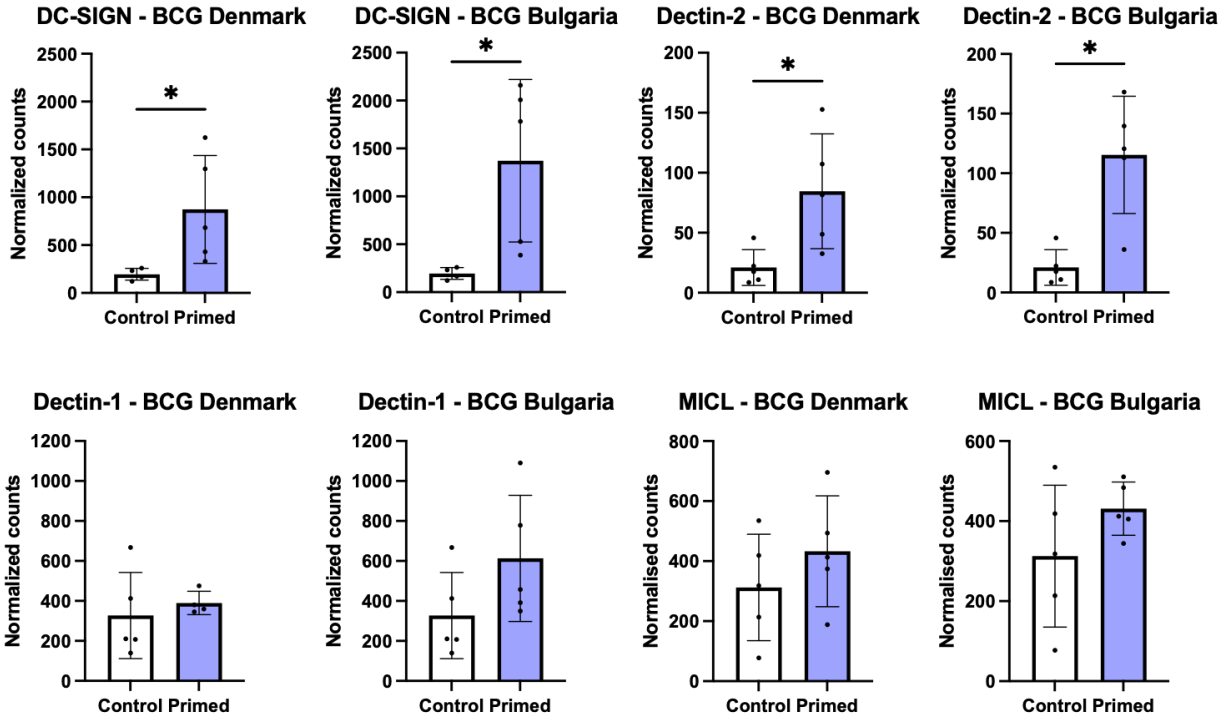

Figure 17. Normalised gene counts comparing glycan-binding protein (GBP) levels in non-primed (white bar, n = 4-5) and BCG-primed (blue bar, n = 4-5) monocytes extracted from 5 different individuals. Two different BCG strains were used to train the monocytes: BCG Bulgaria and BCG Denmark. This priming translated into higher DC-SIGN and Dectin-2 levels, whereas Dectin-1 and MICL did not display clear tendencies. MGL and MR were not detected in this dataset. Outlier tests were followed by Mann-Whitney U tests. Data is represented as Mean ± SD. * $p < 0.05$.

Cumulatively, the different datasets point to a similar conclusion: the priming of monocytes with infectious stimuli leads to a remodelling of the GBPs expressed by these innate immune cells, with the most common hits being receptors with mannose affinity. As far as we are aware, this is the first demonstration of the correlation between the concept of trained immunity and its impact in the remodelling of GBP profile. Based on the results presented in this section, we postulated that pathogen-

derived glycans that are rich in mannose residues, namely fungal α-mannans, could potentially harbour the ability to induce a trained immunity program in monocytes, through the remodelling of GBP expression profile combined with a more pro-inflammatory phenotype.

2. Monocytes supplemented with α-mannan evidenced a primed phenotype

To evaluate if high mannose fungal carbohydrates can pilot the priming of monocytes, we developed an *ex vivo* model using immune cells from healthy donors based of work performed by other groups[157]. For this, we performed a large array of optimizations, where diverse concentrations (from 0,25 μg/mL to 200 μg/mL) of three different stimuli were tested. These consisted of two glycondendrimers, diGlcNAc (dGN) and Man9, and fungal-derived α-mannan. In the end, only dGN and Mannan were selected for further experimentation, as they exhibited the highest training potential. Furthermore, we also tested different methods of delivering this supplementation (dissolved in the medium or coated in the plate), different training timepoints (24 and 48 hours of priming) and addition of other monocyte-maturing stimuli (GM-CSF at 25 ng/mL). Graphical representations of this optimization process can be consulted in **Appendix 1**.

After the optimisations, we opted to not supplement monocytes with GM-CSF, as this stimulus can imprint an activated phenotype in these cells, inducing a bias to our analysis. Moreover, its addition did not improve cell viability significantly. The cells were exposed to coated dGN and Mannan (at 10, 100 and 200 μg/mL) for 24 hours (β-glucan was used as a positive training control and dissolved in the medium[130]). Following this, monocytes were transferred to another plate with only culture media, where they rested for 5 days. Finally, the cells were restimulated with LPS for a 6-hour period, after which further analysis were performed (schematic representation in **Figure 18**). This model allowed us to understand the potency of the various stimuli in instructing a heightened trained immune phenotype.

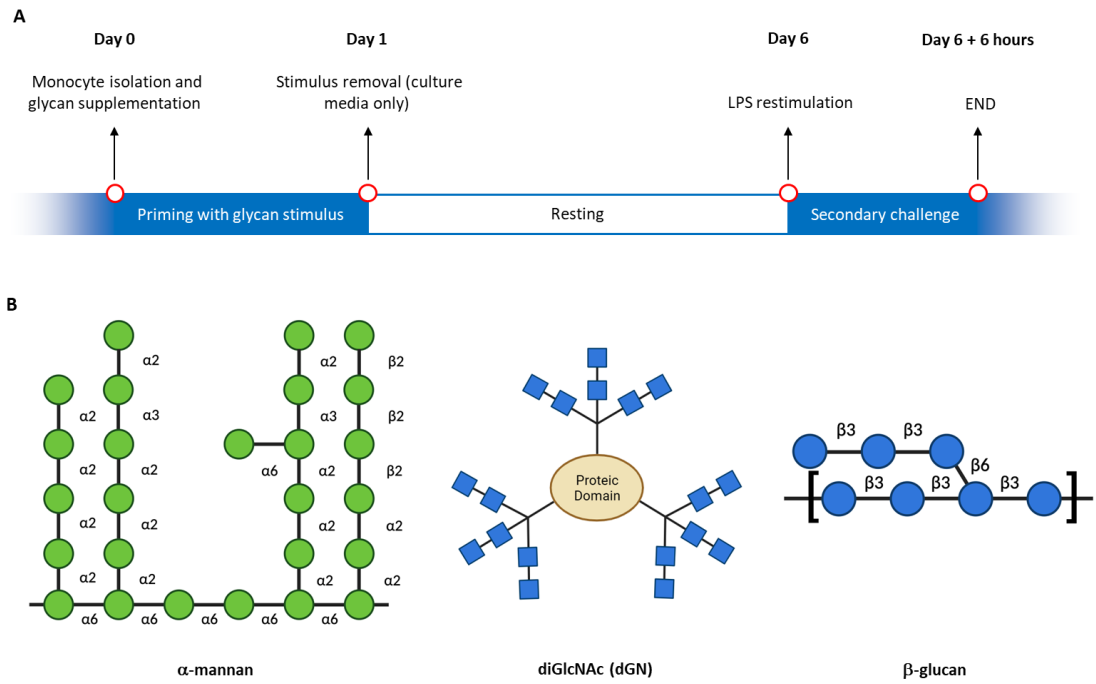

Figure 18. (A) Diagram representation of the experimental procedure employed for the glycan priming of monocytes. After the isolation of the cells, they were exposed to carbohydrate stimuli for 24 hours. This was followed by a 5 day resting period and a 6 hour restimulation period with LPS. (B) Schematic illustration of the structure of the glycan stimuli utilised in the training of the monocytes. α-mannan is built from mannose residues, with an α-1,6 linked backbone connected to several branches. diGlcNAc exposes several GlcNAc adorned domains. β-glucan is constituted by a β-1,3-linked glucose backbone with occasional β-1,6 branches that possess smaller β-1,3 linked chains. Images were created with BioRender.

We started by assessing the expression of CD86 in trained monocytes with flow cytometry. This receptor is an important activation marker and co-stimulatory molecule that binds CD28 in lymphocyte populations. Comparing with the stimulated non-primed monocytes ("Basal + LPS"), β-glucan supplementation led to an increase in the activation of monocytes (**Figure 19-A**). dGN did not influence CD86 levels, but Mannan showcased a positive trend, with an increase in concentration translating into a significant increase in CD86 at the highest concentration of this stimulus. This demonstrates that the monocytes primed with α-mannan displayed higher immune activation (**Figure 19-A**). Afterwards, we explored the GBP expression landscape in the trained monocytes by flow cytometry (**Figure 19-B to 19-E**). We focused our phenotypical analysis on the receptors that stood out in the *in silico* analysis: DC-SIGN, Dectin-1, Dectin-2 and Mannose Receptor. β-glucan didn't induce any significant changes, even though a trend is visible for Dectin-1 levels (**Figure 19-C**). dGN supplementation also yielded similar results, with only Dectin-2 registering expression

alterations, with lower levels at all the concentrations tested for this stimulus (**Figure 19-D**). However, α-mannan priming induced higher Dectin-1 and DC-SIGN levels, even though both lack statistical significance (**Figure 19-B and 19-C**). Curiously, MR and Dectin-2, two receptors capable of recognizing this carbohydrate, presented decreased levels across the range of concentrations, something that is explored in the Discussion section of this thesis. Of note, technical replicates of certain conditions, namely "Mannan 100 μg/mL" and "Mannan 200 μg/mL", presented a limited number of cells, which lead to their exclusion from the analysis and compromised the number of points presented in the graphs in relation to other conditions. Another important note is that Dectin-1 was the only receptor analysed using a non-parametric test due to failing a normality test, even though there are some clear differences in expression of this CTL across the various conditions. Nevertheless, we believe an increase in sample size will resolve this issue.

In our view, these results highlight α-mannan as an imporant glycan with the ability to modulate the GBP expression landscape in monocytes.

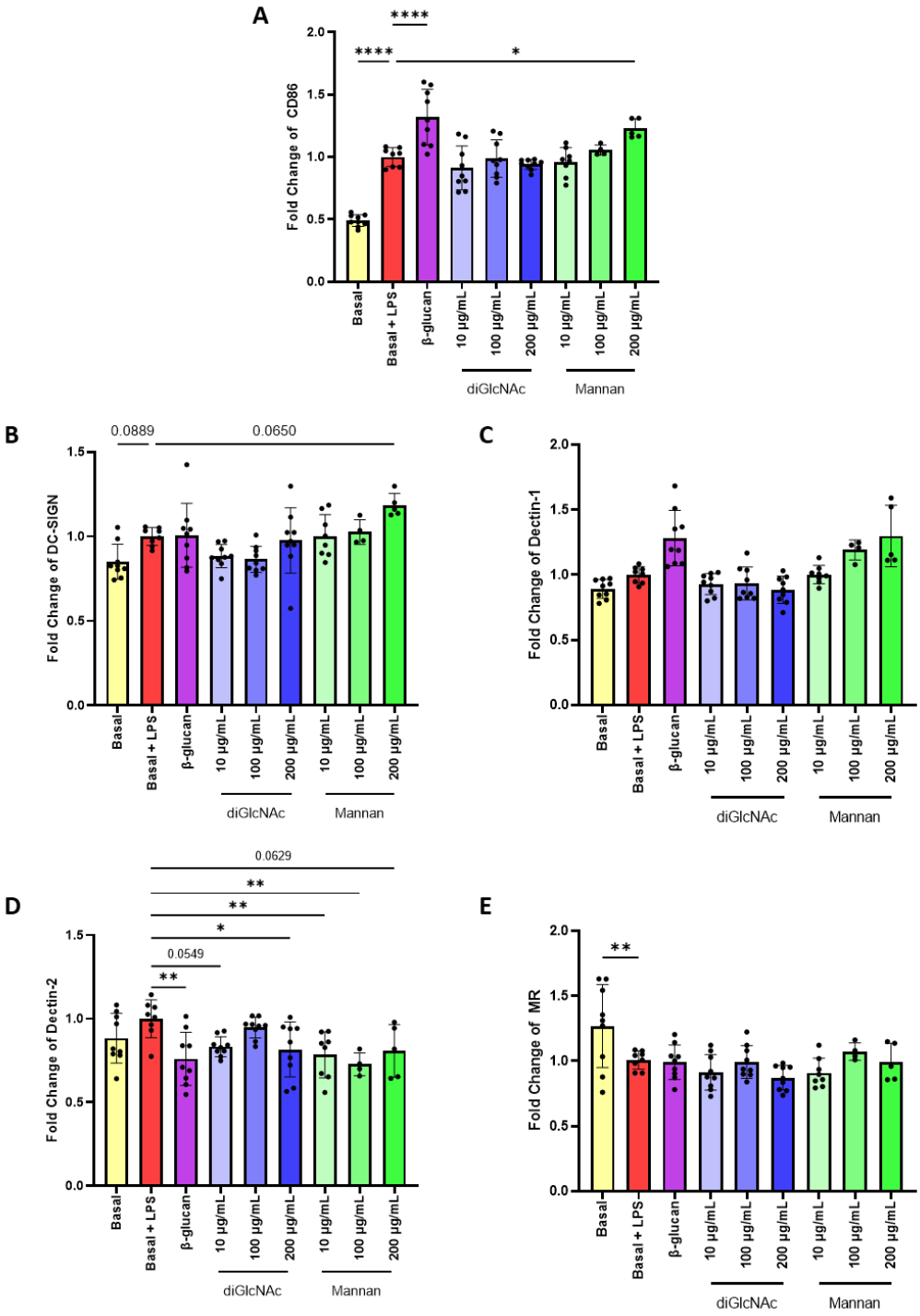

Figure 19. Glycan supplementation of monocytes induced higher levels of CD86 and reprogrammed the expression levels of several pattern recognizing receptors (PRRs). Cultured cells were isolated from two healthy donors and three technical replicates were established from each one (n = 4-9). Monocytes were stained for (A) CD86, (B) DC-SIGN, (C) Dectin-1, (D) Dectin-2 and (E) MR. Results are presented as the fold change of the Median Fluorescence Intensity values normalised to "Basal + LPS" conditions. Outlier tests were followed by Ordinary One-Way ANOVA or Kruskal-Wallis non-parametric ANOVA (depending on normality) and Dunnett's multiple comparison test. Data is represented as Mean ± SD. * $p < 0.05$, ** $p < 0.01$.

An output frequently measured in monocyte training protocols is the production of pro-inflammatory cytokines, such as IL-6 and TNF-α, upon a secondary challenge. To achieve this, we employed the ELISA technique. Indeed, using the stimulated basal condition as a control, β-glucan supplementation led to a massive increase in IL-6 and TNF-α secretion (**Figure 20-A and 20-B**). Once more, dGN priming did not produce significant alterations, whilst mannan exhibited a concentration dependant trend increase in both cytokines' levels, even achieving statistical significance in TNF-α production at the highest concentration (**Figure 20-A and 20-B**). Of note, the non-stimulated cells ("Basal") presented limited secretion of cytokines as expected, which limited the data obtained for this condition. Once again, these results support the hypothesis that α-mannan acts a primer of monocytes, instigating a pro-inflammatory memory-like phenotype.

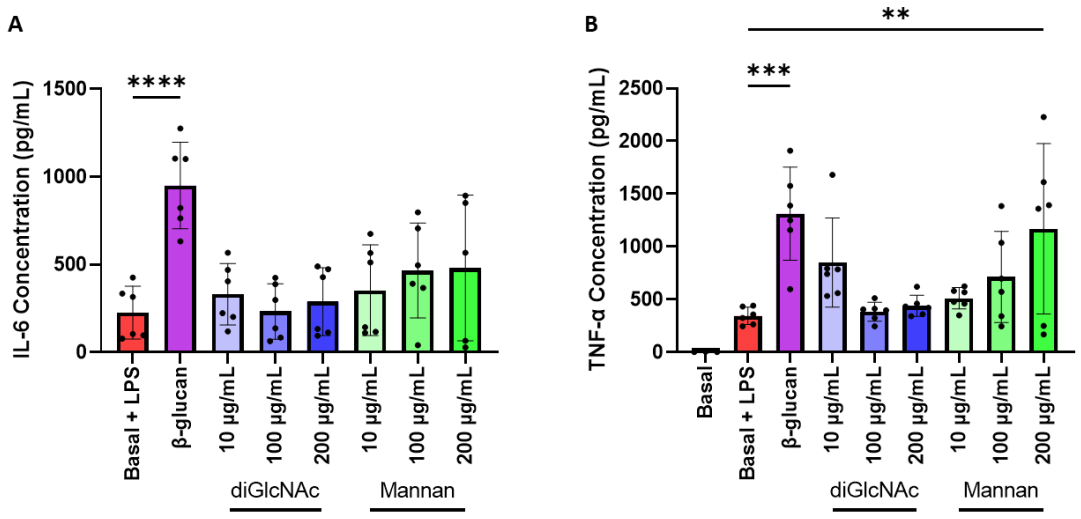

Figure 20. β-glucan and α-mannan primed monocytes to secrete higher levels of pro-inflammatory cytokines. Cultured cells were isolated from two healthy donors and three technical replicates were established from each one (n = 2-6). ELISA assays were performed for IL-6 and TNF-α. Outlier tests were followed by Ordinary One-Way ANOVA and Dunnett's multiple comparison test. Data is represented as Mean ± SD. ** $p < 0.01$, *** $p < 0.001$, **** $p < 0.0001$.

Attempting to further validate this point, we complemented this analysis with an RT-qPCR assessment of two genes, namely *TNF* and *DC-SIGN* (**Figure 21-A and 21-B**), given that levels of both of the resulting proteins had produced the clearest results. β-glucan did not increase the relative expression of *TNF* in relation to stimulated basal conditions ("Basal + LPS"), contradicting the ELISA results (**Figure 21-A**). As for Mannan supplementation, we observe an increasing trend in the mRNA levels of *TNF* in a

concentration dependant manner, but the same was not verified for *DC-SIGN* (**Figure 21-B**). Lastly, dGN demonstrated no relevant impact for both genes, as previously observed. These are preliminary observations that need to be further clarifies in other biological and technical replicates.

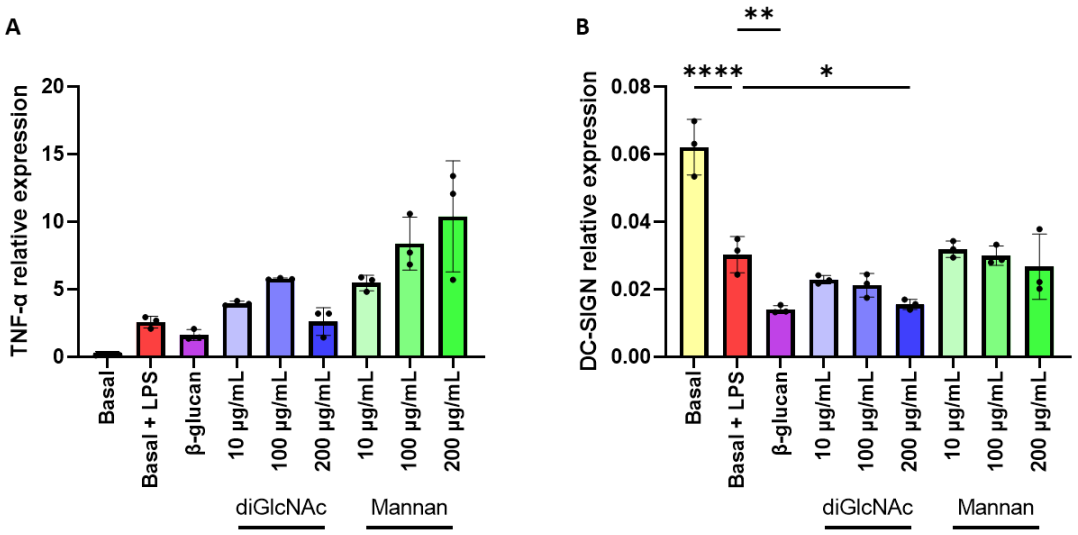

Figure 21. Glycan supplementation of monocytes produced inconsistent RT-qPCR results for (A) *TNF-α* and (B) *DC-SIGN*. For this experiment, only one donor was selected and three technical replicates were established (n = 3). *GAPDH* was used as the housekeeping gene. Outlier tests were followed by Ordinary One-Way ANOVA or Kruskal-Wallis non-parametric ANOVA (depending on normality) and Dunnett's multiple comparison test. Data is represented as Mean ± SD. * $p < 0.05$, ** $p < 0.01$, **** $p < 0.0001$.

This experiment was performed for only one donor due to time constraints. The RT-qPCR *TNF* analysis yielded non-parametric results, with *DC-SIGN* results revealing the opposite. Thus, we believe that an increase in sample size would fix this situation.

All in all, we believe that both the GBP expression and cytokine release analysis allow us to suggest that, in our experimental model, α-mannan may present the capacity to prime and induce a heightened pro-inflammatory state in monocytes, validating our hypothesis. Indeed, even if this statement cannot be made for the transcriptomic realm, this reprogramming translated into a reworked PRR expression landscape at the proteomic level when monocytes were treated with Mannan.

3. Bladder cancer cell lines and glycan-primed monocyte co-cultures

3.1 Bladder cancer cell line glycoprofile characterization

After confirming that the glycan supplementation of monocytes led to their priming, we wanted to evaluate the anti-tumoral capacity of these glycan-trained immune cells. However, before we proceeded with the co-culture of trained monocytes and bladder cancer cell lines, we characterized the surface glycan expression of the latter, as this could have a significant impact on the ability of the immune cells to exert their activity. Indeed, as alluded to in previous sections of this thesis, several glycan structures, such as highly branched complex *N*-glycans, can exert an anti-inflammatory role, supressing immune populations[48]. Furthermore, given the fact we are exploring the impact of GBPs in the immune response of primed monocytes, tumour cells harbouring different levels of certain glycans could directly influence their recognition by the immune cells, manipulating either a pro or anti-inflammatory response.

In this sense, two different bladder cancer cell lines were used: RT112, representative of low grade disease and T24, a model of high grade disease. Even though they originate from tumour samples of different patients, both were resected at the pTa stage, that is, the lesions were confined to the urothelial layer. The glycan signature of both cell lines was obtained by flow cytometry. For this, we employed the use of lectins, molecules with a high affinity for glycans structures. The selected lectins were L-PHA (binds β-1,6-branched complex *N*-glycans), GNA (binds terminal α-1,3-linked mannose residues), SNA (recognizes α-2,6-linked sialic acid residues), ConA (binds oligomannose *N*-glycans) and DC-SIGN BM (recognizes high mannose *N*-glycans and fucose residues). A detailed illustration of their glycan affinities is given in **Table 3** in the Results section.

Looking at the results, it is possible to observe that the T24 cell line, compared to the RT112 cells, displayed lower levels of β-1,6-GlcNAc tetra-antennary *N*-glycans, which was accompanied by a lower α-2,6 sialic acid detection (**Figure 22-A and 22-E**). Furthermore, the T24 cells presented decreased GNA levels in relation to the RT112 cell line, which means that it exhibits lower expression of high-mannose glycans

(**Figure 22-B**). However, the GNA to L-PHA ratio remains similar between both cell lines (**Figure 22-C**). Paradoxically, no differences were observed in the ConA staining and DC-SIGN BM displayed higher binding in the T24 cell line, suggesting a contribution from fucose residues, that are also ligands of DC-SIGN (**Figure 22-D and 22-F**).

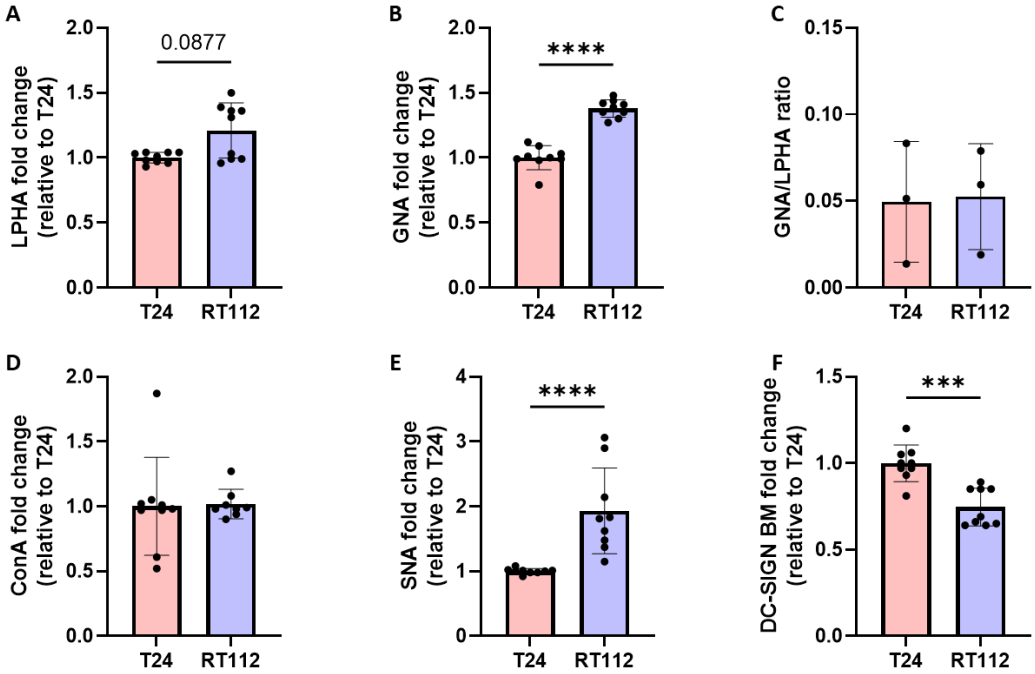

Figure 22. Bladder cancer cell line surface glycan expression profile. Results shown in graphs A to E are the outcome of three different experiments, each one with three technical replicates (n = 9). GNA to L-PHA ratios (graph F) were calculated for each individual experiment for both cell lines, yielding an n = 3. Outlier tests were followed by Mann-Whitney U tests. Data is represented as Mean ± SD. ** $p < 0.01$, **** $p < 0.0001$.

To complement the flow cytometry analysis, we performed a Lectin Blot in order to observe the glycan pattern of all the resolved protein from each cell line. For this, we looked at three of the previously selected lectins: L-PHA, GNA and DC-SIGN BM (**Figure 23**). Consistently, we conclude that both complex and high mannose glycans are more common in the RT112 cell line, corroborating the flow cytometry results (**Figure 23-A and 23-B**). However, DC-SIGN BM demonstrated contradictory results, with the T24 cells showcasing lower levels of ligands for this lectin.

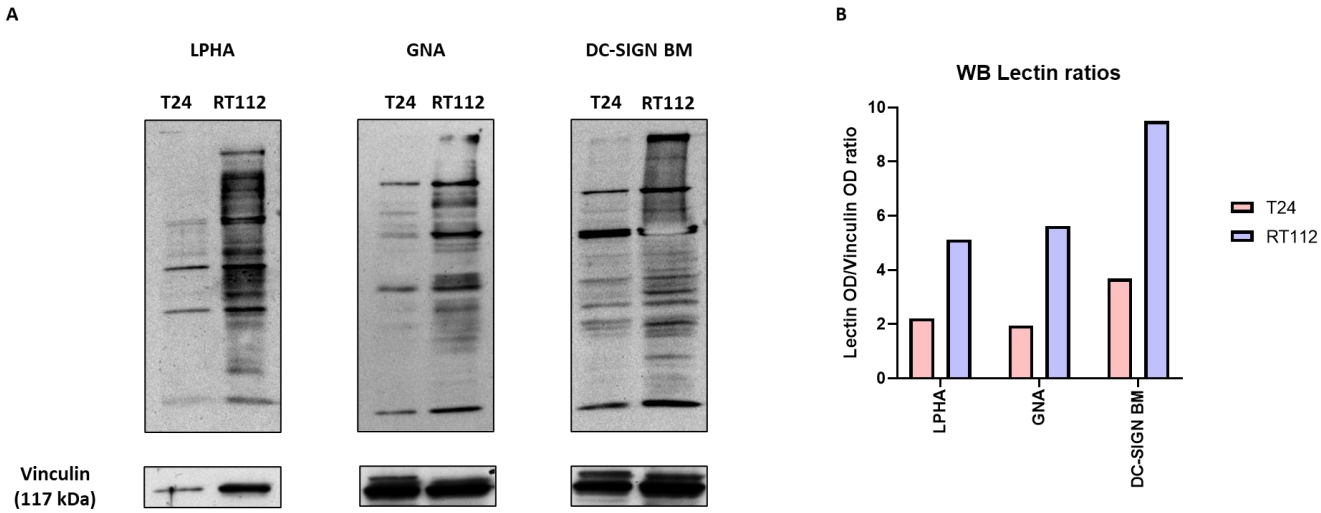

Figure 23. Lectin blot of the total protein lysate for the RT112 and T24 bladder cancer cell lines. Vinculin was used as the housekeeping gene. (A) Scans of the obtained gels. (B) Ratio between the measured Optical Density (OD) of the detected bands using the different lectins and their respective vinculin control.

Overall, these results revealed significant differences in the glycoprofiles of the more aggressive T24 cell line and the lower grade RT112. With this knowledge, we were wanted to assess the potential impact of differing glycomes in the response of glycan-trained monocytes.

3.2 α-mannan primed monocytes displayed higher anti-tumoral activity

After the glycome characterization, we moved onto the co-cultures of the bladder cancer cell lines and glycan-primed monocytes. As was referred previously, the training of monocytes induces a memory-like heightened pro-inflammatory status, equipping these cells with a stronger capacity to deal with secondary threats, such as tumours. Given that dGN did not appear to reprogram the cells, as seen in section 2, this stimulus was not utilised for this part of the work, meaning that the immune cells were trained with β-glucan (positive control) and α-mannan at 200 μg/mL. **Figure 24** presents a diagram of the experimental procedure employed.

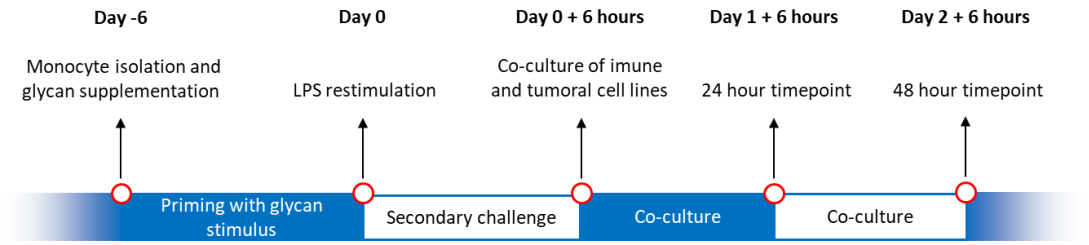

Figure 24. Schematic representation of the co-culture experimental procedure. Initially, monocytes underwent training *in vitro*. Afterwards, the immune cells were restimulated with LPS for 6 hours and cultured with RT112 or T24 bladder cancer cell lines in a 1:10 target:effector ratio. Two different timepoints were used to better evaluate the tumoricidal ability of monocytes: 24 and 48 hours.

Different timepoints, 24 and 48 hours, were tested to get a better understanding of the capacity of trained monocytes to induce tumour cell death in both the RT112 and T24 cell line. The tested target to effector ratio was $1:10^{158}$ and immune cells were obtained from one healthy donor. Unfortunately, and due to lack of time, we only obtained robust results for the T24 cells at the 48-hour timepoint, a topic that is further explored in the Discussion section. Delving into the results (**Figure 25**), we observe that the control with only tumour cells ("T24 control") displayed around 50% live cells, which reflects the potentially suboptimal culture conditions. As for the non-stimulated and stimulated basal monocytes, it is possible to recognize comparable levels of tumour cell viability that are slightly lower than the cell line only control (**Figure 25**). This contradicted our expectations, as the LPS supplementation was anticipated to better prepare the immune cells for the tumour cell challenge. β-glucan priming of monocytes produced another paradoxical result, culminating in levels of live cells comparable to the T24 control condition. Interestingly, the α-mannan trained immune cells lead to a considerable increase of early and late apoptotic cells, indicating that the monocytes were more capable of eliminating the T24 cells. Curiously, necrotic cells were mostly absent when immune cells were present, which can be associated with the phagocytic capacity of monocytes.

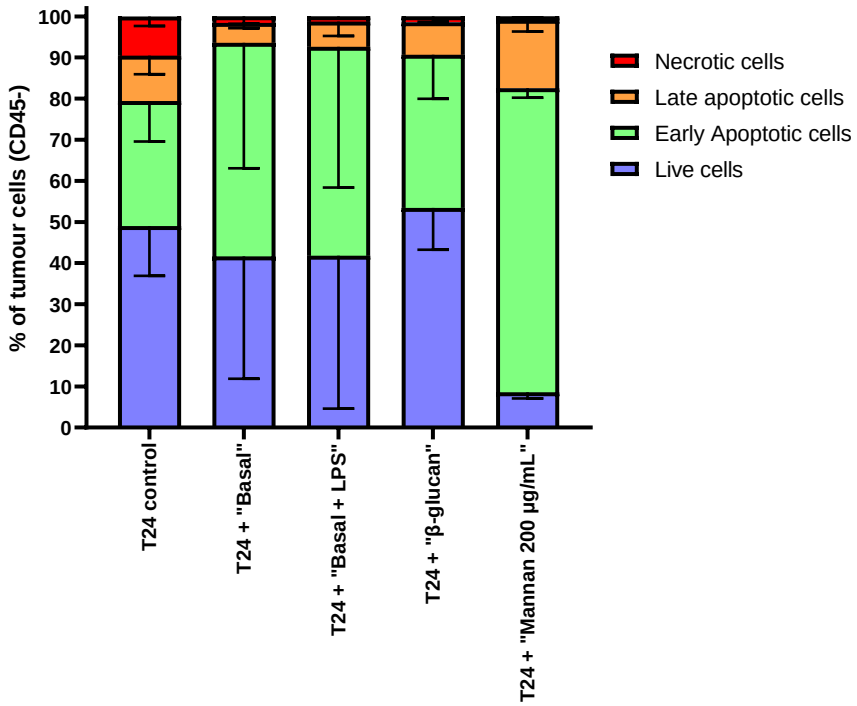

Figure 25. T24 cell line viability after 48 hours of co-culture with trained monocytes. The immune cells were supplemented with either β-glucan or α-mannan at 2,5 ug/ml and 200 ug/mL, respectively, and restimulated for 6 hours with LPS before co-culture with tumour cells. Non-trained monocytes were used as control for the priming of these cells. A further control with only tumour cells was added in this experiment. Monocytes were isolated from one donor and three technical replicates were established (n = 2-3). Cells were stained with CD45, allowing the distinction of tumoral and immune fractions. Furthermore, Annexin V and PI facilitated the evaluation of cell viability, with the percentage (%) of live, early apoptotic, late apoptotic and necrotic cells being displayed for each condition. Outlier tests were followed by a Two-way ANOVA and Dunnett's multiple comparison test. Data is represented as Mean ± SD.

Although several optimizations of this experimental model are necessary in the future (further discussed in the next section), our preliminary data suggests that the priming of monocytes with α-mannan appears to be able to train immune cells with higher anti-tumoral activity, a crucial result that validates our hypothesis, despite needing further confirmation.

4. Characterization of surface receptor expression in monocytes derived from non-muscle invasive bladder cancer patients treated with BCG instillations

As was explored previously in this thesis, in the context of non-muscle invasive bladder cancer (NMIBC), part of the anti-tumoral response urged by BCG instillations is due to the reprogramming of monocytes and the triggering of trained immunity. However, the exact mechanism behind this process is still unknown. As our experimental model demonstrated, certain pathogen-derived carbohydrates possess the ability to increase the levels of certain GBPs, like DC-SIGN and Dectin-1, which lead us to question if BCG harbours the same capacity, as this pathogen also displays glycan moieties at its surface.

For this, we collected a blood sample from an NMIBC patient currently undergoing maintenance BCG immunotherapy. We isolated the monocytes and restimulated them for a 6-hour period with LPS, mimicking our experimental model – cell activation after training (schematic representation on **Figure 26**). Afterwards, we performed the analysis of the previously selected surface receptors by flow cytometry. (**Figure 27**). We observed that the restimulated monocytes presented a tendency for higher CD86 levels, confirming the LPS-induced activation (**Figure 27-A**). As for the GBP expression, no differences were observed (**Figure 27-B to 27-E**), with the exception of a tendency found for an increase of Dectin-1 levels in the restimulated monocytes (**Figure 27-C**). Of note, it is important to highlight the absence of a control condition in this experiment, as we could not get a blood sample from a NMIBC currently undergoing alterne therapies to BCG or subjected to no treatment. Therefore, in this work, we were not able to definitively evaluate the ability of BCG to induce a shift in monocyte PRR expression levels after training.

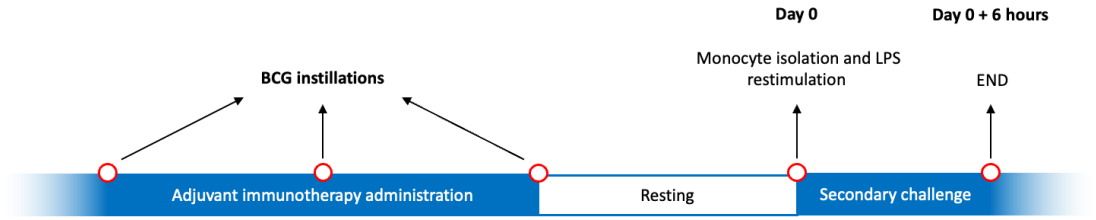

Figure 26. Schematic representation of the experimental procedure employed for the analysis of patient-derived monocytes. Patients underwent a BCG instillation regime that trained the circulating monocytes. We then isolated these cells and rechallenged them with LPS for 6 hours.

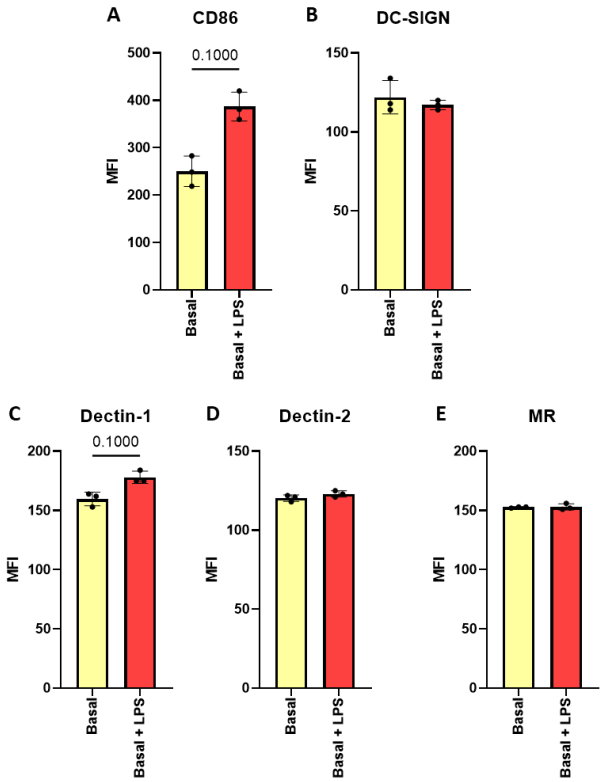

Figure 27. GBP landscape in a BCG treated NMBIC patient. Cultured cells were isolated from one donor and three technical replicates were established (n = 3). Monocytes were stained for (A) CD86, (B) DC-SIGN, (C) Dectin-1, (D) Dectin-2 and (E) MR. Outlier tests were followed by Mann-Whitney U tests. Data is represented as Mean ± SD.

DISCUSSION

Non-muscle invasive bladder cancer (NMIBC) constitutes a serious health problem, being the urothelial malignancy with the highest incidence[1,7]. Even though progression to a more aggressive muscle-invasive stage is not the most likely outcome, it still represents approximately 30% of cases[7,10]. Therefore, it is important to guarantee that we can reduce this risk and limit the progression of NMIBC as early as possible. Currently, high-grade NMIBC malignancies are treated with BCG instillations, as it has been shown that this leads to improved recurrence-free survival[19]. However, not all patients respond and this adjuvant immunotherapy presents some side effects that might compromise the efficacy of the treatment or, in rare scenarios, trigger serious infections[20–22].

It is believed that part of the effectiveness of BCG instillations arises from a phenomenon known as Trained Immunity (TI)[146]. Essentially, this mechanism consists in the epigenetic reprogramming of certain innate immune cells, including monocytes/macrophages, when exposed to an initial stimulus, resulting in a stronger response against a secondary immune challenge[117,118]. Currently, it is largely unexplored whether BCG or other priming stimuli, after inducing this enhanced immune phenotype, can change the glycan-binding protein expression landscape. Therefore, with this project, we set out to study the impact of TI in the expression of pattern recognizing receptors (PRRs) that bind glycans. Moreover, we also explored the potential effect of certain pathogen-derived carbohydrates as inducers of this phenotype, in order to analyse the tumoricidal ability of primed monocytes.

Initially, we analysed publicly available RNA sequencing datasets where monocytes had been exposed to different infectious stimuli that induced a trained phenotype in monocytes[150,155,156]. These pathogens are covered in diverse glycans that can be recognized by the different GBPs expressed by innate immune cells, with some of these structures playing important roles in the pathogenicity of these organisms. For example, the highly mannosylated gp120 protein present in the HIV virus plays an important role in the infection of dendritic cells (DCs) through DC-SIGN[151]. Exploring the transcriptomic datasets, we concluded that several GBPs had their expression altered after exposure to these infectious stimuli. Indeed, the most consistently elevated PRR was DC-SIGN, with Dectin-1, Dectin-2, MR, and MGL also being upregulated in some datasets. This led us to the assumption that the glycans

expressed by the various pathogens played a significant role in the induction of the heightened phenotype displayed by the monocytes. In particular, a good portion of the upregulated PRRs display an affinity to mannose residues. Therefore, we proposed that using a pathogen-derived saccharide, to supplement monocytes *in vitro* could induce a trained phenotype.

With this in mind, we designed our experimental procedure based of previous work in the field[157], focusing fungal mannans and diGlcNAc as our stimuli of interest. Our *in silico* results led us to postulate that Mannan training could potentially result in the reshaping of the glycan binding protein expression landscape in monocytes. Literature on this topic is limited, meaning that little is known about PRR expression alterations in the context of TI. Our FACS analysis focused DC-SIGN, Dectin-2 and MR, as the main hits from the transcriptomic analysis, and Dectin-1, for similar reasons and its importance for TI induced by our positive control. Furthermore, we also analysed CD86 levels, as a marker for the activation of the cells. dGN demonstrated a relatively innocuous influence in the priming of monocytes in respect to all the mentioned receptors. As for cells supplemented with Mannan, it is possible to observe an increasing trend in CD86 levels, with the highest concentration of this stimulus achieving statistical significance. Moreover, DC-SIGN and Dectin-1 expression displayed an increase in the same conditions, highlighting the potential for α-mannan to manipulate the GBP landscape.

In reality, little is known about the potential involvement of most of the receptors we studied in Trained Immunity, with the exception of Dectin-1. Indeed, fungal mannans, being rich in mannose, do not constitute a ligand of this C-Type Lectin, that mainly binds β-glucan, which made its upregulation in cells supplemented with Mannan surprising. One possible explanation could be that this GBP had its levels indirectly increased. It has been shown that, during the recognition of *Candida albicans*, Dectin-1 itself can recruit DC-SIGN to the binding site through actomyosin contractibility[159]. Therefore, a similar reversed mechanism could be at play here, where a receptor that recognizes Mannan is inducing Dectin-1 expression. Nevertheless, the upregulation of Dectin-1 is a positive sign in our view, priming the monocytes for an improved immune response. To be absolutely sure of the relevance of our results, we need to complement our approach with other techniques. As was

alluded to previously, TI is the result of epigenetic alterations that prime innate immune cells to be better equipped to deal with potential threats. Therefore, it would be pertinent to perform an analysis of chromatin markers, particularly in immune response related genes, namely Dectin-1 and the other studied PRRs. For this, we could employ a couple of approaches. The starting point would be the chromatin immunoprecipitation (CHIP), which could then be followed by sequencing (CHIP-seq). For a less specific overview, a western blot analysis could be used after CHIP. With this, we could understand if α-mannan supplementation could induce the epigenetic reprogramming of monocytes, which would constitute strong evidence in favour of our hypothesis.

In contrast, Dectin-2 levels presented lower levels across all conditions. This receptor mainly targets high mannose carbohydrates, with α-mannan being a well-known important ligand of this GBP[160], hence, we expected to observe an increase after priming with this glycan. Taylor *et al.* demonstrated that Dectin-2 is not constitutively expressed by monocytes, with an inflammatory stimulus being required for the upregulation of this receptor[161]. Furthermore, these authors have shown that, in a mouse model, Dectin-2 does not need to be directly bound to be more expressed in monocytes subjected to inflammatory environments, with intravenous LPS prompting higher levels of this PRR. This is quite puzzling, as we provided the monocytes with two stimuli that should either target or potentially elicit this CTL's expression. Nevertheless, our experiments were performed in an *in vitro* setting and in human cells, a different model that might not correlate directly to the *in vivo* mouse procedures. Moreover, on a more speculative note, the training program that Mannan induces might not target Dectin-2 even if this receptor is initially bound, something that could be better understood with, for example, the CHIP-seq technique previously mentioned.

In a similar fashion, MR also presented low levels across the spectrum of tested conditions when compared with the non-stimulated "Basal" setting. This CTL can also recognize fungal mannans[162] and is expressed at a basal level in matured monocytes[163]. We believe that the restimulation with LPS could have caused this generalised decrease in MR expression as it is frequently claimed that this stimulus

can induce the activation of mature myeloid cells, often associated with lower levels of MR in *in vitro* settings[164].

Lastly, DC-SIGN was upregulated in the Mannan supplemented conditions. This CTL, as the name implies, is typically expressed by dendritic cells and is described as undetectable in circulating monocytes[165]. Nevertheless, it has also been found in several tissue macrophage populations[166,167] and other studies where monocytes were isolated and placed in culture also detected DC-SIGN after maturation of the cells[168,169]. Once again, this PRR has the ability to bind α-mannan[170], with this receptor being a good potential candidate for the training of the monocytes in our experimental setting. In fact, DC-SIGN can trigger similar pathways to Dectin-1. The latter, when exposed to β-glucan, activates Raf-1, initiating a crucial signalling avenue that culminates in the establishment of TI[131]. Analogously, Raf-1 can play a vital role in DC-SIGN signalling upon the recognition of certain stimuli, including rich in mannose Man-LAMs and *Candida albicans* cell walls[171]. However, it is worth pointing out that typical response to this mycobacterium glycan structure is an immunosuppressive one[138,141] and the downstream targets of Raf-1 activation differ from Dectin-1[131,171]. Therefore, this parallel could be an interesting route to explore, but with a realistic expectation level. All in all, DC-SIGN being upregulated is, in our perspective, a positive outcome of our experiments, that requires further probing to better understand the potential mechanism.

Additionally, this work placed a heavy focus on CTLs as the potential initiators of glycan induced TI and effectors of the enhanced pro-inflammatory activity. On the one hand, previous evidence from experimentation with other carbohydrate stimuli, such as β-glucan, place members of this group of PRRs at the centre of the mechanism. On the flipside, there are other crucial receptors involved in this process, including Toll-Like Receptors (TLRs). Indeed, TLRs have a vital role in innate immunity and are frequently upregulated in trained monocytes. For instance, BCG vaccination induced a long-term upregulation of TLR4 in these cells[172]. Moreover, it is known that these receptors interact closely with CTLs in many immune responses, including the Dectin-1 and TLR-2 mediated recognition β-glucan[173] and the crosstalk between DC-SIGN and TLRs upon Man-LAM binding[174]. In fact, TLRs have even been implied to be crucial to the recognition of other glycan structures, namely fungal *O*-linked mannosyl

residues[175]. Furthermore, CD14 and TLR4 have also been deemed vital for TNF-α production induced by fungal mannans[176]. Therefore, we believe that other receptors, in particular TLR2 and TLR4, are deserving of some attention in the context of our experimental model and could play an important role in the establishment of the monocyte priming and the potency of their activity. In future testing, it is relevant to address this using similar techniques to the ones showcased in this thesis in conjugation with blocking antibodies of TLRs.

To determine if the glycan supplementation could induce the priming of the cells, we employed ELISA assays for TNF-α and IL-6. Delving into our results, dGN did not induce any relevant alterations, which was somewhat expected, given that previous work from our group in the setting of colitis highlighted that supplementation of other immune populations and mice models with GlcNAc residues resulted in the suppression of their pro-inflammatory activity[177]. Nonetheless, chitin, another component of the fungal cell walls that is rich in GlcNAc, has been linked to a training effect, which prompted us to investigate dGN's priming potential[178]. In contrast, α-mannan supplementation was able to induce an increase in secretion of both the evaluated cytokines, with TNF-α displaying statistical significance at the highest concentration provided. This strongly suggests that fungal mannans possess the ability to prime monocytes. Nevertheless, these findings need to be further validated. Although, it is worth pointing out that the concentrations that were tested were much lower than the ones we adopted and Mannan was dissolved in the culture medium instead of coated. As stated before, CHIP-seq analysis of TNF-α and IL-6 could greatly strengthen this analysis.

Moreover, the effector potential of these trained monocytes was evaluated by the gene expression quantification of the genes coding for the most altered PRR, DC-SIGN (coded by *DC-SIGN*), and most altered cytokine, TNF-α (coded by *TNF*). This constitutes an indirect way of evaluating the epigenetic alterations induced by TI, as a more open chromatin should be more available for elevated mRNA transcription. Briefly, dGN presented no relevant stimulating ability, with Mannan priming inducing a concentration dependant increase in *TNF* mRNA levels. Surprisingly, β-glucan trained monocytes did not upregulate *TNF* mRNA levels as was expected. As for *DC-SIGN*, the RT-qPCR revealed paradoxical results, with the non-stimulated "Basal" condition

displaying a big peek, that was not matched by any of the primed conditions. An important point to make is that, sometimes, mRNA levels do not translate cleanly into protein expression[179], with our results revealing some instances of this. For example, the TNF-α ELISA assay revealed that our positive control, β-glucan, induced a clear upregulation of the secretion of this cytokine, with the PCR analysis yielding transcription levels below the "Basal+LPS" condition. A similar negative correlation can be established for the 200 µg/mL Mannan supplemented monocytes and for the DC-SIGN results. However, a positive remark can be made in relation to this CTL, as the successful detection of its expression at the mRNA level strengthens the validity of our FACS results and reinforces the fact that our cells expressed DC-SIGN. To conclude this topic, it is relevant to mention that the RT-qPCR analysis was performed for one donor only due to time constraints. Thus, the outcome should be interpreted with some care and further experiments with more donors need to be performed to form a more complete picture. With this in mind, we consider that the PCR results do not weaken our previous testing, with the receptor expression and cytokine secretion analysis yielding strong evidence for Mannan exerting a potential training effect in monocytes.

Following this, we wanted to evaluate if the priming of the monocytes could contribute positively to the ability of these cells to eliminate their tumoral counterparts. However, given the fact we one of the elements we are assessing is the expression of various GBPs, it was relevant to characterise the glycome of both the cell lines we intended to use, T24 and RT112, as these receptors can directly bind the various carbohydrates. Indeed, as was touched upon in previous sections, several glycan alterations in cancer cells can manipulate the immune response. For example, high levels of β-1,6 branched *N*-glycans have been demonstrated to mitigate anti-tumoral immunity and favour disease progression[24,48]. On the flipside, some GBPs have been demonstrated to potentiate strong immune responses against tumour cells. Previous work from our group demonstrated that DC-SIGN and MR, when bound to high-mannose epitopes, could improve dendritic cell function[48]. Additionally, Dectin-1 has been postulated to have the ability to recognise *N*-glycan structures, fuelling a strong myeloid-NK cell axis that harbours improved anti-tumoral capacity[112].

To evaluate the glycoprofile of the bladder cancer cell lines, we employed both flow cytometry and a lectin blot procedure. We used several lectins with different glycan affinities, as was explained in the Results section. The results of the flow cytometry experiment revealed that the T24 cell line had lower levels of branched β-1,6 complex (L-PHA), high mannose (GNA) and α-2,6 sialylated (SNA) *N*-glycans compared to the RT112 cells. ConA staining indicated no differences, whilst T24 presented higher levels of DC-SIGN binding motifs. Given the higher GNA levels detected in this cell line, this difference is most likely due to higher fucosylation, important structures in the context of cancer also bound by DC-SIGN[105]. The lectin blot results further corroborate this assessment, as lower levels of mannose terminated and complex branched *N*-glycans were detected in the T24 cell line. However, DC-SIGN BM presented contradictory results, with the RT112 cells being the ones presenting stronger detection with this lectin. In this experiment, whole cell lysates are utilised, justifying the observed paradox. Nonetheless, for our hypothesis, the evaluation of surface glycosylation is more relevant than the total carbohydrate profile, as it will directly interact with the PRRs expressed by the trained monocytes, which gives the flow cytometry results higher importance.

With the glycome characterised, we started the co-culture experiments. We chose a 1:10 target to effector ratio[158] (20 000 cells of each cell line - RT112 and T24 – with 200 000 primed monocytes per well) and two different timepoints (24 and 48 hours). Unfortunately, data could only be retrieved for the 48-hour timepoint with the T24 cell line, something that is explored later in this section. Here, we observed that the Mannan training of the monocytes lead to elevated levels of early and late apoptotic cells when compared to the T24 control (only tumour cells) and the conditions with the non-primed monocytes (T24 + "Basal" and T24 + "Basal + LPS"). Unexpectedly, β-glucan, our positive control, appeared to induce higher tumour cell viability, which goes against what is currently described in the literature[180,181]. We believe that this could be due to a suboptimal experimental setting, where the tumour cells were not properly detached in most conditions. Indeed, the cells were cultured in 96 well U-bottom plates, which could have complicated the detachment with trypsin. On the flipside, β-glucan can induce proliferation of myeloid cells[181] (something that we observed in this experiment), crowding the wells and potentially

making it easier to detach the tumour cells, giving the impression of higher viability. We also believe that the lack of detachment of tumour cells compromised the remaining timepoints for the RT112 (both 24 and 48 hours) and T24 cell lines (24 hours). Therefore, different plates should be considered in the future, as well as different effector to target ratios and other methods to detach the cells. Another curious remark is the lack of necrotic tumour cells in the presence of immune counterparts. This could be due to the natural role of these cells as phagocytes, which culminates in the removal of the necrotic tumour cells[182]. Thus, an assay where the cell lines are previously labelled, for example, using a dye, and then co-cultured is a pertinent way to assess the capacity of these immune cells to phagocyte the tumoral cells or their remains[183]. Furthermore, this could have the added advantage of giving clues to better understand the mechanism behind training induced anti-tumoral activity.

Overall, the results seen for Mannan trained monocytes are a very encouraging first step. Even though we have not explored a potential mechanism in this thesis, the upregulation of DC-SIGN and Dectin-1 could be relevant because, as was previously stated, these receptors have been associated with a potential anti-tumoral role[48,112]. Additionally, a recent paper uncovered relevant results related to the potential of the anti-tumoral capacity of this carbohydrate. Using a variety of tests, Son *et al.*[184] highlighted that Mannan nanoparticles could elicit a very strong tumour supressing response in a variety of mouse models, even inducing complete remission in some cases when paired with a CD4+ T cell stimulating antibody. Moreover, work from our group has recently elucidated the role of high mannose *N*-glycans as important drivers of the pro-inflammatory autoimmune response observed in lupus nephritis[185]. These articles constitute an important validation of our initial premise and further strengthens our results. Nevertheless, further experiments with the tweaks mentioned above are necessary, as we could not obtain a comparison between the viability of both cell lines that present different glycoprofiles, which would help elucidate the role of the GBPs of interest.

Another important element of our hypothesis rested on the potential effects of BCG instillations as drivers of a shift in GBP expression in monocytes derived from NMIBC patients. Indeed, our *in silico* analysis produced encouraging results, with the

dataset where BCG is used as a training stimulus presenting considerable alterations. We were provided with one blood sample from an NMIBC patient in the maintenance stage of treatment, enabling us to perform a FACS analysis. However, the results we observed did not support our premise, as the PRRs of interest showed little to no change, with Dectin-1 being the one receptor that displayed a slight increasing tendency in expression. As expected, the LPS-stimulated cells also presented elevated CD86 levels. It is worth noting that we are missing an essential part of this analysis, as we do not have a non-trained control to compare this data to. In the future, we intend to study monocytes from a higher number of NMIBC patients not only treated with BCG immunotherapy, but also other forms of treatment, namely chemotherapy, allowing us to compare the GBP profile.

As has been the case for most of this discussion, the literature we could uncover on this topic was rather sparse. Whilst there is no doubt that BCG can trigger a TI programme in innate immune cells[143,146], the effect on the GBP landscape is largely unexplored. A few articles, though, touched on the impact of BCG vaccination in the training of monocytes and the levels of some CTLs[143,172]. Indeed, MR was found to be upregulated in the long-term, with Dectin-1 revealing no changes, contradicting the tendencies observed in our testing. However, in hindsight, it is obvious to us that our analysis has some limitations. Other than the already mentioned lack of a control, after monocyte extraction, the cells were immediately restimulated with LPS, leaving little time for the maturation process. This can impact the strength of the immune response[186] and compromise the ability of these immune cells to express certain PRRs, like is the case for DC-SIGN[165] and MR[163], that are not observed in circulating monocytes and require a maturation period to be detected. Ultimately, the results presented in this thesis do not seem to depict the phenotype induced by BCG instillations in NMIBC patients and further studies are needed to correctly assess the expression of the GBPs of interest. For this, the monocytes must be rested for a few days after extraction, allowing them to mature and better reflect their trained phenotype upon rechallenge with a secondary stimulus.

To conclude, we believe that this thesis presents some robust, although preliminary, evidence for fungal mannan being a potential inducer of TI in monocytes, improving their ability to deal with a tumoral challenge through higher cytokine

secretion and improved sensing capacities. This thesis lays down a foundation to build future work upon, where sterile *in vivo* training of monocytes with glycans could become a powerful weapon against cancer.

CONCLUSIONS AND FUTURE PERSPECTIVES

Throughout this thesis, a major hypothesis has been tested: can fungal mannans induce trained immunity in monocytes, increasing their tumoricidal activity? Indeed, we have evidence that supports that *in vitro* supplementation of these innate immune cells with this carbohydrate structure appears to improve their pro-inflammatory cytokine secretion ability and reprogrammed the GBP landscape expression, with increased levels of Dectin-1 and DC-SIGN being reported. Thus, these results point towards the establishment of a pro-inflammatory memory-like phenotype in glycan-primed monocytes. Furthermore, co-culture assays of Mannan-trained monocytes and cancerous cells highlighted the capacity of these immune cells to supress a tumoral challenge. Overall, we consider the work presented in this thesis constitutes strong evidence that supports our hypothesis.

Nonetheless, future experiments are necessary to better understand the mechanisms at play. To start with, the monocyte cell culture protocol needs, in our view, additional refinement. Indeed, during this project, we focused heavily on the establishment of an *ex vivo* model that allowed us to evaluate the priming capacity of certain carbohydrate stimuli, something we believe we achieved. However, for reasons we do not understand, the cell viability was, occasionally, diminished when the monocytes where supplemented with β-glucan and higher concentrations of α-mannan suffered relatively to basal conditions (the total number of cells detected in flow cytometry analysis was lower in these conditions), even though we used concentrations that, at worst, matched what has been reported in literature as not impactful for cell survival[130,184]. For future experimentation, this needs to be addressed.

A major piece of information that our analysis is missing is the analysis of the epigenetic paradigm, a central part of the mechanisms behind TI. Therefore, a CHIP-seq analysis would give us great insight into chromatin alterations that occurred in genes of particular importance to the immune response, such as TNF-α, IL-6 and GBPs of interest. Additionally, to gain further knowledge of the mechanism that could be priming the monocytes upon exposure to Mannan, it would be relevant to analyse PRR expression immediately after exposure to this high-mannose carbohydrate. This would allow the identification of the receptors that could be piloting the epigenetic reprogramming of the monocytes. Moreover, this analysis could be further

complemented with the inhibition of important signalling pathways triggered by the identified GBPs, enabling us to pinpoint the most relevant molecules.

In addition, the co-culture assays had certain limitations, as was alluded to in the Discussion section. Thus, changes should be implemented to strengthen the reported results. We also attempted to establish a correlation between the Mannan-trained monocytes PRR expression and the clinical setting of BCG-treated non-muscle invasive bladder cancer patients. This experimental model, though, was also somewhat compromised and, importantly, the analysis lacked a control group, two elements we must improve in future evaluations.

Focusing the medium to long-term potential of this project, *in vivo* studies in mice models of bladder cancer (and, potentially, other neoplastic diseases) are an interesting prospect, as they would allow for the appraisal of the potential of mannan supplementation and TI as therapeutic options in the context of cancer. Additionally, instead of using fungal mannan in its regular form, functionalization of this carbohydrate through the development of a nanoparticle constituted by a mannan shell could be a very interesting avenue to explore, something that was performed by Son *et al.*[184] with great success. Furthermore, this could allow for the inclusion of other molecules with glycan modulating/immune stimulating properties on the inside of the nanoparticles, providing another layer of treatment to the cancer.

References

1. Sung H, Ferlay J, Siegel RL, et al. Global Cancer Statistics 2020: GLOBOCAN Estimates of Incidence and Mortality Worldwide for 36 Cancers in 185 Countries. *CA Cancer J Clin*. 2021;71(3):209-249. doi:10.3322/caac.21660
2. Mayo M, Potugari B, Bzeih R, Scheidel C, Carrera C, Shellenberger RA. Cancer Screening During the COVID-19 Pandemic: A Systematic Review and Meta-analysis. *Mayo Clin Proc Innov Qual Outcomes*. 2021;5(6):1109-1117. doi:10.1016/j.mayocpiqo.2021.10.003
3. Rucinska M, Nawrocki S. COVID-19 Pandemic: Impact on Cancer Patients. *Int J Environ Res Public Health*. 2022;19(19). doi:10.3390/ijerph191912470
4. Hanahan D, Weinberg RA. The Hallmarks of Cancer. *Cell*. 2000;100:57-70.
5. Hanahan D, Weinberg RA. Hallmarks of cancer: The next generation. *Cell*. 2011;144(5):646-674. doi:10.1016/j.cell.2011.02.013
6. Hanahan D. Hallmarks of Cancer: New Dimensions. *Cancer Discov*. 2022;12(1):31-46. doi:10.1158/2159-8290.CD-21-1059
7. Sanli O, Dobruch J, Knowles MA, et al. Bladder cancer. *Nat Rev Dis Primers*. 2017;3. doi:10.1038/nrdp.2017.22
8. Degeorge KC, Holt HR, Hodges SC. Bladder Cancer: Diagnosis and Treatment. *Am Fam Physician*. 2017;96(8):507-514. www.aafp.org/afp
9. Janković S, Radosavljević V. Risk factors for bladder cancer. *Tumori*. 2007;93(1):4-12. doi:10.1177/030089160709300102
10. Lenis AT, Lec PM, Chamie K. Bladder cancer a review. *JAMA - Journal of the American Medical Association*. 2020;324(19):1980-1991. doi:10.1001/jama.2020.17598
11. Saginala K, Barsouk A, Aluru JS, Rawla P, Padala SA, Barsouk A. Epidemiology of Bladder Cancer. *Med Sci (Basel)*. 2020;8(1). doi:10.3390/medsci8010015
12. Michaud DS. Chronic inflammation and bladder cancer. *Urologic Oncology: Seminars and Original Investigations*. 2007;25(3):260-268. doi:10.1016/j.urolonc.2006.10.002
13. Magers MJ, Lopez-Beltran A, Montironi R, Williamson SR, Kaimakliotis HZ, Cheng L. Staging of bladder cancer. *Histopathology*. 2019;74(1):112-134. doi:10.1111/his.13734
14. Cheng L, Zhang S, MacLennan GT, Williamson SR, Lopez-Beltran A, Montironi R. 2011 - Bladder cancer translating molecular genetic insights into clinical practice. *Hum Pathol*. 2011;42(4):455-481. doi:https://doi.org/10.1016/j.humpath.2010.07.007
15. Cheng L, Lopez-Beltran A, MacLennan GT, Montironi R, Bostwick DG. Neoplasms of the urinary bladder. In: *Urologic Surgical Pathology*. Elsevier; 2008:258-351. doi:10.1016/B978-0-323-01970-5.50008-7
16. Grasso M. Bladder Cancer: A Major Public Health Issue. *European Urology, Supplements*. 2008;7(7):510-515. doi:10.1016/j.eursup.2008.04.001
17. Zhu CZ, Ting HN, Ng KH, Ong TA. A review on the accuracy of bladder cancer detection methods. *J Cancer*. 2019;10(17):4038-4044. doi:10.7150/jca.28989
18. Babjuk M, Burger M, Capoun O, et al. European Association of Urology Guidelines on Non–muscle-invasive Bladder Cancer (Ta, T1, and Carcinoma in Situ). *Eur Urol*. 2022;81(1):75-94. doi:10.1016/j.eururo.2021.08.010
19. Thiel T, Ryk C, Renström-Koskela L, et al. Intravesical BCG treatment causes a long-lasting reduction of recurrence and progression in patients with high-risk non-muscle-invasive bladder cancer. *World J Urol*. 2019;37(1):155-163. doi:10.1007/s00345-018-2375-7
20. Larsen ES, Joensen UN, Poulsen AM, Goletti D, Johansen IS. Bacillus Calmette–Guérin immunotherapy for bladder cancer: a review of immunological aspects, clinical effects and BCG infections. *APMIS*. Published online 2020. doi:10.1111/apm.13011
21. Pettenati C, Ingersoll MA. Mechanisms of BCG immunotherapy and its outlook for bladder cancer. *Nat Rev Urol*. 2018;15(10):615-625. doi:10.1038/s41585-018-0055-4
22. Koch GE, Smelser WW, Chang SS. Side Effects of Intravesical BCG and Chemotherapy for Bladder Cancer: What They Are and How to Manage Them. *Urology*. 2021;149:11-20. doi:10.1016/j.urology.2020.10.039
23. Witjes JA, Bruins HM, Cathomas R, et al. European Association of Urology Guidelines on Muscle-invasive and Metastatic Bladder Cancer: Summary of the 2020 Guidelines. *Eur Urol*. 2021;79(1):82-104. doi:10.1016/j.eururo.2020.03.055

24. Pinho SS, Reis CA. Glycosylation in cancer: Mechanisms and clinical implications. *Nat Rev Cancer*. 2015;15(9):540-555. doi:10.1038/nrc3982
25. Stowell SR, Ju T, Cummings RD. Protein glycosylation in cancer. *Annual Review of Pathology: Mechanisms of Disease*. 2015;10:473-510. doi:10.1146/annurev-pathol-012414-040438
26. Ohtsubo K, Marth JD. Glycosylation in Cellular Mechanisms of Health and Disease. *Cell*. 2006;126(5):855-867. doi:10.1016/j.cell.2006.08.019
27. Moremen KW, Tiemeyer M, Nairn A V. Vertebrate protein glycosylation: Diversity, synthesis and function. *Nat Rev Mol Cell Biol*. 2012;13(7):448-462. doi:10.1038/nrm3383
28. Freeze HH, Boyce M, Zachara NE, Hart GW, Schnaar RL. Glycosylation Precursors. In: *Essentials of Glycobiology*. 4th edition. Cold Spring Harbor (NY): Cold Spring Harbor Laboratory Press; 2022.
29. Reily C, Stewart TJ, Renfrow MB, Novak J. Glycosylation in health and disease. *Nat Rev Nephrol*. 2019;15(6):346-366. doi:10.1038/s41581-019-0129-4
30. Colley KJ, Varki A, Haltiwanger RS, Kinoshita T. Cellular Organization of Glycosylation. In: *Essentials of Glycobiology*. 4th edition. Cold Spring Harbor (NY): Cold Spring Harbor Laboratory Press; 2022.
31. Varki A, Kornfeld S. Historical Background and Overview. In: *Essentials of Glycobiology*. 4th edition. Cold Spring Harbor (NY): Cold Spring Harbor Laboratory Press; 2022:[Internet].
32. Stanley P, Moremen KW, Lewis NE, Taniguchi N, Aebi M. N-Glycans. In: *Essentials of Glycobiology*. 4th edition. Cold Spring Harbor (NY): Cold Spring Harbor Laboratory Press; 2022:[Internet].
33. Aebi M. N-linked protein glycosylation in the ER. *Biochimica et Biophysica Acta (BBA) - Molecular Cell Research*. 2013;1833(11):2430-2437. doi:10.1016/j.bbamcr.2013.04.001
34. Eklund EA, Bode L, Freeze HH. Diseases Associated with Carbohydrates/Glycoconjugates*. In: Kamerling H, ed. *Comprehensive Glycoscience*. Elsevier; 2007:339-371. doi:10.1016/B978-044451967-2/00098-2
35. Vasconcelos-dos-Santos A, Oliveira IA, Lucena MC, et al. Biosynthetic Machinery Involved in Aberrant Glycosylation: Promising Targets for Developing of Drugs Against Cancer. *Front Oncol*. 2015;5. doi:10.3389/fonc.2015.00138
36. Munkley J, Elliott DJ. *Oncotarget 35478 Www.Impactjournals.Com/Oncotarget Hallmarks of Glycosylation in Cancer*. Vol 7.; 2016. www.impactjournals.com/oncotarget/
37. Peixoto A, Relvas-Santos M, Azevedo R, Lara Santos L, Ferreira JA. Protein glycosylation and tumor microenvironment alterations driving cancer hallmarks. *Front Oncol*. 2019;9(MAY). doi:10.3389/fonc.2019.00380
38. Bellis SL, Reis CA, Varki A, Kannagi R, Stanley P. Glycosylation Changes in Cancer. In: *Essentials of Glycobiology*. 4th edition. Cold Spring Harbor (NY): Cold Spring Harbor Laboratory Press; 2022:[Internet].
39. Lau KS, Dennis JW. N-Glycans in cancer progression. *Glycobiology*. 2008;18(10):750-760. doi:10.1093/glycob/cwn071
40. Dobie C, Skropeta D. Insights into the role of sialylation in cancer progression and metastasis. *Br J Cancer*. 2021;124(1):76-90. doi:10.1038/s41416-020-01126-7
41. Keeley TS, Yang S, Lau E. The diverse contributions of fucose linkages in cancer. *Cancers (Basel)*. 2019;11(9). doi:10.3390/cancers11091241
42. Gupta R, Leon F, Rauth S, Batra SK, Ponnusamy MP. A Systematic Review on the Implications of O-linked Glycan Branching and Truncating Enzymes on Cancer Progression and Metastasis. *Cells*. 2020;9(2). doi:10.3390/cells9020446
43. Garnham R, Scott E, Livermore KE, Munkley J. ST6GAL1: A key player in cancer. *Oncol Lett*. 2019;18(2):983-989. doi:10.3892/ol.2019.10458
44. Zhao L, Feng X, Song X, et al. MiR-493-5p attenuates the invasiveness and tumorigenicity in human breast cancer by targeting FUT4. *Oncol Rep*. 2016;36(2):1007-1015. doi:10.3892/or.2016.4882
45. Li Y, Sun Z, Liu B, Shan Y, Zhao L, Jia L. Tumor-suppressive miR-26A and miR-26B inhibit cell aggressiveness by regulating fut4 in colorectal cancer. *Cell Death Dis*. 2017;8(6). doi:10.1038/cddis.2017.281
46. Radhakrishnan P, Dabelsteen S, Madsen FB, et al. Immature truncated O-glycophenotype of cancer directly induces oncogenic features. *Proceedings of the National Academy of Sciences*. 2014;111(39). doi:10.1073/pnas.1406619111

47. Pinho SS, Carvalho S, Marcos-Pinto R, et al. Gastric cancer: adding glycosylation to the equation. *Trends Mol Med*. 2013;19(11):664-676. doi:10.1016/j.molmed.2013.07.003
48. Silva MC, Fernandes Â, Oliveira M, et al. Glycans as Immune Checkpoints: Removal of Branched N-glycans Enhances Immune Recognition Preventing Cancer Progression. *Cancer Immunol Res*. 2020;8(11):1407-1425. doi:10.1158/2326-6066.CIR-20-0264
49. Pinho SS, Figueiredo J, Cabral J, et al. E-cadherin and adherens-junctions stability in gastric carcinoma: Functional implications of glycosyltransferases involving N-glycan branching biosynthesis, N-acetylglucosaminyltransferases III and V. *Biochimica et Biophysica Acta (BBA) - General Subjects*. 2013;1830(3):2690-2700. doi:10.1016/j.bbagen.2012.10.021
50. Allam H, Johnson BP, Zhang M, Lu Z, Cannon MJ, Abbott KL. The glycosyltransferase GnT-III activates Notch signaling and drives stem cell expansion to promote the growth and invasion of ovarian cancer. *Journal of Biological Chemistry*. 2017;292(39):16351-16359. doi:10.1074/jbc.M117.783936
51. Wilczak M, Surman M, Przybyło M. Altered Glycosylation in Progression and Management of Bladder Cancer. *Molecules*. 2023;28(8). doi:10.3390/molecules28083436
52. Azevedo R, Peixoto A, Gaiteiro C, et al. Over forty years of bladder cancer glycobiology: Where do glycans stand facing precision oncology? *Oncotarget*. 2017;8(53):91734-91764. doi:10.18632/oncotarget.19433
53. Sanchez-Fernandez De Sevillaa MC, Morell-Quadrenya L, Gil-Salomb M, Perez-Bacetea M, Llombart-Bosch11 A, Llombart-Bosch A. *Morphometric and Immunohistochemical Characterization of Bladder Carcinoma in Situ and Its Preneoplastic Lesions Key Words Bladder Cancer Carcinoma in Situ Urothelial Dysplasia Morphometry Immunochemistry Lectins Epithelial Differentiation Antigens Blood Group Isoantigens*. Vol 21.; 1992.
54. Yang G, Tan Z, Lu W, et al. Quantitative glycome analysis of N-glycan patterns in bladder cancer vs normal bladder cells using an integrated strategy. *J Proteome Res*. 2015;14(2):639-653. doi:10.1021/pr5006026
55. Afshar M, Gallo RL. Innate immune defense system of the skin. *Vet Dermatol*. 2013;24(1). doi:10.1111/j.1365-3164.2012.01082.x
56. Santaolalla R, Abreu MT. Innate immunity in the small intestine. *Curr Opin Gastroenterol*. 2012;28(2):124-129. doi:10.1097/MOG.0b013e3283506559
57. Woods CM, Hooper DN, Ooi EH, Tan LW, Carney AS. Human lysozyme has fungicidal activity against nasal fungi. *Am J Rhinol Allergy*. 2011;25(4):236-240. doi:10.2500/ajra.2011.25.3631
58. Hariri BM, Cohen NA. New insights into upper airway innate immunity. In: *American Journal of Rhinology and Allergy*. Vol 30. OceanSide Publications Inc.; 2016:319-323. doi:10.2500/ajra.2016.30.4360
59. Nowarski R, Gagliani N, Huber S, Flavell RA. Innate immune cells in inflammation and cancer. *Cancer Immunol Res*. 2013;1(2):77-84. doi:10.1158/2326-6066.CIR-13-0081
60. Németh T, Sperandio M, Mócsai A. Neutrophils as emerging therapeutic targets. *Nat Rev Drug Discov*. 2020;19(4):253-275. doi:10.1038/s41573-019-0054-z
61. Coffelt SB, Wellenstein MD, De Visser KE. Neutrophils in cancer: Neutral no more. *Nat Rev Cancer*. 2016;16(7):431-446. doi:10.1038/nrc.2016.52
62. Gordon S, Taylor PR. Monocyte and macrophage heterogeneity. *Nat Rev Immunol*. 2005;5(12):953-964. doi:10.1038/nri1733
63. Olingy CE, Dinh HQ, Hedrick CC. Monocyte heterogeneity and functions in cancer. *J Leukoc Biol*. 2019;106(2):309-322. doi:10.1002/JLB.4RI0818-311R
64. Sprangers S, Vries TJ de, Everts V. Monocyte Heterogeneity: Consequences for Monocyte-Derived Immune Cells. *J Immunol Res*. 2016;2016:1-10. doi:10.1155/2016/1475435
65. Ruffell B, Coussens LM. Macrophages and Therapeutic Resistance in Cancer. *Cancer Cell*. 2015;27(4):462-472. doi:10.1016/j.ccell.2015.02.015
66. Gordon S, Martinez-Pomares L. Physiological roles of macrophages. *Pflugers Arch*. 2017;469(3-4):365-374. doi:10.1007/s00424-017-1945-7
67. Fujiwara N, Kobayashi K. *Macrophages in Inflammation*. Vol 4.; 2005.
68. Chávez-Galán L, Olleros ML, Vesin D, Garcia I. Much more than M1 and M2 macrophages, there are also CD169+ and TCR+ macrophages. *Front Immunol*. 2015;6(MAY). doi:10.3389/fimmu.2015.00263
69. Yunna C, Mengru H, Lei W, Weidong C. Macrophage M1/M2 polarization. *Eur J Pharmacol*. 2020;877:173090. doi:10.1016/j.ejphar.2020.173090

70. Noy R, Pollard JW. Tumor-Associated Macrophages: From Mechanisms to Therapy. *Immunity*. 2014;41(1):49-61. doi:10.1016/j.immuni.2014.06.010
71. Chen J, Yao Y, Gong C, et al. CCL18 from Tumor-Associated Macrophages Promotes Breast Cancer Metastasis via PITPNM3. *Cancer Cell*. 2011;19(4):541-555. doi:10.1016/j.ccr.2011.02.006
72. Georgoudaki AM, Prokopec KE, Boura VF, et al. Reprogramming Tumor-Associated Macrophages by Antibody Targeting Inhibits Cancer Progression and Metastasis. *Cell Rep*. 2016;15(9):2000-2011. doi:10.1016/j.celrep.2016.04.084
73. Steinman RM, Banchereau J. Taking dendritic cells into medicine. *Nature*. 2007;449(7161):419-426. doi:10.1038/nature06175
74. Vivier E, Artis D, Colonna M, et al. Innate Lymphoid Cells: 10 Years On. *Cell*. 2018;174(5):1054-1066. doi:10.1016/j.cell.2018.07.017
75. Vivier E, Tomasello E, Baratin M, Walzer T, Ugolini S. Functions of natural killer cells. *Nat Immunol*. 2008;9(5):503-510. doi:10.1038/ni1582
76. Artis D, Spits H. The biology of innate lymphoid cells. *Nature*. 2015;517(7534):293-301. doi:10.1038/nature14189
77. Chaplin DD. Overview of the immune response. *Journal of Allergy and Clinical Immunology*. 2010;125(2 SUPPL. 2). doi:10.1016/j.jaci.2009.12.980
78. Luckheeram RV, Zhou R, Verma AD, Xia B. CD4 +T cells: Differentiation and functions. *Clin Dev Immunol*. 2012;2012. doi:10.1155/2012/925135
79. Ohue Y, Nishikawa H. Regulatory T (Treg) cells in cancer: Can Treg cells be a new therapeutic target? *Cancer Sci*. 2019;110(7):2080-2089. doi:10.1111/cas.14069
80. Raskov H, Orhan A, Christensen JP, Gögenur I. Cytotoxic CD8+ T cells in cancer and cancer immunotherapy. *Br J Cancer*. 2021;124(2):359-367. doi:10.1038/s41416-020-01048-4
81. Vantourout P, Hayday A. Six-of-the-best: Unique contributions of γδ T cells to immunology. *Nat Rev Immunol*. 2013;13(2):88-100. doi:10.1038/nri3384
82. Lebien TW, Thomas *, Tedder F. B lymphocytes: how they develop and function. Published online 2008. doi:10.1182/blood
83. Dunn GP, Old LJ, Schreiber RD. The three Es of cancer immunoediting. *Annu Rev Immunol*. 2004;22:329-360. doi:10.1146/annurev.immunol.22.012703.104803
84. Dunn GP, Old LJ, Schreiber RD. The Immunobiology of Cancer Immunosurveillance and Immunoediting. *Immunity*. 2004;21(2):137-148. doi:10.1016/j.immuni.2004.07.017
85. Dunn GP, Bruce AT, Ikeda H, Old LJ, Schreiber RD. *Cancer Immunoediting: From Immuno-Surveillance to Tumor Escape*.; 2002. http://www.nature.com/natureimmunology
86. Vinay DS, Ryan EP, Pawelec G, et al. Immune evasion in cancer: Mechanistic basis and therapeutic strategies. *Semin Cancer Biol*. 2015;35:S185-S198. doi:10.1016/j.semcancer.2015.03.004
87. Han Y, Liu D, Li L. *PD-1/PD-L1 Pathway: Current Researches in Cancer*. Vol 10.; 2020. www.ajcr.us/
88. Grosso JF, Jure-Kunkel MN. CTLA-4 blockade in tumor models: an overview of preclinical and translational research. Published online 2013. doi:10.1158/1424-9634.DCL-5.13.1/2366463/5.pdf
89. Wang M, Zhao J, Zhang L, et al. Role of tumor microenvironment in tumorigenesis. *J Cancer*. 2017;8(5):761-773. doi:10.7150/jca.17648
90. Ellis LM, Hicklin DJ. VEGF-targeted therapy: Mechanisms of anti-tumour activity. *Nat Rev Cancer*. 2008;8(8):579-591. doi:10.1038/nrc2403
91. Taylor ME, Drickamer K, Imberty A, et al. Discovery and Classification of Glycan-Binding Proteins. In: *Essentials of Glycobiology*. 4th edition. Cold Spring Harbor (NY): Cold Spring Harbor Laboratory Press; 2022:[Internet].
92. Rabinovich GA, van Kooyk Y, Cobb BA. Glycobiology of immune responses. *Ann N Y Acad Sci*. 2012;1253(1):1-15. doi:10.1111/j.1749-6632.2012.06492.x
93. Lepenies B, Lee J, Sonkaria S. Targeting C-type lectin receptors with multivalent carbohydrate ligands. *Adv Drug Deliv Rev*. 2013;65(9):1271-1281. doi:10.1016/j.addr.2013.05.007
94. Bochner BS, Zimmermann N. Role of siglecs and related glycan-binding proteins in immune responses and immunoregulation. *Journal of Allergy and Clinical Immunology*. 2015;135(3):598-608. doi:10.1016/j.jaci.2014.11.031

95. Cummings RD, Liu FT, Rabinovich GA, Stowell SR, Vasta GR. Galectins. In: *Essentials of Glycobiology*. 4th edition. Cold Spring Harbor (NY): Cold Spring Harbor Laboratory Press; 2022:[INTERNET].
96. Thijssen VL, Heusschen R, Caers J, Griffioen AW. Galectin expression in cancer diagnosis and prognosis: A systematic review. *Biochimica et Biophysica Acta (BBA) - Reviews on Cancer*. 2015;1855(2):235-247. doi:10.1016/j.bbcan.2015.03.003
97. Liu FT, Rabinovich GA. Galectins as modulators of tumour progression. *Nat Rev Cancer*. 2005;5(1):29-41. doi:10.1038/nrc1527
98. Cagnoni AJ, Giribaldi ML, Blidner AG, et al. Galectin-1 fosters an immunosuppressive microenvironment in colorectal cancer by reprogramming CD8 $^{+}$ regulatory T cells. *Proceedings of the National Academy of Sciences*. 2021;118(21). doi:10.1073/pnas.2102950118
99. Compagno D, Tiraboschi C, Garcia JD, et al. Galectins as Checkpoints of the Immune System in Cancers, Their Clinical Relevance, and Implication in Clinical Trials. *Biomolecules*. 2020;10(5):750. doi:10.3390/biom10050750
100. Duan S, Paulson JC. Siglecs as Immune Cell Checkpoints in Disease. *Annu Rev Immunol*. 2020;38(1):365-395. doi:10.1146/annurev-immunol-102419-035900
101. Stanczak MA, Läubli H. Siglec receptors as new immune checkpoints in cancer. *Mol Aspects Med*. 2023;90:101112. doi:10.1016/j.mam.2022.101112
102. van Houtum EJH, Büll C, Cornelissen LAM, Adema GJ. Siglec Signaling in the Tumor Microenvironment. *Front Immunol*. 2021;12. doi:10.3389/fimmu.2021.790317
103. Dambuza IM, Brown GD. C-type lectins in immunity: recent developments. *Curr Opin Immunol*. 2015;32:21-27. doi:10.1016/j.coi.2014.12.002
104. Mnich ME, van Dalen R, van Sorge NM. C-Type Lectin Receptors in Host Defense Against Bacterial Pathogens. *Front Cell Infect Microbiol*. 2020;10. doi:10.3389/fcimb.2020.00309
105. Nonaka M, Ma BY, Murai R, et al. Glycosylation-Dependent Interactions of C-Type Lectin DC-SIGN with Colorectal Tumor-Associated Lewis Glycans Impair the Function and Differentiation of Monocyte-Derived Dendritic Cells. *The Journal of Immunology*. 2008;180(5):3347-3356. doi:10.4049/jimmunol.180.5.3347
106. Kimura Y, Inoue A, Hangai S, et al. The innate immune receptor Dectin-2 mediates the phagocytosis of cancer cells by Kupffer cells for the suppression of liver metastasis. *Proceedings of the National Academy of Sciences*. 2016;113(49):14097-14102. doi:10.1073/pnas.1617903113
107. Sahasrabudhe NM, Van Der Horst JC, Spaans V, et al. MGL ligand expression is correlated to lower survival and distant metastasis in cervical squamous cell and adenosquamous carcinoma. *Front Oncol*. 2019;9(JAN). doi:10.3389/fonc.2019.00029
108. Dusoswa SA, Verhoeff J, Abels E, et al. Glioblastomas exploit truncated O - linked glycans for local and distant immune modulation via the macrophage galactose-type lectin. *Proceedings of the National Academy of Sciences*. 2020;117(7):3693-3703. doi:10.1073/pnas.1907921117
109. Napoletano C, Rughetti A, Agervig Tarp MP, et al. Tumor-associated Tn-MUC1 glycoform is internalized through the macrophage galactose-type C-type lectin and delivered to the HLA class I and II compartments in dendritic cells. *Cancer Res*. 2007;67(17):8358-8367. doi:10.1158/0008-5472.CAN-07-1035
110. Napoletano C, Zizzari IG, Rughetti A, et al. Targeting of macrophage galactose-type C-type lectin (MGL) induces DC signaling and activation. *Eur J Immunol*. 2012;42(4):936-945. doi:10.1002/eji.201142086
111. Daley D, Mani VR, Mohan N, et al. Dectin 1 activation on macrophages by galectin 9 promotes pancreatic carcinoma and peritumoral immune tolerance. *Nat Med*. 2017;23(5):556-567. doi:10.1038/nm.4314
112. Chiba S, Ikushima H, Ueki H, et al. Recognition of tumor cells by Dectin-1 orchestrates innate immune cells for anti-tumor responses. *Elife*. 2014;3(August2014):1-20. doi:10.7554/eLife.04177
113. Akira S, Uematsu S, Takeuchi O. Pathogen Recognition and Innate Immunity. *Cell*. 2006;124(4):783-801. doi:10.1016/j.cell.2006.02.015
114. Mogensen TH. Pathogen recognition and inflammatory signaling in innate immune defenses. *Clin Microbiol Rev*. 2009;22(2):240-273. doi:10.1128/CMR.00046-08

115. WOUT JW, POELL R, FURTH R. The Role of BCG/PPD-Activated Macrophages in Resistance against Systemic Candidiasis in Mice. *Scand J Immunol*. 1992;36(5):713-720. doi:10.1111/j.1365-3083.1992.tb03132.x
116. Bistoni F, Verducci G, Perito S, et al. Immunomodulation by a low-virulence, agerminative variant of *Candida albicans* . Further evidence for macrophage activation as one of the effector mechanisms of nonspecific anti-infectious protection. *Med Mycol*. 1988;26(5):285-299. doi:10.1080/02681218880000401
117. Netea MG, Quintin J, Van Der Meer JWM. Trained immunity: A memory for innate host defense. *Cell Host Microbe*. 2011;9(5):355-361. doi:10.1016/j.chom.2011.04.006
118. Netea MG, Domínguez-Andrés J, Barreiro LB, et al. Defining trained immunity and its role in health and disease. *Nat Rev Immunol*. 2020;20(6):375-388. doi:10.1038/s41577-020-0285-6
119. van der Heijden CDCC, Noz MP, Joosten LAB, Netea MG, Riksen NP, Keating ST. Epigenetics and Trained Immunity. *Antioxid Redox Signal*. 2018;29(11):1023-1040. doi:10.1089/ars.2017.7310
120. Seeley JJ, Ghosh S. Molecular mechanisms of innate memory and tolerance to LPS. *J Leukoc Biol*. 2017;101(1):107-119. doi:10.1189/jlb.3mr0316-118rr
121. Arts RJW, Novakovic B, ter Horst R, et al. Glutaminolysis and Fumarate Accumulation Integrate Immunometabolic and Epigenetic Programs in Trained Immunity. *Cell Metab*. 2016;24(6):807-819. doi:10.1016/j.cmet.2016.10.008
122. Arts RJW, Joosten LAB, Netea MG. Immunometabolic circuits in trained immunity. *Semin Immunol*. 2016;28(5):425-430. doi:10.1016/j.smim.2016.09.002
123. Netea MG, Joosten LAB, Latz E, et al. Trained immunity: A program of innate immune memory in health and disease. *Science (1979)*. 2016;352(6284):427. doi:10.1126/science.aaf1098
124. Bonilla MC, Fingerhut L, Alfonso-Castro A, et al. How Long Does a Neutrophil Live?—The Effect of 24 h Whole Blood Storage on Neutrophil Functions in Pigs. *Biomedicines*. 2020;8(8):278. doi:10.3390/biomedicines8080278
125. Patel AA, Zhang Y, Fullerton JN, et al. The fate and lifespan of human monocyte subsets in steady state and systemic inflammation. *Journal of Experimental Medicine*. 2017;214(7):1913-1923. doi:10.1084/jem.20170355
126. Patel AA, Ginhoux F, Yona S. Monocytes, macrophages, dendritic cells and neutrophils: an update on lifespan kinetics in health and disease. *Immunology*. 2021;163(3):250-261. doi:10.1111/imm.13320
127. Mitroulis I, Ruppova K, Wang B, et al. Modulation of Myelopoiesis Progenitors Is an Integral Component of Trained Immunity. *Cell*. 2018;172(1-2):147-161.e12. doi:10.1016/j.cell.2017.11.034
128. Cirovic B, de Bree LCJ, Groh L, et al. BCG Vaccination in Humans Elicits Trained Immunity via the Hematopoietic Progenitor Compartment. *Cell Host Microbe*. 2020;28(2):322-334.e5. doi:10.1016/j.chom.2020.05.014
129. Bowman SM, Free SJ. The structure and synthesis of the fungal cell wall. *BioEssays*. 2006;28(8):799-808. doi:10.1002/bies.20441
130. Quintin J, Saeed S, Martens JHA, et al. Candida albicans infection affords protection against reinfection via functional reprogramming of monocytes. *Cell Host Microbe*. 2012;12(2):223-232. doi:10.1016/j.chom.2012.06.006
131. Mata-Martínez P, Bergón-Gutiérrez M, del Fresno C. Dectin-1 Signaling Update: New Perspectives for Trained Immunity. *Front Immunol*. 2022;13. doi:10.3389/fimmu.2022.812148
132. Mangtani P, Abubakar I, Ariti C, et al. Protection by BCG vaccine against tuberculosis: A systematic review of randomized controlled trials. *Clinical Infectious Diseases*. 2014;58(4):470-480. doi:10.1093/cid/cit790
133. Hollm-Delgado MG, Stuart EA, Black RE. Acute lower respiratory infection among Bacille Calmette-Guérin (BCG)-vaccinated children. *Pediatrics*. 2014;133(1). doi:10.1542/peds.2013-2218
134. Moorlag SJCFM, Arts RJW, van Crevel R, Netea MG. Non-specific effects of BCG vaccine on viral infections. *Clinical Microbiology and Infection*. 2019;25(12):1473-1478. doi:10.1016/j.cmi.2019.04.020
135. Arts RJW, Moorlag SJCFM, Novakovic B, et al. BCG Vaccination Protects against Experimental Viral Infection in Humans through the Induction of Cytokines Associated with Trained Immunity. *Cell Host Microbe*. 2018;23(1):89-100.e5. doi:10.1016/j.chom.2017.12.010

136. Zhou KL, Li X, Zhang XL, Pan Q. Mycobacterial mannose-capped lipoarabinomannan: a modulator bridging innate and adaptive immunity. *Emerg Microbes Infect*. 2019;8(1):1168-1177. doi:10.1080/22221751.2019.1649097
137. Zenaro E, Donini M, Dusi S. Induction of Th1/Th17 immune response by Mycobacterium tuberculosis : role of dectin-1, mannose receptor, and DC-SIGN . *J Leukoc Biol*. 2009;86(6):1393-1401. doi:10.1189/jlb.0409242
138. Maeda N, Nigou J, Herrmann JL, et al. The cell surface receptor DC-SIGN discriminates between Mycobacterium species through selective recognition of the mannose caps on lipoarabinomannan. *Journal of Biological Chemistry*. 2003;278(8):5513-5516. doi:10.1074/jbc.C200586200
139. Kang PB, Azad AK, Torrelles JB, et al. The human macrophage mannose receptor directs Mycobacterium tuberculosis lipoarabinomannan-mediated phagosome biogenesis. *Journal of Experimental Medicine*. 2005;202(7):987-999. doi:10.1084/jem.20051239
140. Prigozy TI, Sieling PA. *The Mannose Receptor Delivers Lipoglycan Antigens to Endosomes for Presentation to T Cells by CD1b Molecules*. Vol 6.; 1997.
141. Geijtenbeek TBH, Van Vliet SJ, Koppel EA, et al. Mycobacteria target DC-SIGN to suppress dendritic cell function. *Journal of Experimental Medicine*. 2003;197(1):7-17. doi:10.1084/jem.20021229
142. Yonekawa A, Saijo S, Hoshino Y, et al. Dectin-2 is a direct receptor for mannose-capped lipoarabinomannan of mycobacteria. *Immunity*. 2014;41(3):402-413. doi:10.1016/j.immuni.2014.08.005
143. Kleinnijenhuis J, Quintin J, Preijers F, et al. Bacille Calmette-Guérin induces NOD2-dependent nonspecific protection from reinfection via epigenetic reprogramming of monocytes. *Proc Natl Acad Sci U S A*. 2012;109(43):17537-17542. doi:10.1073/pnas.1202870109
144. Redelman-Sidi G, Glickman MS, Bochner BH. The mechanism of action of BCG therapy for bladder cancer-A current perspective. *Nat Rev Urol*. 2014;11(3):153-162. doi:10.1038/nrurol.2014.15
145. Jiang S, Redelman-Sidi G. BCG in Bladder Cancer Immunotherapy. *Cancers (Basel)*. 2022;14(13). doi:10.3390/cancers14133073
146. van Puffelen JH, Keating ST, Oosterwijk E, et al. Trained immunity as a molecular mechanism for BCG immunotherapy in bladder cancer. *Nat Rev Urol*. 2020;17(9):513-525. doi:10.1038/s41585-020-0346-4
147. Sanchis P, Lavignolle R, Abbate M, et al. Analysis workflow of publicly available RNA-sequencing datasets. *STAR Protoc*. 2021;2(2). doi:10.1016/j.xpro.2021.100478
148. Masters JRW, Hepburn PJ, Walker L, et al. *Tissue Culture Model of Transitional Cell Carcinoma: Characterization of Twenty-Two Human Urothelial Cell Lines*. Vol 46.; 1986. http://aacrjournals.org/cancerres/article-pdf/46/7/3630/2426819/cr0460073630.pdf
149. Bubenik J, Baresova M, Viklick~~ V, Jakoubkova J, Sainerova H, Donner J. *ESTABLISHED CELL LINE OF URINARY BLADDER CARCINOMA (T24) CONTAINING TUMOUR-SPECIFIC ANTIGEN*.; 1973.
150. van der Heijden WA, Van de Wijer L, Keramati F, et al. Chronic HIV infection induces transcriptional and functional reprogramming of innate immune cells. *JCI Insight*. 2021;6(7). doi:10.1172/jci.insight.145928
151. Sato S, Ouellet M, St-Pierre C, Tremblay MJ. Glycans, galectins, and HIV-1 infection. *Ann N Y Acad Sci*. 2012;1253(1):133-148. doi:10.1111/j.1749-6632.2012.06475.x
152. Crispin M, Ward AB, Wilson IA. Structure and Immune Recognition of the HIV Glycan Shield. Published online 2018. doi:10.1146/annurev-biophys
153. Watanabe Y, Allen JD, Wrapp D, Mclellan JS, Crispin M. *Site-Specific Glycan Analysis of the SARS-CoV-2 Spike*. https://www.science.org
154. Casalino L, Gaieb Z, Goldsmith JA, et al. Beyond shielding: The roles of glycans in the SARS-CoV-2 spike protein. *ACS Cent Sci*. 2020;6(10):1722-1734. doi:10.1021/acscentsci.0c01056
155. Theobald SJ, Simonis A, Georgomanolis T, et al. Long-lived macrophage reprogramming drives spike protein-mediated inflammasome activation in COVID-19. *EMBO Mol Med*. 2021;13(8). doi:10.15252/emmm.202114150
156. Bannister S, Kim B, Domínguez-Andrés J, et al. *Neonatal BCG Vaccination Is Associated with a Long-Term DNA Methylation Signature in Circulating Monocytes*. Vol 8.; 2022.

157. Domínguez-Andrés J, Arts RJW, Bekkering S, et al. In vitro induction of trained immunity in adherent human monocytes. *STAR Protoc*. 2021;2(1):100365. doi:10.1016/j.xpro.2021.100365
158. Baron S, Finbloom J, Horowitz J, et al. Near Eradication of Clinically Relevant Concentrations of Human Tumor Cells by Interferon-Activated Monocytes *In Vitro*. *Journal of Interferon & Cytokine Research*. 2011;31(7):569-573. doi:10.1089/jir.2010.0153
159. Choraghe RP, Neumann AK. Dectin-1-Mediated DC-SIGN Recruitment to Candida albicans Contact Sites. *Life*. 2021;11(2):108. doi:10.3390/life11020108
160. Saijo S, Ikeda S, Yamabe K, et al. Dectin-2 Recognition of α-Mannans and Induction of Th17 Cell Differentiation Is Essential for Host Defense against Candida albicans. *Immunity*. 2010;32(5):681-691. doi:10.1016/j.immuni.2010.05.001
161. Taylor PR, Reid DM, Heinsbroek SEM, Brown GD, Gordon S, Wong SYC. Dectin-2 is predominantly myeloid restricted and exhibits unique activation-dependent expression on maturing inflammatory monocytes elicitedin vivo. *Eur J Immunol*. 2005;35(7):2163-2174. doi:10.1002/eji.200425785
162. Yamamoto Y, Klein TW, Friedman H. *Involvement of Mannose Receptor in Cytokine Interleukin-1 (IL-1), IL-6, and Granulocyte-Macrophage Colony-Stimulating Factor Responses, but Not in Chemokine Macrophage Inflammatory Protein 1 (MIP-1), MIP-2, and KC Responses, Caused by Attachment of Candida Albicans to Macrophages*. Vol 65.; 1997. https://journals.asm.org/journal/iai
163. Cummings RD. The mannose receptor ligands and the macrophage glycome. *Curr Opin Struct Biol*. 2022;75:102394. doi:10.1016/j.sbi.2022.102394
164. Allavena P, Chieppa M, Monti P, Piemonti L. From Pattern Recognition Receptor to Regulator of Homeostasis: The Double-Faced Macrophage Mannose Receptor. *Crit Rev Immunol*. 2004;24(3):179-192. doi:10.1615/CritRevImmunol.v24.i3.20
165. Relloso M, Puig-Kröger A, Pello OM, et al. DC-SIGN (CD209) Expression Is IL-4 Dependent and Is Negatively Regulated by IFN, TGF-β, and Anti-Inflammatory Agents. *The Journal of Immunology*. 2002;168(6):2634-2643. doi:10.4049/jimmunol.168.6.2634
166. Tailleux L, Pham-Thi N, Bergeron-Lafaurie A, et al. DC-SIGN Induction in Alveolar Macrophages Defines Privileged Target Host Cells for Mycobacteria in Patients with Tuberculosis. *PLoS Med*. 2005;2(12):e381. doi:10.1371/journal.pmed.0020381
167. Garcia-Vallejo JJ, van Kooyk Y. The physiological role of DC-SIGN: A tale of mice and men. *Trends Immunol*. 2013;34(10):482-486. doi:10.1016/j.it.2013.03.001
168. Chehimi J, Luo Q, Azzoni L, et al. HIV-1 transmission and cytokine-induced expression of DC-SIGN in human monocyte-derived macrophages. *J Leukoc Biol*. 2003;74(5):757-763. doi:10.1189/jlb.0503231
169. Schulz D, Severin Y, Zanotelli VRT, Bodenmiller B. In-Depth Characterization of Monocyte-Derived Macrophages using a Mass Cytometry-Based Phagocytosis Assay. *Sci Rep*. 2019;9(1):1925. doi:10.1038/s41598-018-38127-9
170. Krylov VB, Gómez-Redondo M, Solovev AS, et al. Identification of a new DC-SIGN binding pentamannoside epitope within the complex structure of Candida albicans mannan. *The Cell Surface*. 2023;10:100109. doi:10.1016/j.tcsw.2023.100109
171. Geijtenbeek TBH, Gringhuis SI. Signalling through C-type lectin receptors: shaping immune responses. *Nat Rev Immunol*. 2009;9(7):465-479. doi:10.1038/nri2569
172. Kleinnijenhuis J, Quintin J, Preijers F, et al. Long-Lasting Effects of BCG Vaccination on Both Heterologous Th1/Th17 Responses and Innate Trained Immunity. *J Innate Immun*. 2014;6(2):152-158. doi:10.1159/000355628
173. Ferwerda G, Meyer-Wentrup F, Kullberg BJ, Netea MG, Adema GJ. Dectin-1 synergizes with TLR2 and TLR4 for cytokine production in human primary monocytes and macrophages. *Cell Microbiol*. 2008;10(10):2058-2066. doi:10.1111/j.1462-5822.2008.01188.x
174. Gringhuis SI, den Dunnen J, Litjens M, van het Hof B, van Kooyk Y, Geijtenbeek TBH. C-Type Lectin DC-SIGN Modulates Toll-like Receptor Signaling via Raf-1 Kinase-Dependent Acetylation of Transcription Factor NF-κB. *Immunity*. 2007;26(5):605-616. doi:10.1016/j.immuni.2007.03.012
175. Netea MG. Immune sensing of Candida albicans requires cooperative recognition of mannans and glucans by lectin and Toll-like receptors. *Journal of Clinical Investigation*. 2006;116(6):1642-1650. doi:10.1172/JCI27114

176. Tada H, Nemoto E, Shimauchi H, et al. *Saccharomyces cerevisiae* - and *Candida albicans* - Derived Mannan Induced Production of Tumor Necrosis Factor Alpha by Human Monocytes in a CD14- and Toll-Like Receptor 4-Dependent Manner. *Microbiol Immunol*. 2002;46(7):503-512. doi:10.1111/j.1348-0421.2002.tb02727.x
177. Dias AM, Correia A, Pereira MS, et al. Metabolic control of T cell immune response through glycans in inflammatory bowel disease. *Proceedings of the National Academy of Sciences*. 2018;115(20). doi:10.1073/pnas.1720409115
178. Rizzetto L, Ifrim DC, Moretti S, et al. Fungal Chitin Induces Trained Immunity in Human Monocytes during Cross-talk of the Host with Saccharomyces cerevisiae. *Journal of Biological Chemistry*. 2016;291(15):7961-7972. doi:10.1074/jbc.M115.699645
179. Liu Y, Beyer A, Aebersold R. On the Dependency of Cellular Protein Levels on mRNA Abundance. *Cell*. 2016;165(3):535-550. doi:10.1016/j.cell.2016.03.014
180. Choromanska A, Kulbacka J, Harasym J, Oledzki R, Szewczyk A, Saczko J. High- and low-Molecular Weight oat Beta-Glucan Reveals Antitumor Activity in Human Epithelial Lung Cancer. *Pathology & Oncology Research*. 2018;24(3):583-592. doi:10.1007/s12253-017-0278-3
181. Wani SM, Gani A, Mir SA, Masoodi FA, Khanday FA. β-Glucan: A dual regulator of apoptosis and cell proliferation. *Int J Biol Macromol*. 2021;182:1229-1237. doi:10.1016/j.ijbiomac.2021.05.065
182. Jung M, Weigert A, Mertens C, Rehwald C, Brüne B. Iron Handling in Tumor-Associated Macrophages—Is There a New Role for Lipocalin-2? *Front Immunol*. 2017;8. doi:10.3389/fimmu.2017.01171
183. Bracher M, Gould HJ, Sutton BJ, Dombrowicz D, Karagiannis SN. Three-colour flow cytometric method to measure antibody-dependent tumour cell killing by cytotoxicity and phagocytosis. *J Immunol Methods*. 2007;323(2):160-171. doi:10.1016/j.jim.2007.04.009
184. Son S, Nam J, Kim AS, et al. Induction of T-helper-17-cell-mediated anti-tumour immunity by pathogen-mimicking polymer nanoparticles. *Nat Biomed Eng*. 2023;7(1):72-84. doi:10.1038/s41551-022-00973-4
185. Alves I, Santos-Pereira B, de la Cruz N, et al. Host-derived mannose glycans trigger a pathogenic γδ T cell/IL-17a axis in autoimmunity. *Sci Transl Med*. 2023;15(687). doi:10.1126/scitranslmed.abo1930
186. Takashiba S, Van Dyke TE, Amar S, Murayama Y, Soskolne AW, Shapira L. Differentiation of Monocytes to Macrophages Primes Cells for Lipopolysaccharide Stimulation via Accumulation of Cytoplasmic Nuclear Factor κB. *Infect Immun*. 1999;67(11):5573-5578. doi:10.1128/IAI.67.11.5573-5578.1999

Appendix I – Optimization of the supplementation of monocytes with glycan structures

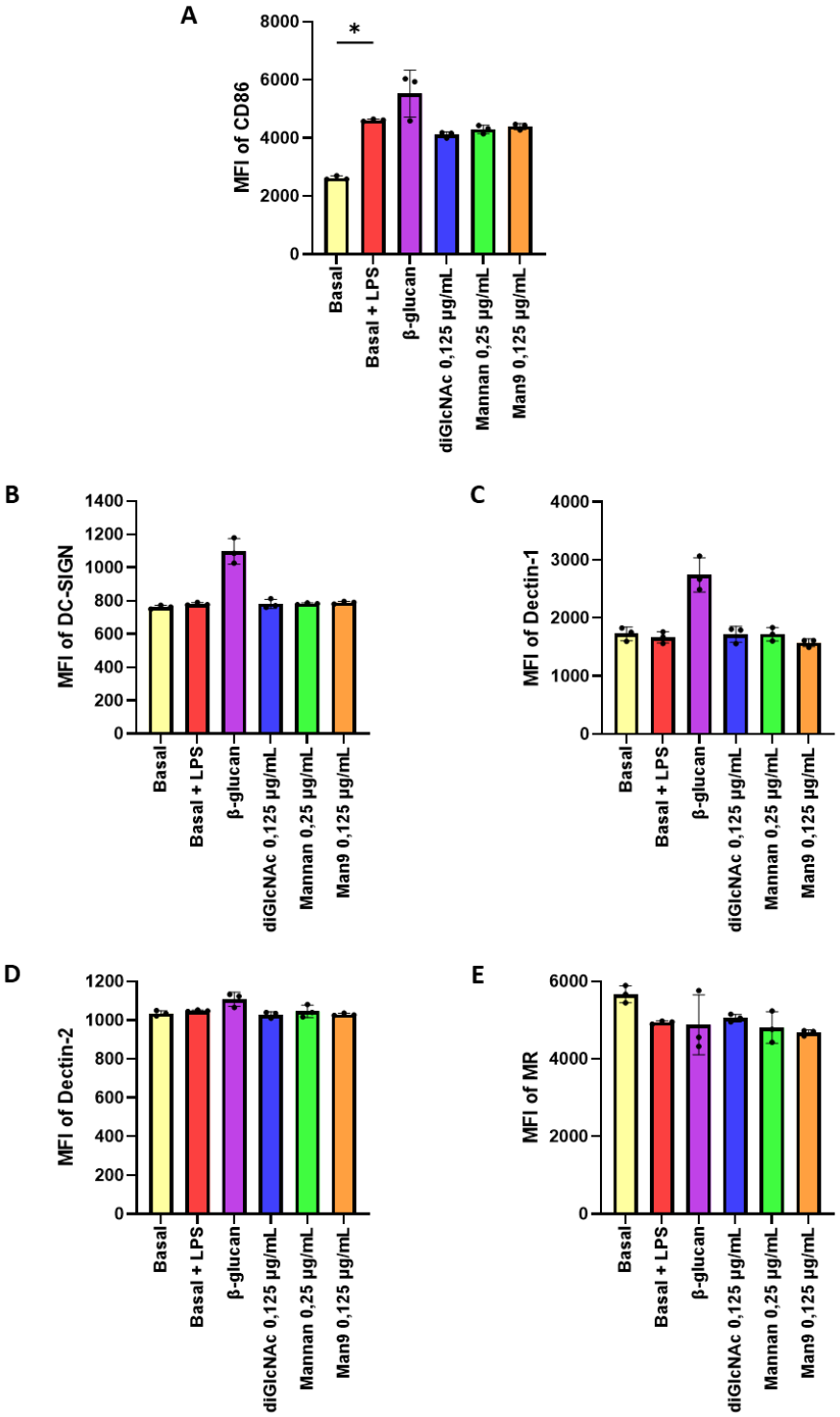

Figure A1. Flow cytometry results of the initial tests for the training of monocytes with various glycan structures. In early experiments, three stimuli were tested: diGlcNAc, Man9 and Mannan. As is possible to observe, the low concentrations of the different stimuli did not lead to the priming of monocytes. Median Fluorescence Intensity (MFI) is shown as Mean ± SD. Outlier tests were followed by Kruskal-Wallis non-parametric ANOVA and Dunnett's multiple comparison test. Data is represented as Mean ± SD. * $p < 0.05$.

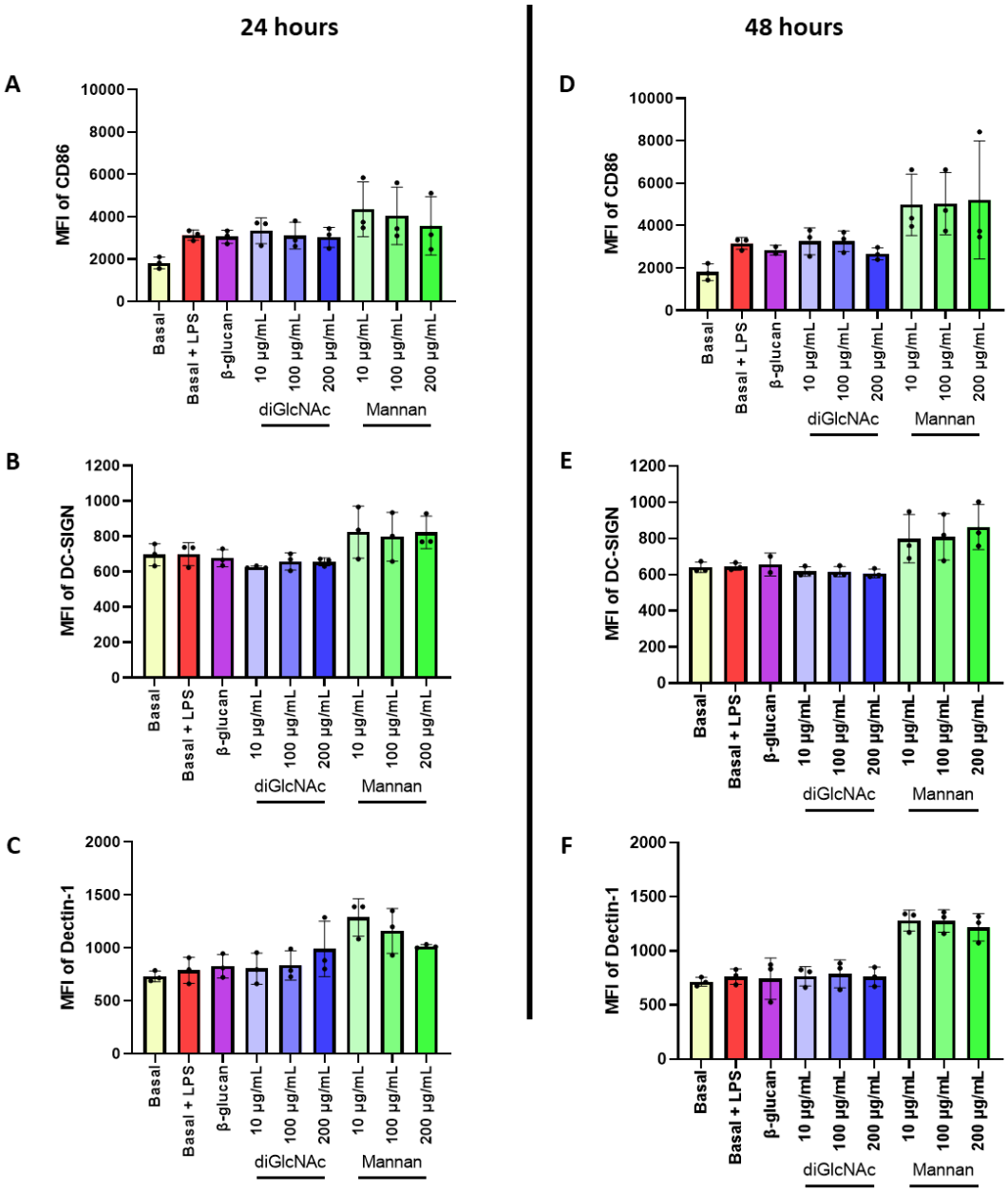

Figure A2. Flow cytometry results of the training of monocytes with various glycan structures after coating and with different periods of priming. For Mannan, coating made a considerable change to the phenotype developed by the monocytes. However, β-glucan did not work as well as in previous tests, prompting us to, once again, supplement the culture medium with this carbohydrate. Training the cells for a longer period (48 hours instead of 24) did not seem to impact the training of the monocytes. Median Fluorescence Intensity (MFI) is shown as Mean ± SD. Outlier tests were followed by Kruskal-Wallis non-parametric ANOVA and Dunnett's multiple comparison test. Data is represented as Mean ± SD.

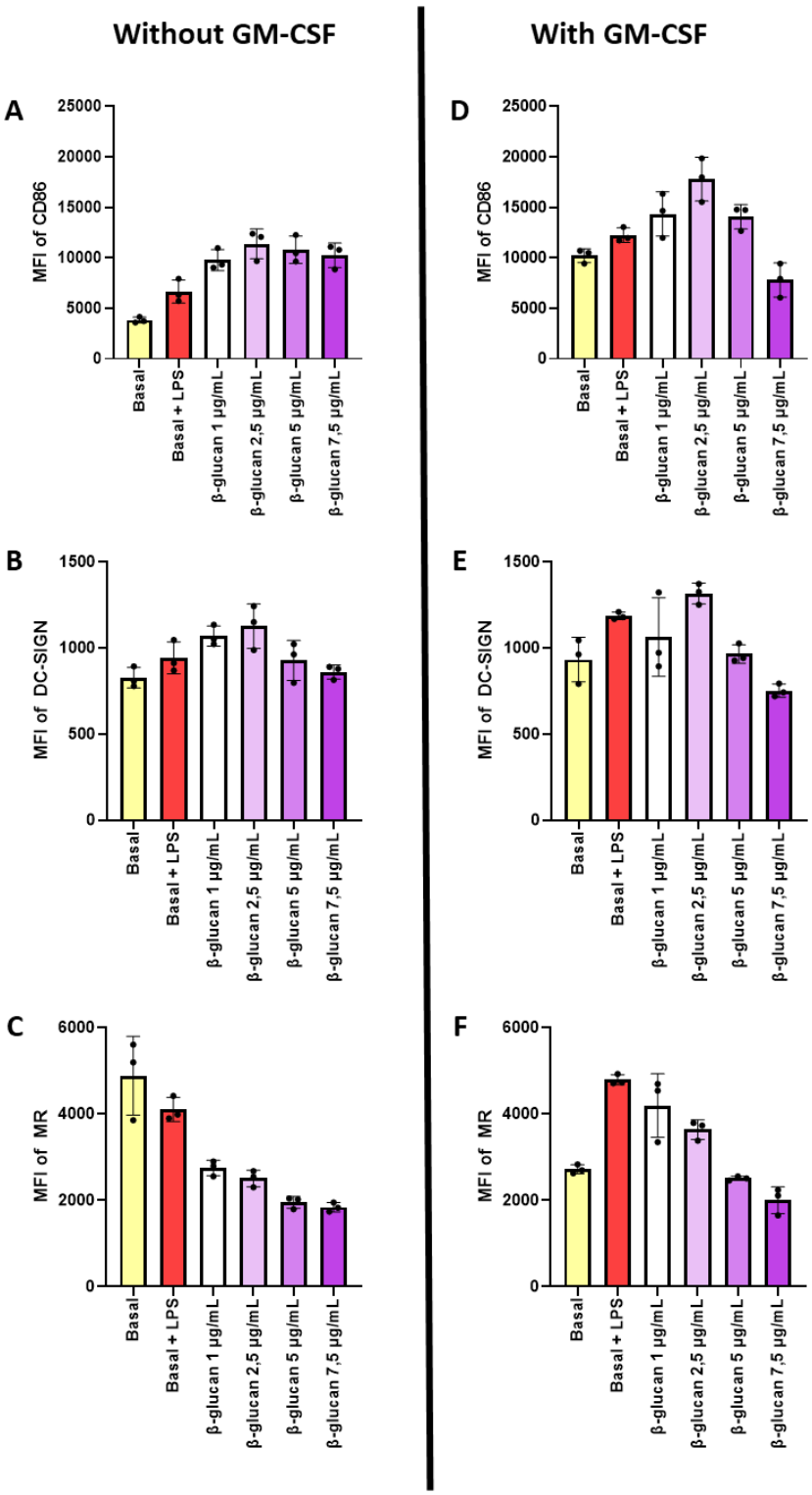

Figure A3. Flow cytometry results of the optimization of the concentration of β-glucan and supplementation with GM-CSF. Higer concentrations of this pathogen-derived glycan compromised the cell viability and did not present a clear benefit in terms of the observed phenotype, which led to the selection of the 2,5 µg/mL concentration for the remaining training experiments. GM-CSF did not have a significant impact on cell viability, but clearly activated these cells more. To avoid this potential bias, we opted to not include it in further procedures. Median Fluorescence Intensity (MFI) is shown as Mean ± SD. Outlier tests were followed by Kruskal-Wallis non-parametric ANOVA and Dunnett's multiple comparison test. Data is represented as Mean ± SD.

Appendix II – Monocytes undergo maturation during the training culture protocol

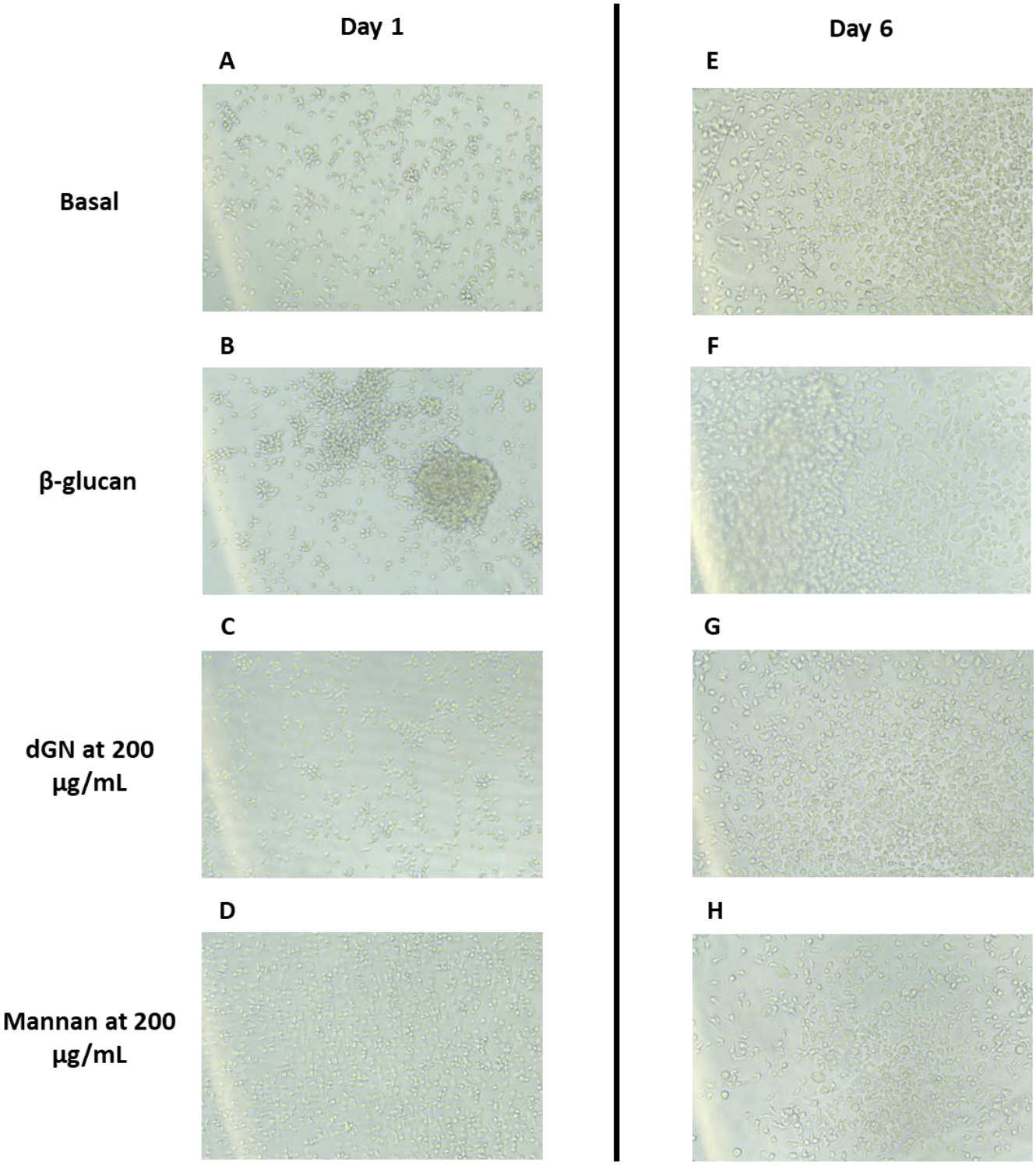

Figure A4. Microscope images of monocytes cultured with different training conditions at day 1 and day 6 after the introduction of the stimuli. The immune cells were subjected to β-glucan (B and F), dGN (C and G) and Mannan (D and H) supplementation, with a control condition (A and E). In general, monocytes present more mature features on day 6, being bigger in size and present less circular and more stellate/irregular shapes. These characteristics are more noticeable in the β-glucan and Mannan supplemented conditions.